Growth of yeast and production of polyhydroxybutyrate using rice wastewater

Afroza Begum, MBBS, MSc

This thesis is submitted to the University of Sheffield for the degree of Doctor of Philosophy

School of Biosciences

University of Sheffield

September 2023

Abstract

Water pollution is a critical global issue aggravated by the release of agricultural runoff, industrial effluents, and domestic sewage into the water bodies. Rice cultivation is a major agricultural activity in Bangladesh that generates substantial amounts of wastewater through the parboiling of rice. This thesis explores the innovative use of rice waste stream as a substrate for conventional yeast, *Saccharomyces cerevisiae*, simultaneously addressing water pollution along with fostering biodegradable polymer, Polyhydroxyalkanoates, and biomass production. Experimental methodologies are outlined encircling the expression of PHA synthase, PhaC1, and PhaC2 from *Pseudomonas mendocina*, an efficient cell factory for biopolymer production in cytosols and peroxisomes of *S. cerevisiae*. The outcome of this research showcases the successful production of polyhydroxybutyrate (PHB) in engineered *S. cerevisiae* cultured in oleate and YPO media. The study encompasses a multifaceted approach with an in-depth analysis of rice waste effluents, investigating their compositions and nutrient content. Analysis of the composition of rice wastewater manifests its potential as a nutrient-rich substrate, laden with organic and inorganic components and makes it an ideal resource for the growth of conventional yeast. Growth of *S. cerevisiae* in rice waste stream including various nutrient supplements displays the potential of rice waste effluent as a rich source of carbon and nutrients, supporting the growth and metabolic activities of yeast. Additionally, the production of biopolymers such as PHB is quantified, offering insights into the feasibility of utilising rice waste effluents as a sustainable biopolymer stock.

Acknowledgements

All praises be to Allah SWT who enlightened me with guidance and blessed me with the strength to complete the thesis and peace and blessings be upon the beloved Prophet Muhammad.

I would like to express my sincere gratitude and appreciation towards my present supervisor, Professor Mike Williamson, whose invaluable support, expertise, and guidance were instrumental in shaping this research project. His exceptional level of drive made me learn many useful and valuable points, which I might have missed otherwise. I would also like to extend heartfelt thanks to my previous supervisor, Dr Ewald Hattema for giving me ample opportunity to get exposure to scientific knowledge and research.

I am also indebted to Dr Donald Watts and all the members of the E-28 lab and the NMR group who provided me with assistance, insights, and constructive feedback throughout the course of this study.

I extend my appreciation to Professor Ipsita Roy (Material Science and Engineering) and her PhD student, Syed Mohammad Daniel Syed Mohamed, whose resources, collaboration, and assistance were indispensable in gathering the required data for this thesis.

I would like to acknowledge the contribution of Professor Morsaline Billah, who brought the rice wastewater samples from Bangladesh to the UK and significantly contributed to the progress of this project.

I would like to pay my special regards to Lab Technician, Anna Foster, Department of Chemistry, for her invaluable help with the ICP-MS analysis which supported me to elevate this work.

I am grateful to all my family members particularly my husband, Dr Khondoker Mehedi Akram, and two beautiful children Araf and Anusha for their support, patience, and understanding of the demanding phases of this research.

Dedication

This thesis is dedicated to the cherished memory of my beloved parents. It is a sincere expression of my gratitude for their unconditional love, selfless sacrifices, and invaluable teachings. Their unwavering influence will always be treasured, and their guidance will serve as a beacon of hope as I confront life's obstacles.

Abbreviations

APS - Ammonium persulphate

ATP- Adenosine triphosphate

C-terminal- Carboxyl-terminal

dH2O- Deionised water

DNA- Deoxyribonucleic acid

DTT - Dithiothreitol

ECL - Enhanced Chemi-Luminescence

EDTA- Ethylenediaminetetraacetic acid

E. coli- Escherichia coli

GC- Gas chromatography

Gpd1 - Glyercol-3-phosphate dehydrogenase 1

GFP- Green Fluorescent Protein

3-HA-CoA – (R)-3-hydroxyacyl-CoA

LiAc – Lithium acetate

M - Molar

MCL – medium chain length

Mdh3 - Malate dehydrogenase 3

Min - Minute(s)

NMR – Nuclear magnetic resonance

N-terminal - Amino-terminal

OD – Optical density

ORF- Open reading frame

PCR- Polymerase chain reaction

PEG – Polyethylene glycol

PEX – Peroxin

PHAs - Polyhydroxyalkanoates

PHB - polyhydroxybutyrate

P. mendocina - Pseudomonas mendocina

PhaC- PHA synthase

phaC- gene encoding PhaC

PLB – Protein loading buffer

PTS – Peroxisome targeting signal

PTS1 - Peroxisomal targeting signal type I

PTS2 - Peroxisomal targeting signal type II

RW – Rice wastewater

S. cerevisiae- Saccharomyces cerevisiae

SCL – short chain length

SDS-PAGE - Sodium dodecyl sulphate polyacrylamide gel electrophoresis

Sec - Second(s)

TCA - Trichloroacetic acid

Ura - uracil

WT- Wild type

YM1 - Yeast minimal medium 1

YM2 - Yeast minimal medium 2

YM2 Ura^- - selective media without uracil

YNB – Yeast nitrogen base

α - Alpha

β - Beta

µ - Micro

µM - Micromolar

Δ Delta

geneΔ - GENE deletion mutant

Table of Contents

List of Figures

Chapter 1:

Chapter 2:

Chapter 3:

Chapter 4:

Chapter 5

List of Tables

Chapter 1: Introduction

1.1 Sustainable resource utilization: the potential of rice waste effluent for biotechnology

Rice is the principal food for half of the world's population and production of rice is a rapidly growing area that produced 510 million metric tons of rice in 2022 (Shahbandeh, 2023). Bangladesh is the fourth biggest rice-producing country in the world and the estimated yield of rice amounted to 52.5 million metric tons in 2021 (Okoroafor, 2023). After the paddy is harvested from the crop fields, it must undergo a series of steps to prepare it for consumption. In Bangladesh, 90% of the paddy undergoes a wet milling process, known as parboiling, which includes soaking, partial boiling, and drying of paddy before the final milling process (Miah *et al.,* 2002).

The prime aim of parboiling rice is to improve the quality of rice by gelatinization of the starch during boiling and to generate chemical and physical alterations in granules in terms of nutritional, economic, and practical perspectives (Miah *et al.,* 2002). Nutrients are transferred from the bran to the endosperm of the granules during the parboiling process. These nutrients include particularly thiamine, as well as vitamins, fibres, proteins, and fats which are abundantly present in rice bran (Paiva *et al*., 2016). The melting temperature of amylose crystallites is above 100°C, and amylose molecules re-bind with each other to form ordered structures during the cooling process which relates to the texture of cooked parboiled rice (Lamberts *et al*., 2009). Starch changes from the crystalline to the amorphous form during parboiling, where continuous fusion and irreversible swelling of starch granules occur and ultimately bring benefits to the grain including retention of nutrients, improving yield by reducing the number of broken grains, sterilization, and improved shelf life (Kumar *et al.,* 2022; Heinemann *et al*., 2005).

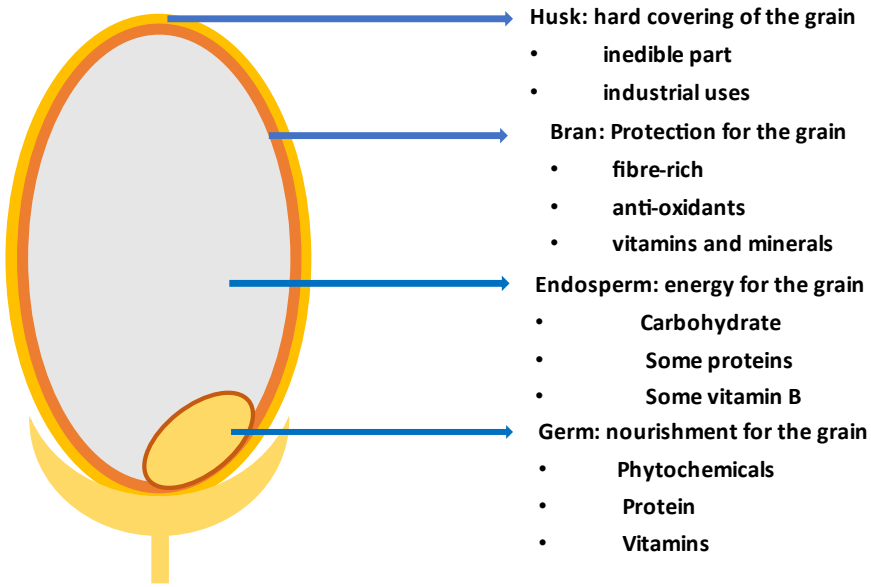

Figure 1.1: Structure of a rice grain, consisting of husk, bran, germ, and endosperm layer. The bran and germ are the most nutritious parts. The germ, often referred to as the seed, is responsible for sprouting into a new plant. It contains a wealth of nutrients, such as vitamin B, beneficial fats, and even protein. The bran, located in the outer layer of the grain, is rich in fibre and antioxidants. On the other hand, the husk (non-edible part) is the hard protecting covering of grain formed from silica and lignin. Modified from Yiu (2021).

Parboiling uses enormous amounts of water (1.5-2.0 L/kg of paddy) and the effluent produced in Bangladesh from 17,000 rice mills constituted 35 billion litres of starch-rich water in 2015 (Afrad *et al.,* 2020). Rice waste effluent produced during the processing of parboiled rice is rich in organic matter and inorganic nutrients that are mostly discharged into the river bodies or on nearby land which ultimately results in the degradation of water quality and nutrient overload in the soil, respectively (Rahman *et al*., 2017). As the rice mills are operated by people with limited knowledge of effluent treatment and environmental impact, disposal of rice wastewater into the river and on land has become a widespread practice in Bangladesh (Arefin and Mallik, 2018). Consequently, there is an urgent need to develop sustainable solutions that mitigate these environmental challenges while simultaneously addressing the growing demand for energy and biodegradable materials.

In order to mitigate the environmental impact, researchers have employed the yeast strain *Pichia pastoris* X-33 to enhance the quality of rice wastewater. As a result, significant reductions of 55% in COD (chemical oxygen demand), 52% in phosphorus, and 45% in nitrogen have been achieved. Biomass generated during this process can be further utilized as a

probiotic resource, providing additional benefits for poultry (Santos *et al*., 2018). Another study explored rice parboiling water as an alternative substrate for the yeast *Phaffia rhodozyma* to produce carotenoids. The findings of this study were promising, indicating that rice parboiling water could serve as an excellent source of nutrients and had the potential for biomass production by the yeast (Rios *et al*., 2015).

The utilization of yeast for rice wastewater treatment has been successfully implemented, resulting in significant reductions in nitrogen, phosphorus, and COD. This application has demonstrated the potential to convert starch, the primary component of rice wastewater, into a carbon source that is favourable for yeast growth. This approach has proven to be beneficial in reducing environmental impact, promoting clean water production, and contributing to improved health and quality of life for human populations (Santos *et al*., 2018).

1.2 Starch: the major nutritional component of rice grain

In human diets, the most common and popular carbohydrate is starch, which is present in enormous amounts in principal foods such as potatoes, rice, corn, wheat, and cassava (Helen, 2021). Starch is composed of two different polymers of glucose that each have a characteristic structure and property, namely amylose (linear) and amylopectin (branched). Generally, 20-25% amylose and 75-80% amylopectin are present in starch (Svihus *et al.,* 2005). Amylose contains approximately 6,000 glucose units in a linear polymer attached by α-1, 4- glycosidic bonds, while amylopectin consists of 10-60 glucose units linked by α-1, 4- glycosidic bonds, along with side chains made of 15-45 glucose units with α-1, 6 chains (Smith and Martin, 1997).

Figure 1.2: The structure of the amylose molecule.

Figure 1.3: The complex structure of the amylopectin molecule. Reproduced from Robyt (2008).

Starch is stored in most green plants as an energy source, collected in semi-crystalline granules (Smith and Martin, 1997). Light energy is used by plants during photosynthesis to convert carbon dioxide to glucose, which delivers chemical energy for metabolism and produces organic compounds such as proteins, lipids, nucleic acid, and cellulose. Plants convert extra glucose into starch (Smith and Martin, 1997). When glucose is stored as starch it becomes water insoluble and therefore osmotically inactive. This allows plants to store glucose compactly but prevents its rapid metabolism (Smith and Martin, 1997; Svihus *et al.*, 2005). The enzymes known as amylases are required to hydrolyse starch into constituent sugars. Amylases hydrolyse α-1, 4-glycosidic linkages in the starch thereby converting it into low molecular weight products for instance maltose, glucose, and maltotriose units (Gupta *et al*., 2003).

1.3 Amylase: catalyses the hydrolysis of starch

Amylases are one of the most significant industrial enzymes in the world enzyme market which occupy about 25% of total production (Gupta *et al*., 2003). Anselme Payen discovered and isolated amylase as diastase in 1833 that acts on α-1, 4-glycosidic bonds, therefore, amylase is also known as glycoside hydrolase (Payen and Persoz, 1833). Amylases are widely categorised into three subtypes alpha (α), beta (β), and gamma (γ), in which the first two types are broadly studied, and α-amylase is faster than β-amylase in action (Gupta *et al*., 2003). A few bacteria, fungi such as yeasts, and animals including humans can produce this enzyme. However, enzymes derived from fungi and bacteria are commonly utilized in industry and research (Gupta *et al*., 2003). Fungal α-amylases are superior to other sources for commercial use. Several species of *Aspergillus, Penicillium*, as well as *Streptomyces rimosus*, and *Thermomyces lanuginosus*, make amylases. *Aspergillus niger* and *Aspergillus oryzae* are the most widely used species for amylase production (Gupta *et al*., 2003). The United States Food and Drug Administration declared *A. niger* as “Generally recognized as Safe” due to its high tolerance of acid and capability to avoid bacterial contamination easily (Shafique *et al.,* 2010).

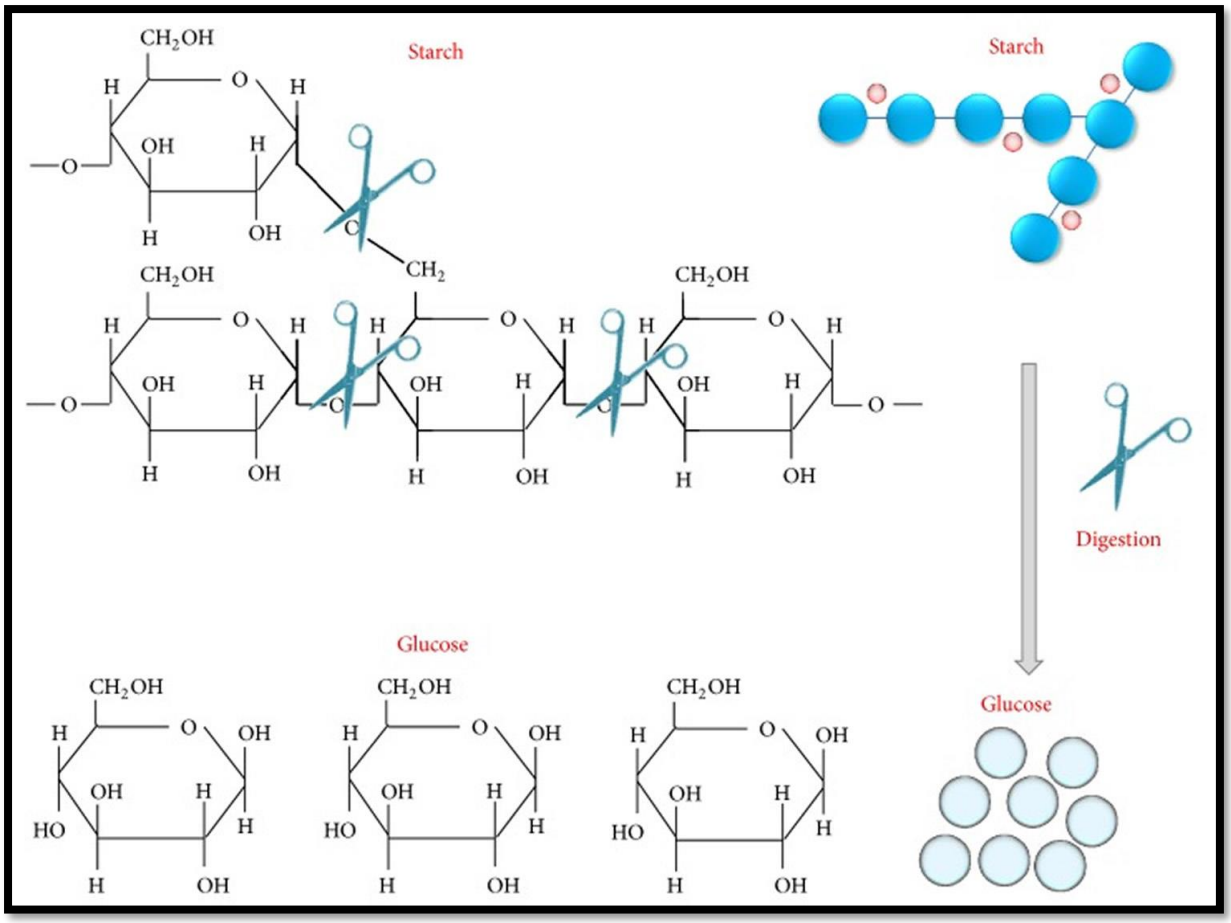

Figure 1.4: Diagrammatic representation of starch hydrolysis by amylase. Starch is a polysaccharide and by the action of amylase, it releases either monosaccharide (glucose) or disaccharide (maltose) (adapted from Gopinath *et al.,* 2017).

Yeast cells are naturally capable of making amylases, but the amount produced is too low to break down significant quantities of starch. However, after pretreatment of starch with alpha and beta amylase enzymes, yeasts grow and feed on those simple sugars (Sherri, 2023). Therefore, one possible approach is to add amylases to the waste stream for breaking down complex carbohydrates into simpler sugars that yeast can readily utilise and grow. Alternatively, yeast strains can be engineered with an amylase gene, to produce their own amylases. This can allow for in-situ saccharification of complex substrates to improve substrate utilisation in wastewater, reducing the need for external enzymes for yeasts (Cripwell *et al.,* 2019).

1.4 Yeasts in Biotechnology

Yeasts are eukaryotic, unicellular, microfungi that are found extensively in nature and can be isolated from aquatic, terrestrial as well as atmospheric environments (*SGDWiki,* 2019). Yeasts have been used by humans for millennia to produce alcoholic beverages and later also for processing food (Nocon *et al*., 2014). There are three major application areas in biotechnology for yeasts such as, *in vivo* biotransformation, generation of recombinant proteins, and metabolites production (Nocon *et al*., 2014).

Figure 1.5: Diagram represents a unicellular yeast cell surrounded by cell wall followed by periplasm, plasma membrane and cytoplasm or inside of the yeast containing intracellular nucleus, mitochondria, peroxisome, vacuole, golgi, endoplasmic reticulum including secretory vesicles.

Biotechnologists marked *S. cerevisiae* and its close relatives as conventional yeasts which are characterized by extreme growth in high concentration of sugar and final disposal of ethanol as a by-product (Rozpedowska *et al*., 2011). In 1996, the DNA sequence of the *S. cerevisiae* twelve million base pair genome was determined, which is regarded as a landmark in biotechnology (Goffeau *et al*., 1996). Scientists since then have published the genome sequences of many yeast species including, *Schizosaccharomyces pombe*, *Candida albicans*, and *Cryptococcus neoformans* (Wood *et al.,* 2002). Glucose or sucrose are the typical carbon substrates for yeast bioprocessing, which are derived from starch containing foods. As industrial biotechnology is expanding, researchers are searching for alternative carbon sources and are engineering strains to utilise these carbon sources to produce chemicals.

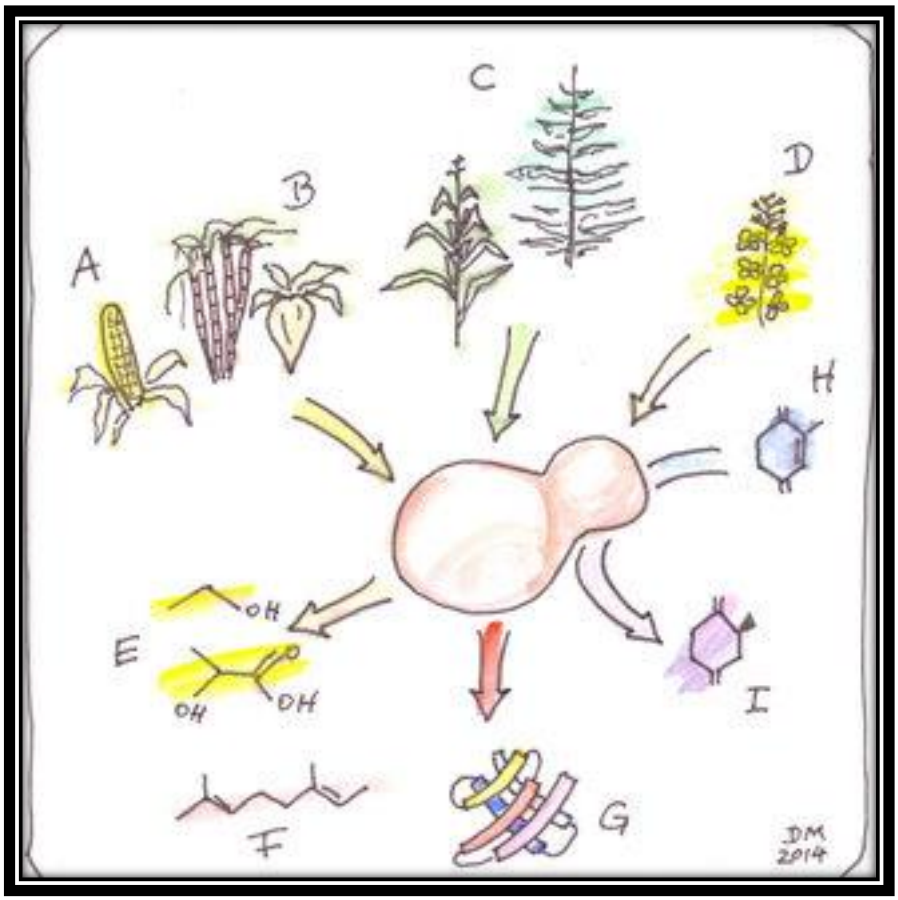

Figure 1.6: Diagram that demonstrates principal carbon derivatives in bioprocesses of yeast originated from corn starch (A), sugar cane or beet (B), lignocellulose (C), crude glycerol (D). A few wild and engineered yeast strains make products from the substrate like primary (E) or secondary (F) metabolites or recombinant (G) proteins. Furthermore, a complex substrate (H) in terms of whole cell biocatalysis is converted biochemically into a product (I) through the metabolic transformation of yeast cells. Chemical structures are for illustrative purposes only (Adapted from Mattanovich *et al.,* 2014).

The production of metabolites from yeast is a biotechnological process in which yeast microorganisms are employed to synthesize and accumulate various organic compounds, often of industrial or pharmaceutical importance. Yeasts, particularly *Saccharomyces cerevisiae*, are widely used for metabolite production due to their well-understood genetics, ease of genetic manipulation, and robust growth characteristics (Breuer *et al*., 2002). These microorganisms can be engineered to synthesize target metabolites by harnessing their natural metabolic pathways or introducing heterologous pathways. For instance, ethanol production is a well-known application, where *S. cerevisiae* is engineered to ferment sugars into ethanol efficiently (Azhar *et al.,* 2017). However, several challenges are associated with metabolite production from yeasts.

One of the primary challenges is optimizing metabolic pathways to enhance metabolite yields and productivity. Metabolic engineering techniques involve modifying yeast strains to redirect metabolic fluxes toward the desired metabolite (Yang *et al*., 1998). Achieving a balance between biomass growth and metabolite production is crucial, as excessive production of one may hinder the other. Another challenge is the efficient extraction and purification of metabolites from yeast cultures. Some metabolites may be intracellular, while others are secreted into the culture medium (Sasidharan *et al*., 2012). Developing cost-effective and environmentally sustainable methods for metabolite recovery is essential. Additionally, downstream processing can be challenging, especially for high-value or sensitive metabolites. The ability to fine-tune and control these conditions allows for the efficient conversion of raw materials, such as sugars or waste substrates, into valuable metabolites (Sasidharan *et al*., 2012).

1.5 Peroxisomes: versatile and highly adaptive organelles

The import of proteins into peroxisomes in yeast is a highly orchestrated and precisely regulated process critical for the organelle's proper function. Peroxisomes are membrane-bound organelles involved in various metabolic processes, including fatty acid degradation, hydrogen peroxide detoxification, and the synthesis of specific lipids and metabolites (Lazarow and Fujiki, 1985; Van den Bosch *et al*., 1992; Fidaleo, 2010). In mammals, peroxisomes primarily play a role in the β-oxidation of very long-chain and branched fatty acids, while the processing of short, medium, and long-chain fatty acids occurs mainly in the mitochondria. The sequence of reactions involved in β-oxidation is similar for both peroxisomes and mitochondria, but they differ in terms of substrate specificity. Yeast and plants depend exclusively on peroxisomes for the process of β-oxidation (Fidaleo, 2010). In yeast, peroxisomes are involved in various processes such as β-oxidation, the breakdown of methanol and amino acids, as well as the synthesis of lysine (Al-Saryi *et al*., 2017; Brown and Baker, 2003). To ensure functionality, peroxisomes must import specific enzymes and proteins. The process of protein import into peroxisomes primarily relies on two well-characterized peroxisomal targeting signals (PTS) and a set of dedicated peroxins (Pex proteins). For the successful importation of specific proteins and enzymes to peroxisome, PTS signals and peroxins are required to work together (Walter and Erdmann, 2019).

Peroxisomal matrix proteins are produced by ribosomes in the cytoplasm and subsequently transported into peroxisomes after the process of translation (Lazarow and Fujiki, 1985). The majority of peroxisomal matrix proteins possess one of two peroxisomal targeting signal (PTS) sequences embedded within their polypeptide structures. The most prevalent peroxisomal targeting signal (PTS) is known as PTS1, which consists of a conserved tripeptide consensus

sequence of (S/A/C)-(K/R/H)-L. This PTS1 sequence is typically located at the very end of the C-terminus of peroxisomal matrix proteins (Gould *et al*., 1989). The PTS2, in contrast, is less frequently observed. It is situated close to the N-terminus of the protein and is characterized by the consensus sequence (R/K) -(L/V/I/Q)-X-X-(L/V/I/H/Q) -(L/S/G/A/K)-X-(H/Q) -(L/A/F) (Swinkels *et al*., 1992). These PTS signals serve as specific recognition tags for the peroxisomal import machinery. Upon synthesis in the cytosol, proteins containing PTS1 or PTS2 signals are recognized by the cytosolic receptors, Pex5 and Pex7, respectively, and form complexes with their respective cargo proteins, constituting the receptor-cargo complexes. Pex5 is responsible for binding PTS1-containing cargo, while Pex7 recognizes PTS2-containing cargo. These receptor-cargo complexes then shuttle to the peroxisomal membrane, where docking occurs through interactions with proteins such as Pex14 (Walter and Erdmann, 2019).

Upon docking, the cargo-loaded receptor complex facilitates the formation of transient import pores on the peroxisomal membrane. These pores allow the translocation of the cargo protein from the cytosol into the peroxisomal matrix. The exact mechanism of pore formation is not fully elucidated but involves the coordination of various peroxins (Meinecke *et al*., 2016). Following translocation, cargo protein is released into the peroxisomal matrix, and the receptor needs to be recycled for further rounds of import. Pex5 undergoes a process called mono-ubiquitination, a modification that is crucial for its recycling. The Pex4-Pex22 complex catalyses the ubiquitination. The ubiquitinated Pex5 is recognized by the AAA ATPase complex consisting of Pex1 and Pex6 (Miyata and Fujiki, 2005). This complex extracts ubiquitinated Pex5 from the peroxisomal membrane and recycles it back to the cytosol. In the cytosol, the ubiquitin is removed from Pex5 by the action of a deubiquitinating enzyme, Pex4. In the case of PTS2-containing proteins, the PTS2 signal is cleaved off after import, and the mature protein remains in the peroxisomal matrix. Once inside the peroxisome, the imported protein can undergo processing and folding as required for its function within the organelle.

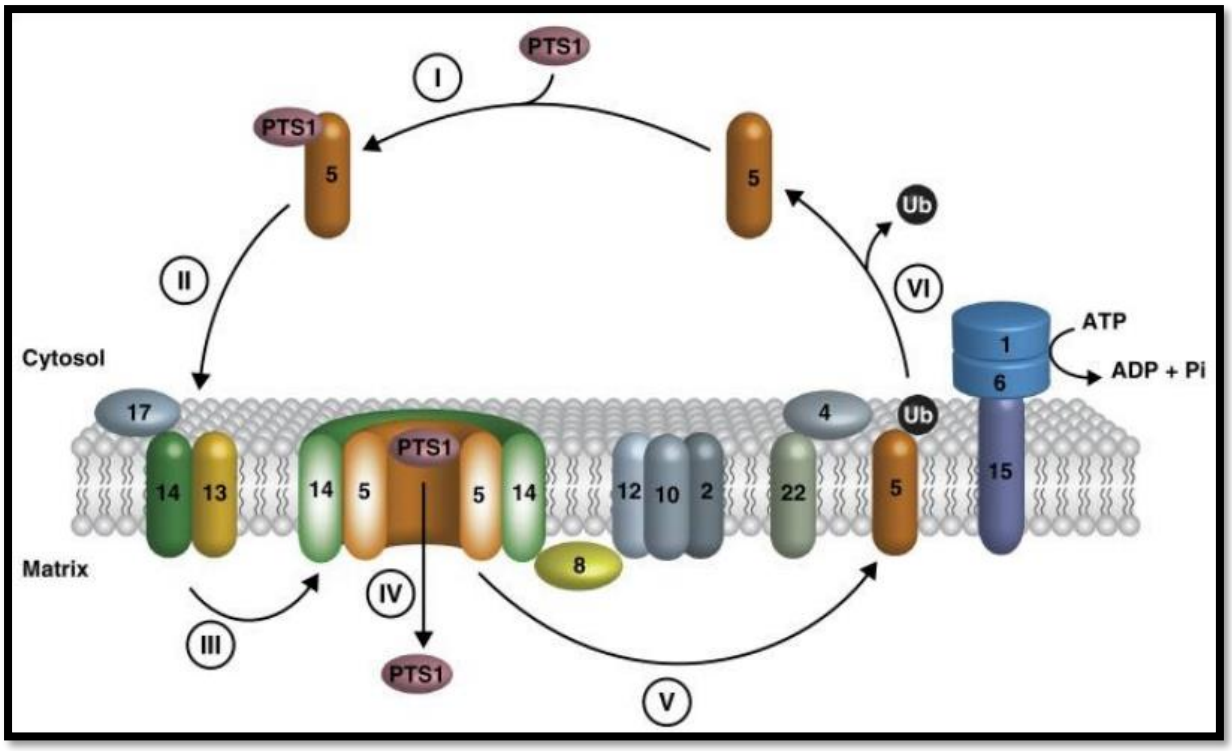

Figure 1.7: The schematic diagram depicts the process by which peroxisomal matrix proteins are imported (Hettema *et al.,* 2014). (I) Proteins containing a peroxisomal targeting signal of type 1 (PTS1) are recognized and bound by the import receptor Pex5 in the cytosol. (II) The receptor, loaded with cargo, is then directed to the peroxisomal membrane where it binds to the docking complex. (III) The receptor forms a transient pore with Pex14. (IV) The cargo proteins are imported into the peroxisome through an unknown mechanism before being released from the receptor. (V) The import receptor is then mono-ubiquitinated. (VI) Finally, the import receptor is released from the peroxisomal membrane in an ATP-dependent manner.

1.6 Peroxisome biogenesis and role of Pex3

The process of peroxisome biogenesis is a complex and highly regulated pathway that ensures the formation and maintenance of functional peroxisomes within the cell (Okumoto *et al.,* 2020). Understanding this process is crucial for unravelling the roles of peroxisomes in cellular physiology. The disruption of specific genes in yeast, such as the PEX3 gene, allows scientists to create mutants with defective peroxisome biogenesis. PEX3 is a key player in peroxisome biogenesis, particularly in the early stages of peroxisomal membrane assembly. The absence of PEX3, as seen in the *pex3Δ* mutant, results in a significant impairment in peroxisome formation. The PEX3 gene encodes a protein essential for the import of peroxisomal

membrane proteins (PMPs) and is crucial for the growth and division of peroxisomes (Okumoto *et al.,* 2020).

The process of peroxisome biogenesis involves several steps. First, peroxisomal matrix proteins are synthesized in the cytoplasm and imported into the peroxisome. PEX3 is involved in the targeting and insertion of PMPs into the peroxisomal membrane. The peroxisomal membrane then elongates, and small vesicles bud off from the endoplasmic reticulum (ER), contributing to peroxisome growth. Finally, the mature peroxisomes are formed through a series of fission events (Lazarow and Fujiki, 1985). In the context of studying peroxisome biogenesis, the use of mutants like *pex3Δ* provides valuable insights into the specific roles of genes and proteins in this intricate process. The defective peroxisome biogenesis observed in these mutants directly impacts cellular functions, especially those reliant on peroxisomal activities. Consequently, the study of these mutants aids in uncovering the molecular mechanisms governing peroxisome formation, and it sheds light on the broader implications for cellular metabolism, lipid homeostasis, and redox regulation (Fang *et al.,* 2004).

1.7 Polyhydroxyalkanoates

Petrochemical-derived plastics are commonly non-biodegradable because of their complex structure and high molecular mass, and they can remain in soil, landfill, and water bodies for a long period (Akaraonye *et al.,* 2010). The awareness of harmful consequences of petroleum-based plastics by the environmental bodies have been raised all over the world (Raza *et al*., 2018). This concern has led a global scientific movement to produce eco-friendly, biodegradable, and biocompatible polyesters and plastics. Polyhydroxyalkanoates (PHAs) are produced by several microorganisms and act as diverse polyesters that have already attracted attention as an alternative to petroleum-based polymers (Muneer *et al.,* 2020).

PHAs are a diverse group of storage polymers made up of hydroxy fatty acids. They are synthesized by different types of bacteria and archaea. PHAs are produced when there is an excess of carbon sources but limited availability of nutrients, leading to inhibited growth. These polymers are stored as insoluble granules within the cell cytoplasm, typically 0.2-0.5 µm in diameter, and a phase contrast light microscope is required for visualisation because of their high refractivity. Alternatively staining dyes such as the oxazine dyes Nile Blue, Sudan Black B, or Nile Red could be utilised for visualisation (Muneer *et al*., 2020). However, when the carbon supply becomes scarce, enzymes associated with the granules, called PHA depolymerases break down the PHA releasing carbon and providing energy (Rehm,2021).

"This image has been removed by the author of this thesis for copyright reasons".

Figure 1.8: Transmission electron microscopic view of bacteria (Pseudomonad) filled with PHAs, arrow is indicating PHA granule. The scale bar is 1µm.

In 1926, PHA was first discovered by the French scientist Lemoigne in the form of PHB (Poly 3-hydroxybutyrate) in *Bacillus megaterium* (Lemoigne, 1926). The natural polyester PHAs consist of 3-, 4-, 5-, 6- hydroxyalkanoic acids that are thermoplastic in nature, and the polyester core is made of either protein or phospholipid. The general structure of PHAs is illustrated in Figure 1.8, where R is the side chain that includes alkyl groups that vary from methyl (C1) to tridecyl (C13) and n refers to the number of monomer units in the polymer chain, which varies from 100 to 30,000 (Muneer *et al*., 2020).

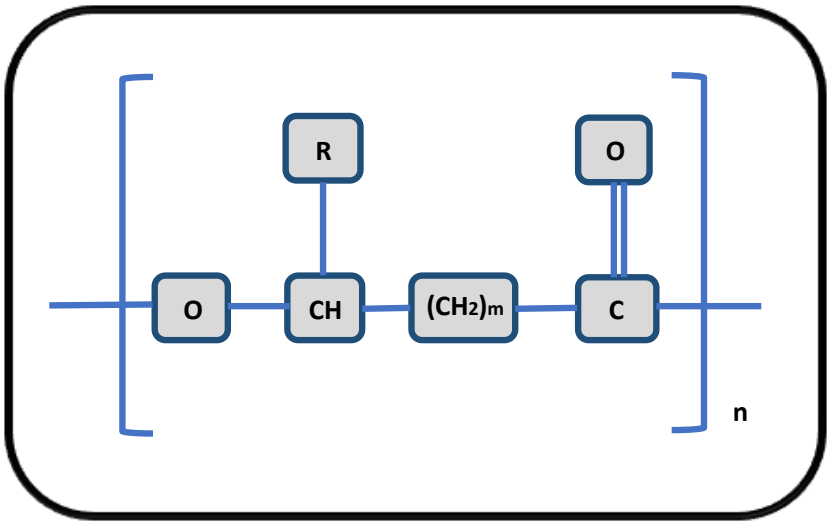

Figure 1.9: Chemical Structure of PHA. Here, R refers to the side chain that can contain 1-13 carbons, m-1, 2or 3 while n refers to the number of repeating units and can be 100 to many thousands. Modified from (Muneer *et al*., 2020).

In terms of the number of carbons in their side chains, PHAs are classified into short chain length (SCL), medium chain length (MCL), and long chain length (LCL) types (Kunasundari and Sudesh, 2011). There are 3-5 carbon atoms present in SCL-PHAs such as poly 3-hydroxybutyrate (P3HB), poly 4 hydroxybutyrate (P4HB), and poly3-hydroxyvalerate (P3HV) or the copolymer P(3HB-co-3HV). Medium-chain lengths PHAs have 6–14 carbon atoms as for example homopolymer poly 3-hydroxyhexanoate (P3HHx), poly3-hydroxyoctanoate (P3HO) and copolymers such as P(3HHx-co-3HO) (Kim and Lenz, 2001) and more than 14 carbon atoms are present in LCL-PHAs, but these are less studied.

Figure 1.10: This diagram represents structure of PHAs depending on the classification, showing commonly synthesized scl-PHAs, such as, 3-hydroxybutyrate (3HB), 3-hydroxyvalerate (3HV) and mcl-PHAs, for instance, 3-hydroxyhexanoate (3HHx), 3-hydroxyoctanoate (3HO), 3-hydroxydecanoate (3HD), 3-hydroxydodecanoate (3HDD).

PHAs composed of mostly medium-chain-length (MCL) monomers are elastomeric in nature, whereas PHAs composed of mostly short-chain-length (SCL) monomers are often stiff and brittle. However, SCL-MCL PHA copolymers can have properties between the two states and this copolymer reduces the crystallinity as well as melting point of the polymer, which leads to improvement in the processing, flexibility and strength of the polymer (Kim and Lenz, 2001). The mechanical properties of PHA can be changed by blending, modifying the surface or combining PHA with other polymers.

PHA biosynthetic pathways are linked directly or indirectly with several metabolic pathways including Krebs cycle, glycolytic and pentose phosphate pathways, amino acids and fatty acids biosynthesis and degradation pathways (Lu, J *et al*., 2009). Acetyl-CoA is the key precursor for biosynthesis of many short chain length (SCL) and medium chain length (MCL) PHAs (Meng, D.C *et al*., 2014).

There are three well-known PHA bio-synthetic pathways, based on biosynthesis using acetyl-CoA derived from basic metabolism such as glycolysis, using intermediates produced by fatty acid degradation (β-oxidation) and intermediates produced during fatty acid biosynthesis as described in figures 1.11, 1.12 and 1.13 respectively (Anjum *et al*., 2016). In bacteria, PHA synthetic genes are reside within an operon that includes a *phaA* (β-ketothiolase), a *phaB* (NADPH-dependent acetoacetyl coenzyme A reductase), and a *phaC* (synthase) (Pohlmann *et al*., 2006). The glucose molecule is converted into acetyl-CoA by glycolysis, two acetyl-CoA molecules undergo condensation by the enzyme β-ketothiolase, encoded by PhaA, and

produce acetoacetyl-CoA. The next step is the reduction of Acetoacetyl-CoA by Acetoacetyl-CoA reductase encoded by PhaB to produce (R)-3-hydroxybutyryl-CoA. Finally, Pha synthase encoded by PhaC polymerizes this monomer to form PHAs (Anjum *et al*., 2016; Verlinden *et al.,* 2007).

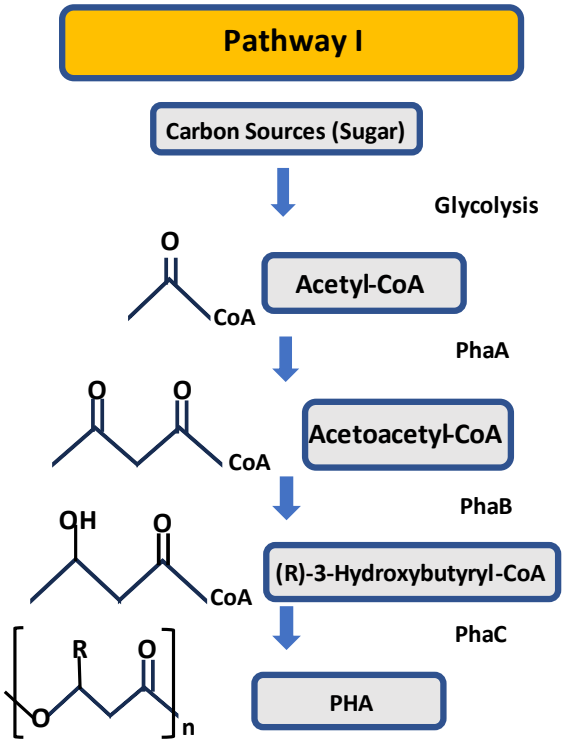

Figure 1.11: PHA synthesis metabolic pathway I. Modified from (Verlinden *et al*., 2007).

The beta-oxidation pathway is a well-known metabolic pathway involved in the synthesis of PHA (Anjum *et al.,* 2016; Verlinden *et al.,* 2007). It begins with the breakdown of fatty acids into acetyl-CoA unit. The acetyl-CoA is then further metabolized to produce a molecule called (R)-3-hydroxyacyl-CoA. This intermediate is subsequently converted to (R)-3-hydroxyacyl-CoA monomers, which act as building blocks for PHA synthesis. Once the monomeric unit, as for example, 3-hydroxyacyl-CoA, is produced through the β-oxidation pathway, they undergo polymerization to form PHA chains (Anjum *et al.,* 2016; Verlinden *et al.,* 2007). The polymerization procedure involves the action of an enzyme called PHA synthase. This enzyme catalyses the condensation of the monomeric units, linking them together to form PHA chains. The resulting polymer can have varying properties depending on the types of

monomeric units incorporated and the polymerization strategy employed (Anjum *et al*., 2016; Verlinden *et al*., 2007).

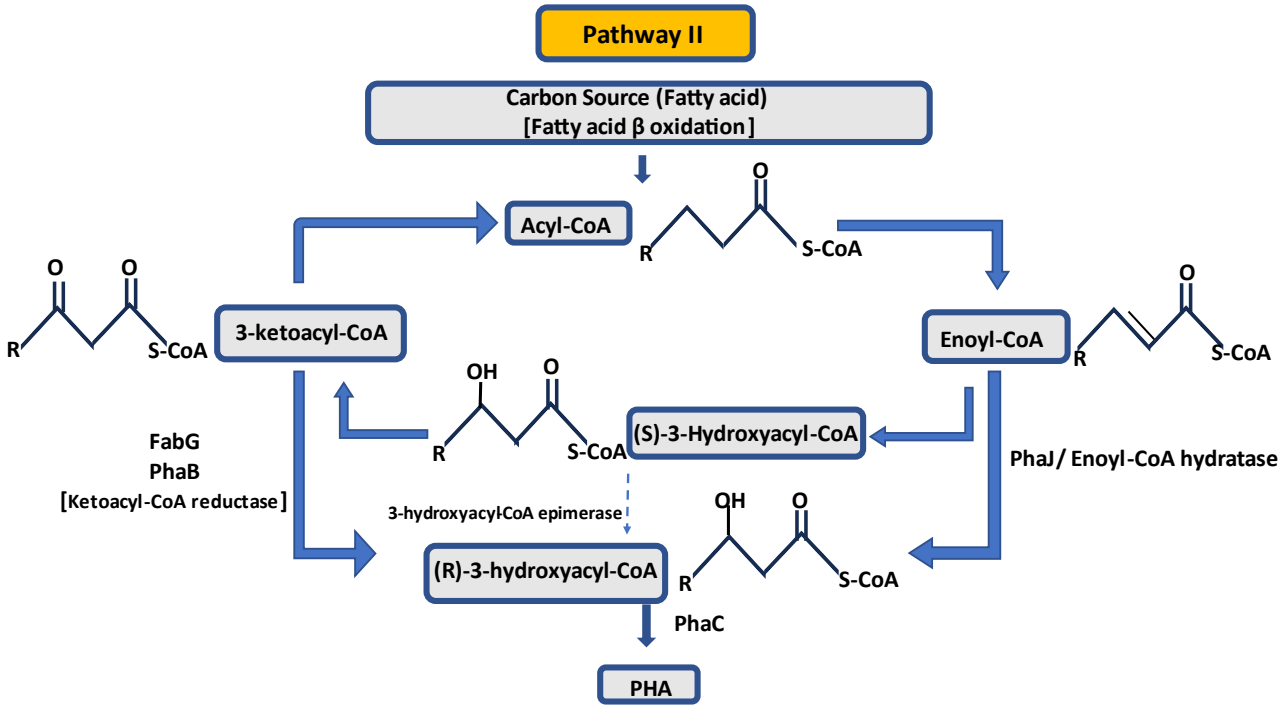

Figure 1.12: PHA synthesis Pathway II. Modified from (Verlinden *et al*., 2007).

Pathway III is of significant interest because it involves fatty acid biosynthesis and ultimately generates monomers for PHA synthesis from structurally unrelated, inexpensive, simple carbon sources such as glucose, sucrose and fructose (Anjum *et al*., 2016; Verlinden *et al*., 2007). In the fatty acid biosynthetic pathway, the process starts with the conversion of glucose or other carbon sources to acetyl-CoA. The acetyl-CoA is then converted to malonyl-CoA through a series of enzymatic reactions. The malonyl-CoA is subsequently converted to (R)-3-hydroxyacyl-CoA which are converted from their Acyl Carrier Protein (ACP) form to the CoA form by the enzyme Acyl-ACP-CoA transacylase which is encoded by PhaG. These (R)-3-hydroxyacyl-CoA molecules are then polymerized to form PHA (Anjum *et al.,* 2016; Verlinden *et al*., 2007).

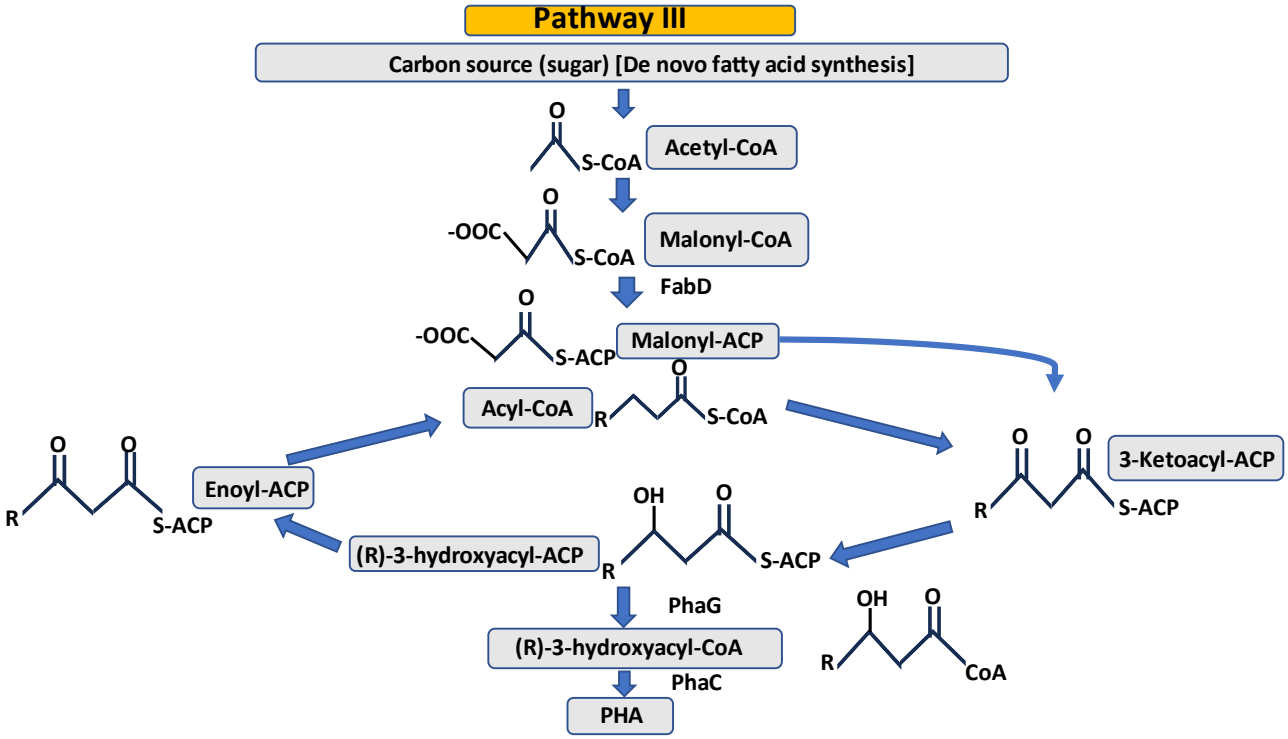

Figure 1.13: PHA synthesis pathway III. Modified from (Verlinden *et al*., 2007).

Both eukaryotic and prokaryotic microorganisms are enabled to produce various types of PHAs (Rehm, 2009). Even though *S. cerevisiae* does not naturally produce PHA, it serves as a valuable model organism for investigating PHA production. Since *S. cerevisiae* naturally synthesizes the PHA monomers known as 3-HA-CoAs, it is enabled to compartmentalize PHA biosynthesis within peroxisomes. Therefore, *S. cerevisiae* is a suitable platform for studying PHA production due to its native production of PHA monomers and its capability to localize PHA biosynthesis to peroxisomes (Haddouche *et al*., 2011; Poirier *et al*., 2001; Zhang *et al.,* 2006). Previous study established that *S. cerevisiae* can express PHAs by utilizing 3-hydroxyacyl coenzyme A intermediates through fatty acid metabolism (Zhang *et al.,* 2006). Feeding of appropriate substrates are also essential to produce polymers by yeast whether it is even, odd or combined numbered monomers (Zhang *et al*., 2006). Researchers are focusing on finding new ways of cost effective PHA production, by utilizing several waste materials for microorganisms as carbon source to accomplish long term environmental and economic benefit (Alvi *et al*., 2014). One source of carbon could be the rice waste stream for further exploration and development.

Rice wastewater provides a rich source of nutrients, including carbohydrates, proteins, and minerals, which can support the growth and metabolic activities of yeast. By utilizing this

waste effluent as a growth medium for yeast, we can effectively transform an environmental burden into a sustainable resource for biomass production.

1.8 Sustainable solutions: Role of PHAs in green plastics

Polyhydroxyalkanoates (PHAs) have emerged as a promising candidate in the realm of green plastics, often referred to as bioplastics, which are derived from renewable resources. Green plastics refer to environmentally friendly polymers and PHAs fit this definition perfectly as they are derived from natural sources and produced from various microorganisms through the fermentation process (Kovalcik *et al.,* 2019). Additionally, PHAs are designed to be biodegradable or have a lower environmental impact compared to conventional plastics. The biodegradability of PHAs means that they can be broken down by microorganisms into natural byproducts such as H_2O and CO_2. This characteristic addresses the persistent pollution issues associated with conventional plastics that can take centuries to decompose (Muthuraj *et al*., 2021).

PHAs possess several qualities that make them attractive for environmentally friendly applications. The potential use of PHAs in green plastics spans various applications. They can be utilized in packaging materials, disposable cutlery, cups, plates, bottles, and other single-use items (Kovalcik *et al.,* 2019). PHAs are versatile and can be engineered to exhibit properties similar to conventional plastics while still being biodegradable (Muthuraj *et al*., 2021). This makes them suitable for a range of everyday products without compromising performance. In addition to their biodegradability, PHAs are biocompatible, a characteristic that makes them particularly attractive for various biomedical applications (Pulingam *et al*., 2022; Zhang *et al.,* 2022). Biocompatibility refers to the ability of a material to interact harmoniously with living organisms without causing adverse effects. Their ability to seamlessly interact with biological systems, coupled with their biodegradability and tunable properties, positions PHAs as promising candidates for medical implants, drug delivery systems, tissue engineering, and other applications where compatibility with living organisms is of utmost importance. The ongoing research and development in this field continue to unveil new possibilities for harnessing PHAs in innovative and biocompatible solutions (Pulingam *et al*., 2022; Zhang *et al.,* 2022). As awareness of environmental issues grows and regulations on single-use plastics tighten, the adoption of PHAs is likely to increase, paving the way for a more sustainable future in the realm of materials and packaging.

1.9 Aims and objectives

To achieve the aims and objectives of this project, an industrial biotechnology route has been applied by employing a conventional yeast, *S. cerevisiae* to produce green bioplastics, PHAs. Chapter 3 aims to express PHA synthase into peroxisomes and cytosols of *S. cerevisiae* to produce PHAs in engineered yeast.

Chapter 4 aims to comprehend and identify the chemical components present in rice wastewater. Rice wastewater is a byproduct generated during the processing of rice, and its composition can vary based on the specific processing methods employed. To achieve this objective, a comprehensive analysis of the wastewater was conducted, involving techniques such as Inductively Coupled Plasma spectroscopy, and Nuclear Magnetic resonance spectroscopy. This analysis established organic and inorganic compounds, nutrients, and potential pollutants present in the rice wastewater. Understanding the chemical constituents is crucial for developing effective strategies and exploring its suitability as a feedstock for conventional yeast.

The waste effluents from rice mills predominantly contain starch, an excellent source of carbon for the yeast. The main benefit of using yeasts is, that the molecular machinery of yeasts has been well studied and this eukaryotic organism is the most widely used for industrial production of fuels and chemicals (Rocha *et al*., 2010). Rice wastewater made here for this project, employing yeast strains capable of utilizing this waste effluent, optimizing the fermentation process for maximum biomass and PHAs production (Chapter 5).

Chapter 2: Materials and Methods

2.1 Chemicals and enzymes

The chemicals, primers and other materials utilised in this study were mostly supplied by MERCK formerly known as Sigma-Aldrich. Growth media components were supplied by Difco Laboratories, ForMedium and Fisher Scientific UK. PCR buffers, dNTPs and DNA polymerases were purchased from Bioline UK. Gel extraction kits and Miniprep kits were supplied by Qiagen. Restriction enzymes and buffers were provided by New England Biolabs (NEB). Equipment used for DNA and protein work was supplied by BioRad. Buffers for protein work were provided by Geneflow.

2.2 Strains and plasmids

2.2.1 Strains

Table 2.1: The yeast strains used in this study.

Strain	Genotype	Source
BY4741 WT	*MATa his3Δ1 leu2Δ0 met15Δ0 ura3Δ0*	Euroscarf
BY4742 WT	*MATα his3Δ1 leu2Δ0 lys2Δ0 ura3Δ0*	Euroscarf
pex3Δ	*BY4742 pex11Δ::kanMX4*	Euroscarf
atg36Δ	*MATA his3-1 leu2-0 met15-0 ura3-0 atg36Δ::KanMX4*	Euroscarf
mdh3/gpd1Δ	*MATA his3-1 leu2-0 met15-0 ura3-0 gpd1Δ::KanMX4 mdh3Δ::SpHis5*	(Al-Saryi *et al.*, 2017)

Table 2.2: The *Escherichia coli* strain used in this study.

E. coli strain	Genotype	Purpose	Source
DH5α	*supE44 ΔlacU169 (Φ80 lacZ ΔM15) hsdR17 recA1 endA1gyrA96 thi-1 relA1*	Amplification of plasmids and recovery of plasmid DNA from *S. cerevisiae* following in vivo homologous recombination	(Hanahan, 1983)

2.2.2 Plasmids

Plasmids used in this study are tabulated in Table 2.3. Plasmids were made by either a homologous recombination-based approach in *S. cerevisiae* or by conventional restriction digestion and ligation followed by transformation into *E. coli*. Promoters, recombinant tags, open reading frames and terminators were introduced into the restriction sites of the multiple cloning sites.

Table 2.3: The list of plasmids used in this study.

Plasmid Name	Vector backbone	Promoter/ Terminator	Insert	Marker	Source
pEW322	Ycplac33	*TPI/PGK1*	MCS	Ura3	Lab stock
pEW351	Ycplac33	*TPI/PGK1*	*GRD19*	Ura3	Lab stock
pEW355	Ycplac33	*TPI/PGK1*	*GFP-GRD19*	Ura3	Lab stock
Ycplac33	_	_	Empty	Ura3	Lab stock
pAB01	pEW355	*TPI/PGK1*	*GFP-PhaC1-PTS1*	Ura3	This study
pAB02	pEW355	*TPI/PGK1*	*GFP-PhaC1*	Ura3	This study
pAB03	pEW355	*TPI/PGK1*	*GFP-PhaC2-PTS1*	Ura3	This study

pAB04	pEW355	*TPI/PGK1*	*GFP-PhaC2*	Ura3	This study
pAB05	pEW355	*TPI/PGK1*	*PhaC1-PTS1*	Ura3	This study
pAB06	pEW355	*TPI/PGK1*	*PhaC1*	Ura3	This study
pAB07	pEW355	*TPI/PGK1*	*PhaC2-PTS1*	Ura3	This study
pAB08	pEW355	*TPI/PGK1*	*PhaC2*	Ura3	This study
pAB09	pEW351	*TPI/PGK1*	*PhaC1-PTS1*	Ura3	This study

2.3 Growth media

Components for cell growth media were dissolved in Millipore water and mixed with a magnetic stirrer, then autoclaved to sterilisation at 121°C. Antibiotics or amino acid stocks were added to their final concentration when the autoclaved media had cooled to about 50°C. The reagents required to make growth media are listed in Table 2.4.

Table 2.4: Growth media and their constituents.

Culture media	Constituents with concentration
YPD	1% Yeast extract, 2% Peptone, 2% D-glucose
2TY	1% yeast extract, 1.6% Bacto-tryptone, 0.5% NaCl. Kanamycin or Ampicillin was added to autoclaved media whenever required to final concentrations of 50 µg/ml and 75 µg/ml respectively.
Yeast Minimal Medium 1 YM1 (For selection of all auxotrophic markers)	0.5% Ammonium Sulphate, 0.17% Yeast nitrogen Base without Amino acids and Ammonium sulphate, 2% Galactose, D-Glucose or Raffinose. Adjusted to pH 6.5 with NaOH and after autoclaving relevant amino acid stocks were added.

Yeast Minimal Medium 2 YM2 (For selection of Uracil auxotrophic marker)	0.17% Yeast Nitrogen Base without Amino acids and Ammonium sulphate, 0.5% Ammonium Sulphate, either 2% D-Glucose or Raffinose or Galactose, 1% Casamino acids. Adjusted to pH 6.5 with NaOH. 0.3% Leucine and 0.2% Tryptophan were added after autoclaving.
Amino Acid stocks	Amino acid stocks were added to YM1 and YM2 as per requirement from 100x stocks to final concentrations of 20 ng/ml (Tryptophan, Methionine, Histidine-HCl) or 30 ng/ml (Leucine, Lysine-HCl).
Solid Media	2% (w/v) Agar was added to liquid growth media followed by autoclaving. Media was poured into sterile petri dishes (Sterilin) while it was cooled and left to set at room temperature. Once prepared, plates were stored at 4°C.

2.4 Bacterial genomic DNA isolation

DNA purification from the Gram-negative bacterium*, Pseudomonas mendocina* CH50 was performed by following the steps described in Cold Spring Harbor protocol (Green and Sambrook, 2017). 5 ml of an overnight bacterial culture which was grown in 2TY media, was transferred to a 1.5 ml microcentrifuge tube followed by centrifugation for 30 sec at room temperature. After removal of the supernatant, 400 µl of TE (pH 8.0) was added. The bacterial pellet was dispersed by vortexing twice for 20 sec each time. 50 µl of 10% SDS, and 50 µl of proteinase K (20 mg/mL in TE, pH 7.5) were added afterwards to lyse the cells. The bacterial lysate was then incubated for 1 hour at 37°C.

At this stage, the digested lysate was too viscous to handle. The DNA was sheared by three to five passages through a 26-gauge needle to reduce its viscosity. 500 µl of a 1:1 mixture of phenol: chloroform was added for extraction and the top of the microcentrifuge tube was closed and the two phases were mixed by gentle vortexing. The upper layer was transferred to a fresh microcentrifuge tube and the aqueous phase was extracted twice with 500 µl of chloroform. The supernatant was transferred to a fresh Eppendorf tube, added 25 µl of 5M NaCl and 1ml of 95% ethanol, then vortexed and centrifuged for 10 min at 4°C and carefully removed the residual ethanol with a micropipette. The open tube was left on the bench for about 15 min afterwards.

The damp-dry pellet was dissolved in 100 µl of TE (pH 8.0), with 5 µl of ribonuclease A (5mg/mL in TE, pH 8.0). The solution was then incubated for 30 min at 37°C. 40 µl of 5M ammonium acetate and 250 µl of isopropanol were added after incubation. The closed tube was stored briefly for 10 min at room temperature. The DNA was then recovered by centrifugation (10 min at room temperature). The pellet was washed twice with 70% ethanol and the residual ethanol was carefully removed with a micropipette. The tube was left open on the bench for 15 min. The damp-dry pellet was dissolved finally in 100 µl of TE (pH 8.0). The concentration of DNA was measured with a Nanodrop machine, and the DNA was stored at -20°C.

Table 2.5: Reagents required for Gram-Negative Bacterial DNA Isolation. Solutions were sterilized by autoclaving for 20 min at 15 psi (1.05 kg/cm²) on liquid cycle and stored at room temperature.

Solutions	Reagents required
5M Ammonium acetate	38.5 g up to 100mL dH_2O
5M Sodium chloride	29.2 g NaCl up to 100mL dH_2O
TE buffer (10x)	100 mM Tris-Cl, 10 mM EDTA (pH 8.0)
Proteinase K	20 mg/ml in 1xTE pH 7.5
Ribonuclease A	5 mg/ml in TE (pH 8.0)
10% SDS	10 g up to 100 ml dH_2O
Phenol: chloroform	1:1 (v/v)
Ethanol	95% and 70% in dH_2O (v/v)

2.5 DNA procedures

2.5.1 Polymerase Chain Reaction (PCR)

PCR was used to amplify specific regions of DNA. VELOCITY™ or MyTaq™ DNA polymerase was used to amplify DNA. 25 µl reactions were made up in PCR tubes. PCR reactions were prepared with the detailed reagents on ice with the DNA polymerase added last. The reagents used are detailed in Table 2.6.

Table 2.6: PCR reaction mixture composition.

Component	Velocity DNA Polymerase	My Taq DNA Polymerase
Reaction buffer	5 µl 5x Hi-Fi buffer	5 µl 5x MyTaq™ buffer
Forward primer	2.5 µl forward primer (5 µM working stock from a 100 µM stock)	2.5 µl forward primer (5 µM working stock from a 100 µM stock)
Reverse primer	2.5 µl reverse primer (5 µM working stock from a 100 µM stock))	2.5 µl reverse primer (5 µM working stock from a 100 µM stock)
dNTPs	1.5 µl 2.5mM dNTPs (0.15 mM)	_
Template	1 µl (gDNA or plasmid)	1 µl (gDNA or plasmid)
DNA polymerase	0.25 µl VELOCITY™ polymerase (1.25 unit)	0.25 µl MYTAQ™ DNA polymerase (1.25 unit)
dH20	12.25 µl dH_20	13.75 µl dH_20

PCR reactions were run in a thermocycler with the lid preheated to 100°C to prevent condensation in the PCR tubes. The PCR conditions used are detailed in Table 2.7. The annealing temperature was calculated depending on the GC/AT content of the individual primers used. To get approximate annealing temperature following equation was used:

Annealing temperature (TA°C) = Melting temperature (TM°C) - 5°C

where (TM°C) = 4 x (#G + #C) + 2 x (#A + #T); Mostly, 5µl of PCR product was loaded on an agarose gel to see if a product of the required size had been produced. The primers used for various PCRs in this study are listed in Table 2.8.

Table 2.7: PCR conditions. PCR conditions were set up as detailed. Steps 2-4 were repeated for 30 cycles in each PCR reaction.

Steps	Velocity DNA Polymerase	MyTaq DNA Polymerase
Initial denaturation	95°C 3 min	95°C 3 min
Denaturation	95°C 30 sec	95°C 30 sec
Annealing	50-65°C 30 sec	50-65°C 30 sec
Elongation	72°C 15 sec/kb	72°C 30 sec/kb
Final elongation	72°C 10 min	72°C 10 min

Table 2.8: The primers used in this study. Here, 'F' and 'R' stand for 'forward' and 'reverse' respectively.

Name code	Sequence (5' to 3')	Description
VIP4189 F	GGATGAACTATACAAAGGAGCAGGTGCGGGATCCATGAGTGAACAAGAATAACGAAGAC	Primers of PhaC1 from *P. mendocina* into *S. cerevisiae* with PTS1 and GFP
VIP4190 R	AATTGATCTATCGATAAGCTTTTATAATTTAGAATGTAATGGACCGTCGACGCGTTCGTGTACATAGGTGC	Primers of PhaC1 from *P. mendocina* into *S. cerevisiae* with PTS1 and GFP
VIP4191 F	GGCATGGATGAACTATACAAAGGAGCAGGTGCGGGATCCATGCGAGACAAGTCGAACCC	Primers of PhaC2 from *P. mendocina* into *S. cerevisiae* with PTS1 and GFP
VIP4192 R	AAAATTGATCTATCGATAAGCTTTTATAATTTAGAATGTAATGGACCGTCGACGCGGATATGCACGTAGGTGC	Primers of PhaC2 from *P. mendocina* into *S. cerevisiae* with PTS1 and GFP
VIP4256 R	AAAATTGATCTATCGATAAGCTTTTAGTCGACTCAGCGTTGGTGTACATAGG	Primers of PhaC1 from *P. mendocina* into *S. cerevisiae* with GFP without PTS1
VIP 4268 F	CTATACAAAGGAGCAGGTGCGGGATCCATGCGAGACAAGTCGAACCC	Primers of PhaC2 from *P. mendocina* into *S. cerevisiae* with PTS1 and GFP

VIP 4269 R	GAAAAAAATTGATCTATCGATAAGCTTTTATAATTTAGAATGTAATGGACCGTCGACGCGGATATGCACGTAGGTGC	Primers of PhaC2 from *P. mendocina* into *S. cerevisiae* with PTS1 and GFP
VIP 4270 R	AAAAATTGATCTATCGATAAGCTTTCAGCGGATATGCACGTAGG	Primers of PhaC2 from *P. mendocina* into *S. cerevisiae* with GFP without PTS1
VIP 4300 R	AAAAATTGATCTATCGATAAGCTTTCAGCGTTCGTGTACATAGG	Primers of PhaC1 From *P. mendocina* into *S. cerevisiae* with GFP without PTS1

Name code	Sequence (5' to 3')	Description
VIP4368 F	AACACATACATAAACGAGCTCGGATCCATGCGAGACAAGTCGAACCCG	Primers of PhaC2 from *P. mendocina* into *S. cerevisiae* without PTS1 and GFP
VIP4369 F	AAACACATACATAAACGAGCTCGGATCCATGAGTGACAAGAATAACGAAGAC	Primers of PhaC1 from *P. mendocina* into *S. cerevisiae* without PTS1 and GFP
VIP4423 F	ATACATAAACGAGCTCAAAATGAGTGACAAGAATAACGAAG	Primers of PhaC1 without stop-codon from *P. mendocina* into *S. cerevisiae* with PTS1 and without GFP
VIP4424 R	TTGATCTATCGATAAGCTTTTATAATTTAGAATGTAATGGACCGCGTTCGTGTACATAGGTGC	Primers of PhaC1 without stop-codon from *P. mendocina* into *S. cerevisiae* with PTS1 and without GFP
VIP4433 R	TTGATCTATCGATAAGCTTTCAGCGTTCGTGTACATAGG	Primers of PhaC1 with stop codon from *P. mendocina* into *S. cerevisiae* without GFP and PTS1
VIP4434 F	AAACACATACATAAACGAGCTCAAAATGCGAGACAAGTCGAATCC	Primers of PhaC2 without stop codon from *P. mendocina* into *S. cerevisiae* with PTS1 without GFP
VIP 4435 R	ATTGATCTATCGATAAGCTTTTATAATTTAGAATGTAATGGACCACGGATATGCACGTAGGTGC	Primers of PhaC2 without stop codon from *P. mendocina* into

		S. cerevisiae with PTS1 without GFP
VIP 4436 R	AAATTGATCTATCGATAAGCTTTCAACGGATATGCACGTAGGT	Primers of PhaC2 with stop codon from *P. mendocina* into *S. cerevisiae* without PTS1 and GFP

2.5.2 Agarose gel electrophoresis

PCR product, plasmid, digested plasmid and gel-extracted DNA samples were examined by agarose gel electrophoresis. Generally, 1% and 0.7% agarose gels were prepared by melting 0.5 g and 0.35 g of high-grade agarose powder respectively in 50 ml of 1x TAE (40 mM Tris-acetate, 1 mM EDTA), and adding ethidium bromide to a final concentration of 0.5 µg/ml. 6x loading buffer (0.25% bromophenol blue, 0.25% xylene cyanol FF, 30% (v/v) glycerol) was added to samples to give a 1x final concentration. A DNA marker (Bioline Hyper ladder I) was run alongside the DNA samples to estimate the size of DNA fragments. Gels were run in 1xTAE buffer at a constant voltage of 95V for 40 minutes. DNA bands were examined using an ultraviolet transilluminator imaging system (GeneSys).

2.5.3 Restriction digest

The restriction digest was performed using restriction endonucleases and carried out in a volume of 25 µl which contained 2.5 µl 10x NEB CutSmart™ Buffer, 1 µl each restriction enzyme required and 0.5-2 µg plasmid DNA. The volume was made up to 25 µl with dH2O. Restriction digests were prepared on ice and incubated at 37°C for a period varying from 2 hours to overnight.

2.5.4 DNA gel extraction

DNA was run on an agarose gel as detailed in Section 2.5.2 and visualised on a long wavelength UV transilluminator. The relevant DNA bands were excised from the gel using a sterile scalpel and gel extractions were performed using the QIAquick gel extraction kit (Qiagen) according to the manufacturer's instructions.

2.5.5 Ligation

Each ligation reaction was made in a final volume of 20 µl. A 3:1 insert: vector molar ratio was used with 50 ng digested, gel extracted vector added to the relevant amount of digested, gel extracted insert. The concentrations of nucleic acid samples were determined using a nanodrop spectrophotometer. To calculate the concentrations, the instrument was blanked with the corresponding buffer, and small aliquots (typically 2 µl) of each sample were pipetted onto the sample pedestal. The Nanodrop measured the concentration values of DNA. 2 µl 10x ligase buffer and 0.5 µl T4 DNA ligase (Promega) was added and the reactions were made up to 20 µl with dH2O. Ligation reactions were incubated for at least 2 hours at room temperature but were preferentially left overnight for optimal ligation and transformed into chemically competent *E. coli* cells the following day.

2.5.6 Homologous recombination-based cloning

Homologous recombination-based DNA editing in *S. cerevisiae* was employed for gene cloning, to introduce tag, gene or both into a vector. Target open reading frame was amplified by PCR using primers designed to anneal to the start and the end of a region of interest and to have 18-20 nucleotides as flanking regions identical to each side of the desired insertion sites in the vector. The vector was digested using restriction enzymes at the insertion site. PCR fragment and linearized vector were transformed into yeast by high efficiency yeast transformation (Section 2.7.3). Upon homologous recombination the vector is circularised, a procedure also referred to as gap-repair incorporating the PCR product (Figure 2.1). Recombinant plasmid carrying cells were identified by growth on selective yeast medium.

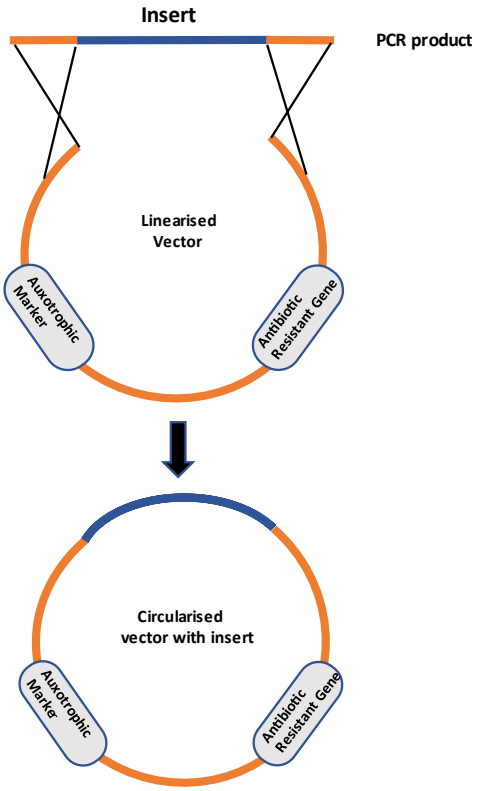

Figure 2.1 Construction of plasmid by homologous recombination in *S. cerevisiae*. PCR product consists of insert (blue) and nucleotide overhangs (orange) are about 18-20 nucleotide long. These overhangs are identical nucleotide sequences between the PCR product and a linearized plasmid. Once transformed into yeast the linearized vector and the PCR product undergo homologous recombination and that results in the circularised plasmid with insert.

2.5.7 Plasmid miniprep

E. coli DH5α cells with plasmid were grown overnight in 5 ml of 2TY medium containing an appropriate antibiotic. QIAprep Spin Miniprep Kit by Qiagen was used to perform Plasmid miniprep. 5 ml 2TY-ampicillin overnight culture was centrifuged for 3 minutes at maximum speed. Cells were resuspended in 250 µl of resuspension buffer. To lyse the cells, 250 µl of lysis buffer was added and immediately mixed by inverting the tube multiple times until the solution becomes clear. 350 µl of neutralisation buffer was then added and the tube was inverted thoroughly 4-6 times for mixing. Afterwards, the tube was centrifuged at highest speed for 10 minutes. To increase the efficiency, 250 µl of column preparation buffer was

added to the spin column, centrifuged for 1 minute, and discarded the flow-through. At this stage, 800 µl supernatant was transferred into spin columns, centrifuged for 1 minute at 13000 rpm and discarded the flow-through. 500 µl of binding buffer was added to the column and centrifuged at 13000 rpm for 1 minute. The column was washed with 750 µl of wash buffer, and plasmid eluted into a fresh Eppendorf tube with 50 µl of elution buffer by centrifugation for 1 minute at 13,000 rpm.

2.5.8 DNA sequencing

To confirm the sequence, plasmids were sequenced by Source Bioscience using their Sanger sequencing method. The obtained sequence data was analysed using SnapGene and ClustalW multiple sequence alignment online tool (http://www.genome.jp/tools-bin/clustalw).

2.6 *E. coli* protocols

2.6.1 Preparation of chemical competent *E. coli* DH5α cells

E. coli DH5α chemically competent cells were prepared by following the rubidium chloride method (Hanahan, 1983). *E. coli* DH5α cells were streaked out from -80°C, on a 2TY plate without antibiotics and incubated overnight at 37°C. The next day a single colony was inoculated into 5 ml of 2TY and grown overnight at 37°C on an oscillating shaker at 200 rpm. The following morning, after measuring OD600 of overnight culture, a secondary culture of 200ml 2TY in a 1 litre flask was prepared and inoculated with an OD600 of 0.05. Cells were grown at 37°C on an oscillating shaker at 200 rpm until OD600 reached 0.5 (mid-log phase), then placed on ice for 15 minutes. The culture was transferred from the flask into four 50 ml sterile falcon tubes and centrifuged at 4°C for 10 minutes at 3000 rpm. The supernatant was discarded, and the pellets were resuspended in 35 ml of RF1 described in Table 2.9. 2 tubes and left on ice for 15 minutes. The tubes were centrifuged at 3000 rpm for 10 minutes at 4°C as before. The supernatant was discarded and 8 ml of RF2 (Table 2.9) was used to resuspend each pellet before combining the two to make 16 ml. 200 µl aliquots were taken and put into pre-cooled Eppendorf tubes before flash freezing in liquid nitrogen and finally stored at -80°C.

Table 2.9: The components of the solutions RF1 and RF2. Required to produce chemically competent (RbCl) *E. coli* DH5α cells.

RF1 (pH 5.8)	RF2 (pH 6.8)
Rubidium Chloride (100 mM)	MOPS (10 mM)
Manganese Chloride (50 mM)	Rubidium Chloride (10 mM)
Potassium Acetate (30 mM)	Calcium Chloride (75 mM)
Calcium Chloride (10 mM)	15% (w/v) Glycerol
15% (w/v) Glycerol	

2.6.2 Production of electrocompetent *E. coli* cells

1L of 2TY medium was inoculated from overnight grown cells to start a secondary culture starting with OD600 0.05. The cells were grown at 37°C with shaking until OD600 0.5. The culture was divided between four 500 ml, sterile centrifuge buckets and left on ice to chill for 15 minutes. Subsequently, the cells were harvested by centrifugation at 3,000 rpm for 15 min using a pre-cooled Sigma 4-K15 centrifuge (12166-H rotor).

After harvesting, the supernatant was discarded, and the pellet was resuspended in 125 ml sterile 10% glycerol (ice-cold) and pooled two buckets together. The cells were harvested again as above, supernatant was poured off and cells were resuspended in 125 ml sterile 10% glycerol (ice cold). The harvesting was done for a third time and the cells were resuspended in 30 ml sterile ice cold 10% glycerol. After a final centrifugation, the supernatant was removed and both pellets were resuspended in 0.35 ml of ice cold sterile 10% glycerol and then combined to give a 0.7 ml suspension in 50 ml falcon tube. The cells were aliquoted out into 40 µl in each pre-cooled 1.5 ml Eppendorf tube followed by snap freezing in the liquid nitrogen and stored at - 80°C. All centrifugation steps were performed at 4°C.

2.6.3 Transformation of chemically competent *E. coli*

Chemically competent DH5α cells were removed from storage at -80°C and thawed on ice. 1 µl plasmid DNA or 10 µl ligation mixture was added to 50 µl or 100 µl cells respectively in an Eppendorf tube and mixed very gently by resuspending a few times. The tube was incubated on ice for 20-30 minutes. The cells were heat shocked in a water bath at 42°C for 2 minutes then placed back on ice for 5 minutes. 900 µl 2TY media was added and the tube was then incubated at 37°C for 30-45 minutes. The tube was centrifuged at 8,000 rpm for 1 minute and 850 µl supernatant was removed leaving about 50 µl 2TY media and cells. The cells were resuspended gently then plated onto 2TY agar media with the appropriate antibiotic and incubated overnight at 37°C.

2.6.4 Transformation of electrocompetent *E. coli*

40 µl of *E. coli* DH5α electrocompetent cells were removed from storage at -80°C and thawed on ice. 10 µl of 10x diluted gDNA was added to the electrocompetent cells and the reaction mixture was transferred to a 2 mm electroporation cuvette (Fisher) on ice. The cuvette was placed in the electroporation chamber on the electroporator (MicroPulser by BIORAD), and the cells were electroporated using the setting EC2 (V=2.5kV). 600 µl 2TY was added immediately, resuspended 2-3 times and transferred to a fresh 1.5 ml Eppendorf tube. Subsequently, the tube was incubated at 37°C for 30 minutes. The tube was then centrifuged for 5 minutes at 5000 rpm, and the supernatant was removed. The cell pellet was plated onto 2TY agar plate with the appropriate antibiotic and incubated overnight at 37°C before being stored at 4°C.

2.7 *S. cerevisiae* protocols

2.7.1 Yeast growth and maintenance

Yeast strains were grown at 30°C on either solid media or in liquid media on an oscillating shaker at 200 rpm. Amino acids were added to media for auxotrophic strains as required.

2.7.2 One step transformation

Yeast strains were transformed with plasmid DNA using the One Step method (Chen *et al.,* 1992). Cells were inoculated into 3 ml of appropriate media (commonly YPD) and grown on a shaker at 200 rpm for overnight at 30°C. The following day, 200 µl of the culture was harvested by centrifugation for 1 minute at 12,000 rpm in an Eppendorf tabletop centrifuge. The supernatant was then removed and 1 µl plasmid DNA (100ng-400ng), 5 µl (50 µg) of single stranded DNA (ssDNA) from Salmon sperm and 50 µl one step buffer (0.2M LiAc pH 5.0, 40% (w/v) PEG 4000 (polyethylene glycol), 0.1M DTT) were added to the cell pellet and mixed by vortexing. The tube was incubated at room temperature for several hours (usually 3-5 hours) with occasional vortexing. The tube was heat shocked afterwards, for 30 minutes at 42°C in a water bath, vortexed again, finally the cell suspension was plated onto relevant selective solid media. Plates were incubated for 2-3 days at 30°C to obtain transformants.

2.7.3 High efficiency transformation

High efficiency yeast transformations were performed to create plasmids according to the Lithium Acetate protocol (Gietz and Woods, 2002) using the chemicals listed in Table 2.10. Yeast strains were grown overnight in 3 ml YPD liquid medium at 30°C with shaking at 200 rpm. The next morning, the optical density (OD600) of the culture was measured in a Jenway spectrophotometer at 600nm wavelength and the appropriate amount of overnight culture was added to 5 ml YPD to give an OD of 0.1. Cells were grown at 30°C on an oscillating shaker at 200 rpm until they reached exponential phase (OD600=0.5). The cells were then centrifuged at 2500 rpm for 5 minutes at room temperature and the supernatant was discarded. The pellet was washed in 1 ml sterile water, centrifuged as before then washed in 1 ml 1xTE/LiAc solution. The supernatant was completely removed, and the pellet was resuspended in 50 µl 1xTE/LiAc. 5 µl digested vector (0.2-0.5 µg), 5 µl PCR product, 5 µl (50 µg) ssDNA and 300 µl 40% PEG 4000 was added to 50 µl resuspended pellet in an Eppendorf tube. Vector was linearized for overnight (500 ng vector, 0.5 µl restriction enzyme, 2.5 µl 10X buffer, and water was added to achieve final volume of 25 µl). The reaction was left at room temperature for 30 minutes, incubated at 30°C for 30 minutes then heat shocked in a 42°C water bath for 15 minutes. The cells were harvested by centrifuging for 30 seconds at 8000 rpm, the supernatant discarded, and the pellet resuspended in 50 µl 1xTE. The cells were then plated on selective agar media and incubated for 2-3 days at 30°C.

Table 2.10: Components of the solutions required for high efficiency yeast transformation.

Solution	Reagents
1xTE/Lithium Acetate solution	1 ml 10x TE (0.1M Tris-HCl and 0.01M EDTA) (pH 7.4) 1 ml 1M Lithium Acetate solution (pH 7.5) 8 ml dH20 (for 10 ml).
40% Polyethylene Glycol solution	500 µl of 10X TE, 500 µl of LiAc, 4 ml of 50% PEG 3350 (for 5 ml).
1x TE	1 ml 10xTE, 9 ml dH_20
10X TE	100 mM Tris pH8.0, 10 mM EDTA pH8.0

2.7.4 Yeast genomic DNA isolation

S. cerevisiae (BY4741) cells were grown overnight in 5ml YPD media. The cells were then harvested by centrifugation in 2ml screw cap tubes, pellet on pellet at 12000 rpm for 1 minute and removed supernatant. The pellet was resuspended in 1ml sterile water and centrifuged at12000 rpm for 1 minute.

After the supernatant was poured off, cells were re-suspended in remaining volume, and 200 ul TENTS solution (20 Mm Tris-Cl pH 8, 1 mM EDTA, 100 mM NaCl, 2% Triton 100X, 1% SDS), 200 µl 0.5 mm diameter glass beads and 200 µl phenol/chloroform were added into the tube. The tube was put into a bead beater and beaten sample for 45 seconds at high speed. Afterwards, the sample was centrifuged at 12000 rpm for 30 seconds followed by adding 200 µl TENTS, vortexed and spun at 12000 rpm for 5 minutes. Supernatant was transferred into a new 1.5 ml tube, 200 µl phenol/chloroform was added, vortexed and centrifuged for 5 minutes at 12000 rpm. After spinning, 300 µl supernatant was transferred into a new 1.5 ml tube, where DNA was precipitated by adding 30 µl 3M NaAc pH 5.2 along with 825 µl 100% ethanol. The tube was vortexed and left on ice for 15 minutes followed by centrifuged at 12000 rpm for 15 minutes.

After removing the supernatant, pellet was washed in 300-500 µl 70% ethanol and centrifuged at maximum speed for 5 minutes and supernatant was again removed. The pellet was then dissolved in 200 µl 1X TE+ RNase mixture (1 µl RNAse (10 mg/ml) per 100 µl TE) and

incubated at room temperature for 10 minutes. Thus, DNA was precipitated and air dried. The dry pellet was then re-suspended in 50 ul 1X TE and stored at -20.

2.7.5 Fluorescence microscopy

Cells were visualised and analysed with an epifluorescence microscope (Axiovert 200M; Carl Zeiss, Inc.) equipped with band-pass filters (Carl Zeiss, Inc. and Chroma), Exfo X-cite 120 excitation light source, a digital camera (Orca ER; Hamamatsu Phototonics), a Plan-Fluar 100x/1.45 NA or Plan-Apochromat 63x 1.4 NA objective lens (Carl Zeiss, Inc.). Image acquisition was performed using Volocity software (PerkinElmer). Fluorescence images were routinely collected as 0.5 µm z-stacks and processed further in ImageJ/FIJI. Brightfield images were processed where necessary to highlight the circumference of cells in magenta.

2.7.6 Bioinformatics analysis

NCBI, UniProt, Addgene, *Saccharomyces* Genome Database (SGD) were researched as the vital source for all DNA and protein sequences, gene and protein functions, regulations, expressions, and interactions.

2.8 PHA Synthesis

For the PHAs production experiment, yeast strains were initially transformed with plasmid DNA using the One Step method and grown for 2 days, the cells were then inoculated on YM2 selective media with 2% glucose as a pre-culture media and shaken at 200 rpm overnight at 30°C.

Overnight cultures of cells were inoculated in PHA production media in Erlenmeyer/Conical flasks with orbital shaking of 200 rpm at 30°C. In order to improve PHAs synthesis, different production media, inoculation concentration, media volume, and experimental length were employed. The procedure was repeated with different production media (see table 2.13) and volume (50, 100, 200, 600 ml), several inoculation concentrations (10, 15, 20 OD600nm) and cultivation period (2, 3,4, 6 days) to optimise PHAs production. At the end of the step, the whole culture was harvested and centrifuged. Collected cell pellets were washed with distilled water before freezing at -80°C and subsequently freeze dried for 24 hours.

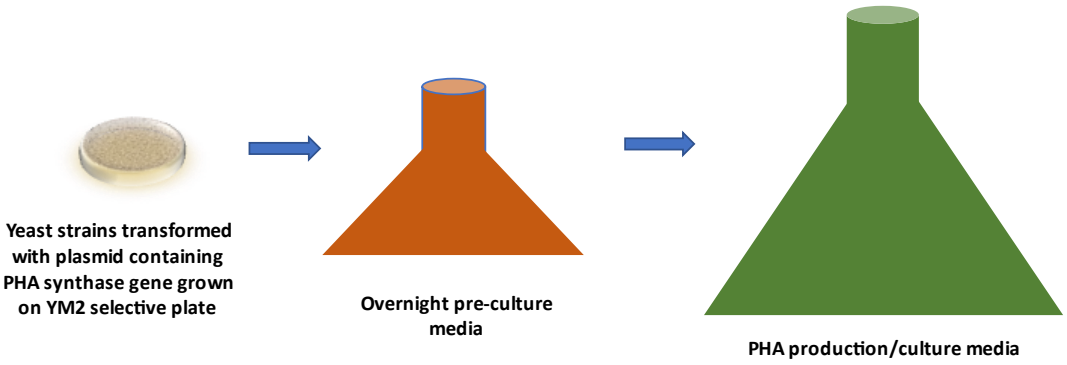

Figure 2.2: Schematic presentation of PHA production stages. Yeast strain transformed with plasmid containing PHA synthase gene was grown on selective YM2 plates and cells were then inoculated in pre-culture media for overnight to achieve a high concentration of cells (dark orange flask). Afterwards, the culture was used to inoculate PHA production media to accumulate PHA (green flask).

Table 2.11: Reagents required for PHA production experiments.

Solution	Reagents
Oleate media	0.5% ammonium sulphate, 0.2% yeast nitrogen base without amino acids and ammonium sulphate, 1% casamino acid, 0.2% (v/v) Tween-80, 0.12% (v/v) oleate, 400 µl NaOH and 50 mM phosphate buffer combined in dH2O to 900 ml using a magnetic stirrer, then autoclaved. 0.3% (v/v) glucose and 1% (v/v) leucine and tryptophan added after autoclaving.
Glucose media	0.5% ammonium sulphate, 0.2% yeast nitrogen base without amino acids and ammonium sulphate, 1% casamino acid, 2% glucose, 400 µl NaOH and 50 mM phosphate buffer combined in dH2O to 900 ml using a magnetic stirrer, then autoclaved. 1% (v/v) leucine and tryptophan added after autoclaving.

Minimal media	0.25% ammonium sulphate, 6% glucose, 400 µl NaOH and 50 mM phosphate buffer combined in dH2O to 900 ml using a magnetic stirrer, then autoclaved. 1% (v/v) leucine, 1% (v/v) tryptophan, 0.2% yeast nitrogen base without amino acids and ammonium sulphate dissolved in 100 ml dH2O, filtered and added 10 ml to media after autoclaving.
YPO media	2% Bacto-peptone, 1% yeast extract, 0.2% (v/v) Tween-80, 0.12% (v/v) oleate, 400 µl NaOH and 50 mM phosphate buffer combined in dH2O to 900 ml using a magnetic stirrer, then autoclaved.

Solution	Reagents
Mineral salt media 1	2% glucose, 0.07% ammonium sulphate, 1% disodium phosphate, 0.27% monopotassium phosphate, 0.015% calcium chloride, 0.01% magnesium chloride, 0.1% fatty acid (oleic acid), 0.2% detergent Tween 80, combined in dH2O to 450 ml using a magnetic stirrer, then autoclaved. 1% (v/v) leucine and tryptophan added after autoclaving. Throughout the process, a pH of 6 was automatically maintained by adding 10M NaOH.
Mineral salt media 2	0.05% ammonium sulphate, 0.46% disodium phosphate, 0.4% monosodium phosphate, 0.2% yeast nitrogen base without amino acids and ammonium sulphate, 0.2% decanoic acid, 1% yeast extract combined in dH_2O to 450 ml using a magnetic stirrer, then autoclaved. 0.3% (v/v) glucose and 1% (v/v) leucine and tryptophan added after autoclaving. Throughout the process, a pH of 6 was automatically maintained by adding 10M NaOH.
Mineral salt media 3	0.054% urea, 0.46% disodium phosphate, 0.4% monosodium phosphate, 0.2% yeast nitrogen base without amino acids and ammonium sulphate, 0.5% dodecanoic acid, 0.1% oleic acid, 0.2% detergent Tween 80% combined in dH_2O to 450 ml using a magnetic stirrer, then autoclaved. 0.3% (v/v) glucose and 1% (v/v) leucine and tryptophan added after autoclaving. Throughout the process, a pH of 6 was automatically maintained by adding 10M NaOH.

Nitrogen deficient media	0.46% disodium phosphate, 0.4% monosodium phosphate, 0.2% yeast nitrogen base without amino acids and ammonium sulphate, 0.5% dodecanoic acid, 0.1% oleic acid, 0.2% detergent Tween 80%, combined in dH_2O to 450 ml using a magnetic stirrer, then autoclaved. 0.3% (v/v) glucose and 1% (v/v) leucine and tryptophan added after autoclaving. Throughout the process, a pH of 6 was automatically maintained by adding 10M NaOH.

2.9 Protein Procedures

2.9.1 TCA protein extraction

To confirm the expression of PhaC1 and PhaC2 in yeast cells and check for protein truncation, protein samples for western blotting were prepared by resuspending the 15 OD600nm samples in 0.2M NaOH and 0.2% β- mercaptoethanol in order to cell lysis and left the mixture on ice for 10 minutes. Subsequently, 71 µl of 40% (w/v) TCA (Trichloro acetic acid) solution was added for protein precipitation and left on ice again for 10 minutes. Samples were then centrifuged at 4°C for 5 minutes at 13,000 rpm and the supernatant was removed leaving the precipitated protein. The pellet was neutralised in 1M Tris Base (pH 9.4). Then 90 µl of 1x PLB was added to above mixture and boiled for 10 minutes at 95°C. Sample were ready to use for SDS-PAGE.

Protein loading dye (4x): 250 mM Tris pH 6.8, 9.2% (w/v) SDS, 40% (w/v) Glycerol, 0.2% (w/v) Bromophenol brilliant blue, 100 mM DTT.

2.9.2 SDS-PAGE

Sodium Dodecyl Sulphate Polyacrylamide Gel Electrophoresis (SDS-PAGE) was performed for protein separation as described by (Sambrook and Russell, 2006). 10% gels were prepared using the reagents shown in Table 2.12. When the gel polymerised and was ready for loading, 10 µL of each protein sample was loaded onto the SDS-PAGE gel for analysis. 3 µl of CSL-BBL Tris-Glycine 4-20% pre-stained protein ladder was loaded onto each SDS-PAGE gel. All empty gel lanes were loaded with 10 µL of PLB. Once loaded, the gel was run at 100V through stacking, then increased to 130V for through resolving in Tris-Glycine-SDS running buffer.

Protein running buffer (10X): 30.28 g Tris Base, 144.13 g Glycine, 1% (w/v) SDS, dH20 up to 1L.

Table 2.12: SDS-PAGE gel reagents.

Chemicals	Resolving gel (10%)	Stacking gel (4%)
Protogel (0.8% bisacrylamide solution, 30% acrylamide)	3.3 ml	0.65 ml
Resolving buffer (0.4% SDS, 1.5M Tris-HCl) (pH 8.8)	2.6 ml	_
Stacking buffer (0.4% SDS, 0.5M Tris-HCl) (pH 6.8)	_	1.25 ml
10% Ammonium persulfate (APS)	100 µl	50 µl
Tetramethylethylenediamine (TEMED)	10 µl	5 µl
dH20	4.1 ml	3.05 ml

2.9.3 Western blot analysis

Protein samples were separated by SDS-PAGE and transferred from the gel to a nitrocellulose membrane. Bio-Rad Mini Trans-Blot Electrophoretic Transfer apparatus was used for protein transfer at a constant current of 200 Milliamps (mA) for 2 hours in western blot transfer buffer. After transfer, a ponceau stain was used to check the presence of protein and equal loading. To prevent non-specific antibody binding, membrane was blocked with 15 ml of 2% milk in 1X TBS-T for 1-hour rocking at room temperature or overnight at 4°C. The membrane was rinsed several times with TSB-T buffer and a 1:3000 dilution of the anti-GFP primary antibody was added and incubated rocking at room temperature for 1 hour. The primary antibody was discarded, and the membrane washed multiple times with TSB-T. The secondary antibody (goat anti-mouse) was then added and incubated rocking at room temperature for 1 hour. After a final wash with TBS-T, blots were developed using Enhanced Chemi-Luminescence (ECL) substrates and tagged proteins were detected and imaged using multiple long exposures in the Syngene GBox imaging system.

Table 2.13: Reagents required for western blotting.

Solution	Reagents required
Transfer buffer	15.13 g Tris Base, 56.25 g Glycine, 4L dH2O, 1L Methanol.
TBS 10X	24.23 g Tris HCl, 80.06 g NaCl mix in 800 ml ddH2O. Adjust pH to 7.6 with HCl and top up to 1 L.
TBST	To make 1 L: 100 ml of 10X-TBS in 900 ml ddH2O with 1 ml Tween20.
1X Ponceau stain	0.1% (w/v) Ponceau S in 5% (v/v) acetic acid
Primary anti-GFP antibody	1:3000 (3 µl in 10 ml TBS-T buffer)
Secondary goat anti-mouse antibody	1:4000 (2.5 µl in 10 ml TBS-T buffer)

2.10 Nile red analysis

Nile red assay was carried out in this study to serve as an independent and qualitative indicator of intracellular PHAs content (Zuriani *et al*., 2013). At the beginning, recombinant yeast cells were grown in PHAs production media until late stationary phase. Cells were then harvested and stained with Nile red to perform Nile red assay.

Primary stock of Nile red stain was prepared earlier by adding 10 mg of Nile red to 10 ml of dimethyl sulfoxide (DMSO), making the concentration 3.14 µmole/ml. A secondary stock of Nile red dye was prepared with a final volume of 1000 µl with the concentration of 0.4 µmole/ml by adding 128 µl from primary stock with 872 µl DMSO. Subsequently, 20 µl from secondary stock of Nile red was added to 1 ml of cell suspension and vortexed vigorously. An aliquot of suspension was pipetted into a black 96-well microplate. The fluorescence intensity was measured at excitation and emission wavelength 535 nm and 605 nm respectively

(Zuriani *et al*., 2013) using SkanIt software in a Thermo Scientific Varioskan multimode microplate reader.

2.11 Rice wastewater production

This study investigated the utilization of rice wastewater as a substrate for the culture of engineered yeast to produce biomass and PHAs to establish a cost-effective and sustainable strategy.

To begin, raw rice grains were soaked in water to soften the outer husk. The soaking time typically took 6-8 hours. After soaking, the rice was drained and loaded into a large pot, where it was boiled for about 20-30 minutes. Once the rice boiling process was completed, the wastewater produced during soaking and parboiling was autoclaved to investigate the potential of utilizing rice waste effluent as a low-cost substrate to grow recombinant yeast capable of producing biomass and PHAs.

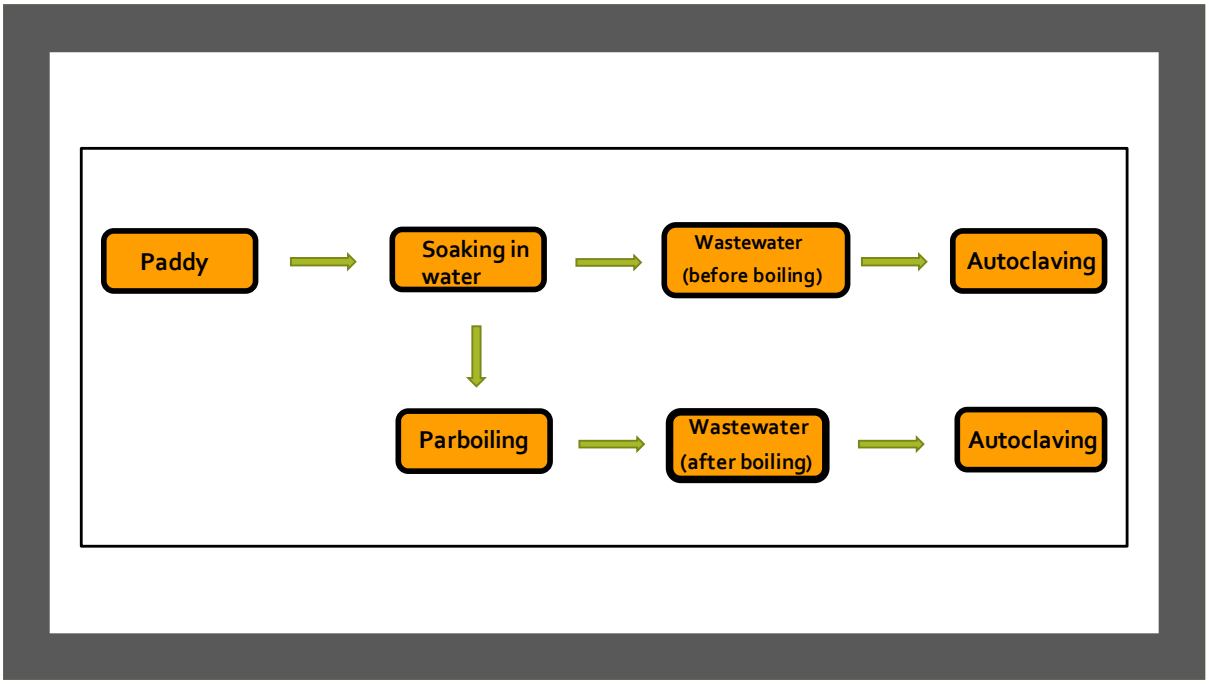

Figure 2.3: Flow chart shows the steps followed for generating rice wastewater in this study.

Through the optimisation of fermentation parameters, such as temperature, pH, and nutrient availability this study explored the potential of PHAs production by the engineered yeast cultivated in rice waste effluent. To enhance the nutrient content, several supplements were added to rice wastewater before cultivation and details are in Table 2.14. The inoculum was prepared transferring a colony of *S. cerevisiae* to YM2 selective media and cultivated at 200 rpm in shaker and 30 °C for overnight as pre-culture step. The cultivation was performed in conical flasks of 250 ml, containing 50 ml of parboiled effluent (PE), inoculated with 10% (v/v) of *S. cerevisiae* and agitated at 200 rpm for 48 hours, samples were taken periodically to determine cell growth by optical density. The pH in PE was found 5.8 before autoclaving which was preferrable for *S. cerevisiae* as it is an acidophilic organism. Finally, the whole culture was harvested and centrifuged. Collected cell pellets were washed with distilled water before freezing at -80°C and subsequently freeze dried before analysis for 24 hours.

Table 2.14: Different treatment and specific supplements added to rice wastewater in this study.

Treatment	Supplementation
Rice wastewater only	N/A
Rice wastewater + Glucose	Glucose was added at a final concentration of 10 g/L, mixed with a magnetic stirrer and sterilized at 121°C for 20 minutes using an autoclave.
Rice wastewater + Yeast extract	Yeast extract was added at a final concentration of 10 g/L, mixed with a magnetic stirrer and sterilized at 121°C for 20 minutes using an autoclave.
Rice wastewater + Glucose + Yeast extract	10 g/L glucose, 10 g/L yeast extract mixed with rice wastewater and sterilized at 121°C for 20 minutes using an autoclave.
Rice wastewater + Amylase	Amylase was added after sterilisation of rice wastewater (at 121°C for 20 minutes) using an autoclave, at a final concentration of 0.2 g/L, mixed with a magnetic stirrer.

2.12 Inductively Coupled Plasma Spectroscopy

Analysis was conducted using an Agilent 7500ce ICP-MS instrument with shield torch in hot plasma (no reaction gas) mode. Samples were diluted by a factor of 2, 10 or 100 and then filtered using Whatman Filter Paper No 540. Sample introduction used a MiraMist (Agilent) nebulizer and a pump speed of 0.3 revolutions per second. The argon carrier gas flow rate was 1.05 L/min. Acquisition was in spectrum mode with a 0.1s integration time for low level elements or 0.01s for more concentrated elements with 3 replicates. The masses were mostly selected based on the manufacturer's recommendation, which intends to maximise the intensity of the signal, by using the more abundant isotope, whilst avoiding isometric and common polyatomic interferences. Commercially available certified reference materials (Sigma-Aldrich/Supelco TraceCERT Standard for ICP; Fisher scientific Spex Certiprep standards; VWR/BDH inorganic reference standard) were used for calibration and were made up using 1% nitric acid. For the calibrations, the commercial standards were diluted to about 4-5 different concentrations around the level expected in the sample dilutions. These solutions were run on the ICP-MS and a calibration curve was produced. This curve was used to calculate the concentration in the samples.

2.13 NMR

2.13.1 NMR Sample preparation

This protocol was developed based on a published chloroform-sodium hypochlorite dispersion method. To extract PHAs as treatment with sodium hypochlorite alone can cause severe degradation resulting in molecular weight reduction of PHAs, so chloroform was used as a shield to prevent degradation (Hahn *et al*., 1993). 0.7 ml 5% (v/v) sodium hypochlorite solution and 1 ml of deuterated chloroform ($CDCl_3$) were added to each sample of freeze-dried cells. Subsequently, the mixture was vortexed for 10 minutes and incubated on a shaker at 200rpm for two hours to overnight at 30°C. After extraction, samples were centrifuged at 1500xg for 10 minutes to induce phase separation and obtained three separate phases after centrifugation. The upper phase was hypochlorite solution, the middle phase contained some undisrupted cells, and the bottom phase was chloroform containing polymer. The bottom organic layer of $CDCl_3$ was removed and transferred to a 5mm NMR tube.

2.13.2 NMR analysis

To determine the presence of polyhydroxyalkanoates in engineered yeast, NMR spectra were measured in Chloroform-d (CDCl3). NMR experiments were conducted on a Bruker DRX-600 spectrometer at 298 K operating Topspin 4.0.5 on mag5. All samples were tuned and shimmed, and the 90° pulse length was set automatically using spectrometer routines. Typical 1D spectra were acquired into 32768 points (acquisition time 1.70 s) with 64 scans, taking approximately 5 minutes per spectrum. TOCSY spectra were acquired using the Bruker dipsi2etgp pulse program, with 256 increments of 2048 points. HSQC spectra were acquired using the Bruker hsqcetgpsisp2.2 pulse program, with 250 increments of 1600 points.

2.14 Methanolysis of Polyhydroxyalkanoates samples for GC analysis

The determination of low concentrations of polymers using Gas Chromatography is superior to other methods (Braunegg *et al*., 1978). 2 ml of chloroform was added to 10-20 mg of freeze-dried cell pellets and vortexed. Subsequently, 2 ml of methanolic sulphuric acid was added to the mixer and vortexed again. Secure the tube with the cap. Methanolic sulphuric acid was prepared with an 85:15 ratio of methanol to sulphuric acid. The mixing should be done slowly on an ice bath inside a fume hood due to the exothermic reaction. The ratio of methanolic sulphuric acid should be 1:1 with the samples for methanolysis.

The tubes were heated at 100 °C for 4 hours in a heating block and shaken intermittently in the first three 10 minutes. After cooling the tubes at room temperature, 2 ml of distilled water was added to the mixture. The mixture was vortexed generously and incubated for an hour, or ideally overnight to form separate layers. The organic layer at the bottom part was collected using a Pasteur pipette the next day and transferred it into another vessel containing around 10 mg of sodium sulphate to dry.

4 µl of methyl benzoate was pipetted into 1996 µl of chloroform to make 0.2% (v/v) or 2000 mg/l concentration of methyl benzoate stock solution. The stock solution was added to the methanolized samples as an internal standard. Finally, the organic phase containing the resulting methyl ester group was transferred into GC vials for analysis by GC spectrophotometer.

2.15 Gas Chromatography

The analytical instrumentation used for this experiment was the Perkin Elmer XL autosampler. The chromatographic column, Zebron ZB-5plus capillary GC column, which is known for its performance characteristics in gas chromatography was chosen for the analysis. The injection volume was precisely set at 0.5 µl to ensure precision and reproducibility in the sample introduction. The temperature program in the chromatographic oven commenced at 60°C and remained there for 3 minutes. Afterward, a controlled temperature ramp was initiated, increasing at a rate of 10°C per minute until reaching a final temperature of 230°C. The system was then maintained at this final temperature for a further 2 minutes. To facilitate the transportation of the components in a sample through the chromatographic column, hydrogen gas was employed as the carrier gas.

2.16 Statistical analysis

The statistical significance of the data analysis was evaluated using one-way ANOVA with the Brown-Forsythe test in GraphPad Prism 10, which enabled us to determine whether there were any significant differences between the test and control samples. The p-value less than 0.0001, obtained from this test was used to determine the level of significance between the samples.

Chapter 3: Expression of PHA synthase from *P. mendocina* in various locations of *S. cerevisiae* cells

3.1 Introduction

Polyhydroxyalkanoates (PHAs) illustrate a family of biopolymer compounds with vast potential as sustainable alternatives to traditional plastics. The biodegradable and biocompatible polymers have attracted considerable attention from researchers for addressing the environmental and sustainability challenges posed by conventional petrochemical-originated plastics (Zhang *et al*., 2006). These polymers are synthesized and accumulated by numerous microorganisms as intracellular granules for carbon and energy storage under nutrient-deficient conditions (Zhang *et al.,* 2006). PHAs exhibit similar properties to those of conventional plastics but are environmentally friendly and can be degraded by microorganisms. The purified plastic has a wide range of applications from green packaging, coating, and production of biodegradable bulk commodities such as bottles, containers, and higher value medical products for instance stents, drug delivery constructs, implants, medical devices, and tissue engineering scaffolds (Muneer *et al*., 2020).

PHA production involves the intricate interaction of various enzymatic processes, integrating the key enzyme known as PHA synthase (Meng, D.C *et al*., 2014). To catalyse the polymerisation of hydroxy acyl-CoA substrates to PHA chains, the key enzyme PHA synthase is essential. PHA synthase has specificity towards several substrates and its regulation plays a crucial role in defining the polymer composition (Meng, D.C *et al*., 2014). PHA synthase is classified based on substrate specificity along with the molecular weight of the produced polymer. PHA synthase, prevalent in *Pseudomonas mendocina*, which is a gram-negative, soil-dwelling bacterium, belongs to the *Pseudomonas* genus, known for its remarkable metabolic versatility and adaptability to various environmental conditions. *P. mendocina* has been extensively studied due to its capacity to degrade a wide range of organic compounds. Additionally, it has garnered attention in biotechnology for its ability to produce polyhydroxyalkanoates (PHAs). In *P. mendocina*, there are two key enzymes that play pivotal roles in PHA biosynthesis, known as PhaC1 and PhaC2. These enzymes are responsible for the polymerization of hydroxyalkanoate monomers into PHA chains. The ability of *P. mendocina* to produce PHAs via PhaC1 and PhaC2 has led to investigations into optimizing PHA production for numerous applications (Mozejko-Ciesielska *et al.,* 2019). While they share similarities, there are notable differences between PhaC1 and PhaC2 in terms of their structural characteristics, substrate specificity, and regulatory roles (Mezzolla *et al*., 2018). PhaC1 and PhaC2 differ in their structural features. These distinctions are often manifested in the catalytic domains responsible for polymerization. Structural studies have revealed

variations in the active sites and binding regions of these enzymes, indicating that they may interact differently with hydroxyalkanoate substrates. Substrate specificity is a key point of differentiation between PhaC1 and PhaC2. These enzymes often exhibit preferences for specific types of hydroxyalkanoate monomers. PhaC1 may favour certain monomers over others, and its substrate specificity might differ from that of PhaC2 (Chen *et al.,* 2006; Mezzolla *et al*., 2018). PhaC2 is capable of incorporating both short-chain-length 3-hydroxybutyrate and medium-chain-length 3-hydroxyalkanoates (mcl 3HA) into PHA, while PhaC1 displays a preference for mcl 3HA for polymerization. PhaC1 exclusively utilizes mcl 3HA as a substrate for PHA biosynthesis, whereas PhaC2 can accommodate both mcl 3HA and short-chain-length 3-hydroxybutyrate (Chen *et al*., 2006). This selectivity plays a crucial role in determining the composition and properties of the resulting PHA polymer. Furthermore, PhaC1 and PhaC2 enzymes may have different regulatory mechanisms and expression patterns within microbial cells. The regulation of PHA synthesis is often linked to cellular metabolic states and environmental conditions.

Most of the research regarding PHA has highlighted prokaryotic organisms because of their inherent PHA production capability. Nonetheless, eukaryotic organisms such as *Saccharomyces cerevisiae* offer a distinctive platform to produce PHA due to robust genetics, ease of cultivation, established metabolic pathways, and the potential to compartmentalise the production of PHA in distinct cellular organelles. This study aims to explore the expression of the PHA synthase gene from *P. mendocina* in different compartments of *S. cerevisiae* such as peroxisome and cytosol in order to manipulate substrate availability, precursor utilisation, and protein localisation. The engineering of the PHA synthase gene from *P. mendocina* in *S. cerevisiae* involves a set of molecular biology and genetic engineering techniques such as gene cloning, selection of promoter and terminators, plasmid construction followed by transformation. Subsequent experiments encompass the strategies employed to produce PHA in various media and quantification.

Engineering the PHA synthase gene from *P. mendocina* into *S. cerevisiae* offers a distinct opportunity to explore the production of polymer in the eukaryotic system. It also provides some advantages of exploring inexpensive and sustainable carbon sources, for instance, rice wastewater for engineered yeast that would harvest the polluting constituents present in the waste stream and incorporate them during growth. These endeavours could lead the way for the development of holistic approaches to PHA biosynthesis in the eukaryotic host and would add value to the waste stream.

3.2 Construction of plasmids

The successful expression of the PHA synthase genes, PhaC1, and PhaC2 from *P. mendocina* within *S. cerevisiae* targeting both peroxisomes and cytosols, required meticulous design and construction of a series of plasmids to facilitate the expression and targeted localisation. This section outlines the plasmid construction strategies implemented for this study.

The genomic DNA (gDNA) from the Gram-negative bacterium*, P. mendocina* was purified by following the steps (Chapter 2, Section 2.4) described in the Cold Spring Harbor protocol (Green and Sambrook, 2017). In the beginning, gDNA isolated from *P. mendocina* was employed as a template to expedite the amplification of both genes, PhaC1 and PhaC2 that encode PHA synthase. The process of amplification was carried out utilising the Polymerase Chain Reaction (PCR) technique with gene-specific primers designed to incorporate restriction enzyme recognition sites, along with introducing overhangs that were complementary to the expression vector, pEW355 (Figure 3.1). To incorporate the PHA synthase gene into the vector plasmid pEW355, we employed restriction enzymes, BamHI-HF and HindIII-HF to excise the GRD19 open reading frame (ORF) to allow the insertion of the PHA synthase gene (Figure 3.1). For creating plasmids without GFP protein, the vector plasmid was linearised with restriction enzymes SacI-HF and HindIII-HF to remove ORF and GFP genes from the plasmid. We introduced finally the linearised vector pEW355 and suitable PCR fragments into wildtype (WT) *S. cerevisiae* (YEH703) exploiting the High-Efficiency Yeast transformation technique to accomplish homologous recombination (Figure 3.2).

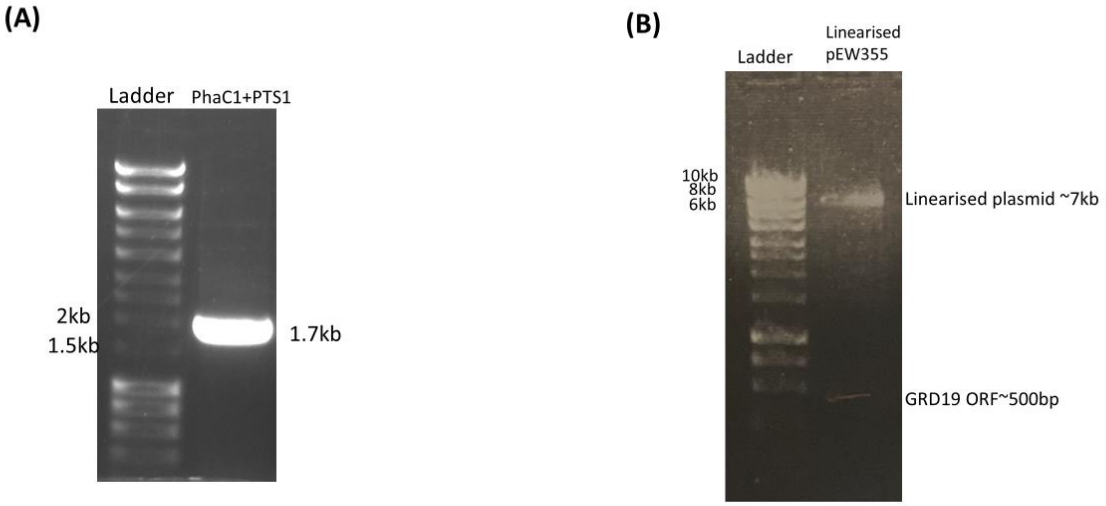

Figure 3.1: (A) The agarose gel image illustrates the results of a polymerase chain reaction (PCR) targeting the PhaC1 ORF (Open Reading Frame) with specific primers designed to include the Peroxisomal Targeting Signal 1 (PTS1) sequence. The amplification aims to confirm the presence of the PhaC1 gene with the specific PTS1 sequence. The presence of clear and well-defined band along with expected size (1.7kb) confirms the successful amplification of the PhaC1 ORF with the inclusion of the PTS1 sequence. **(B)** Agarose gel electrophoresis depicting the digestion of the plasmid vector pEW355 with BamHI and HindIII restriction enzymes to remove ORF. This resulted in a linearized plasmid of approximately 7kb, which was then prepared for PhaC1 insertion.

S. cerevisiae vector plasmid, pEW355 was chosen because it is a CEN/ARS1 plasmid that contains both yeast centromere sequence and an autonomous replication sequence derived from yeast chromosomes to be useful for cloning and expression of genes in yeasts. Additionally, pEW355 has the capability of driving strong gene expression containing TPI and PGK1 as promoter and terminator respectively. The TPI promoter is a well characterised and strong constitutive promoter available for expression in *S. cerevisiae*. The TPI promoter is derived from the gene encoding triose phosphate isomerase, an abundant glycolytic enzyme in yeast and other organisms (Ralser *et al*., 2006). It can drive the transcription of both the antibiotic-resistant gene along with gene of interest in a hybrid vector. The TPI promoter is stable and consistent, as it does not depend on external factors or inducers for its activity and ensures continuous expression of the inserted gene in yeast cells (Ralser *et al.,* 2006).

Therefore, the TPI promoter was the suitable choice for this study which required constant expression of a heterologous gene in yeast cells. Restriction sites were chosen based on compatibility with the expression vector, pEW355, and downstream localisation. The complementary overhangs allowed the genes to be introduced into the linearised vector by the homologous recombination method (Figure 3.2).

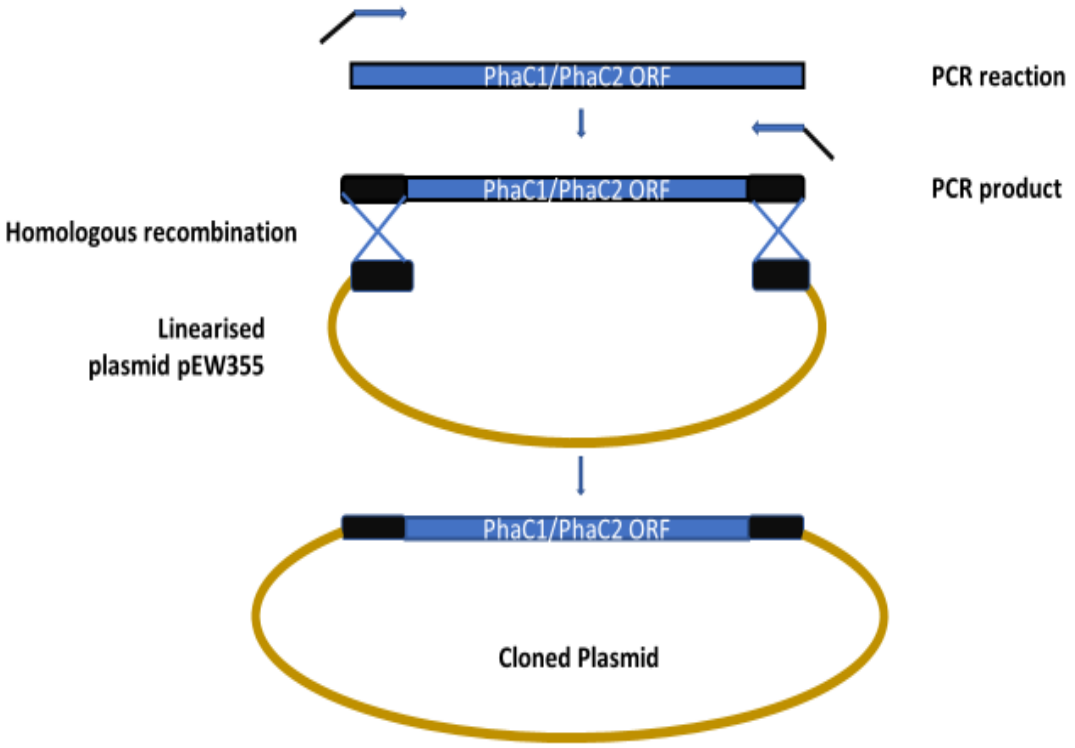

Figure 3.2: Plasmid reconstruction in *S. cerevisiae* by homologous recombination.
SnapGene-designed primers contain a nucleotide extension marked with arrows, which is identical between a linearised plasmid (pEW 355), and the PCR product shown in black. The PhaC1/PhaC2 gene of interest, represented by a blue block, was amplified using these primers. Homologous recombination between the linearised plasmid and the PCR product resulted in the cloning of the plasmid along with the PhaC1/PhaC2 gene of interest.

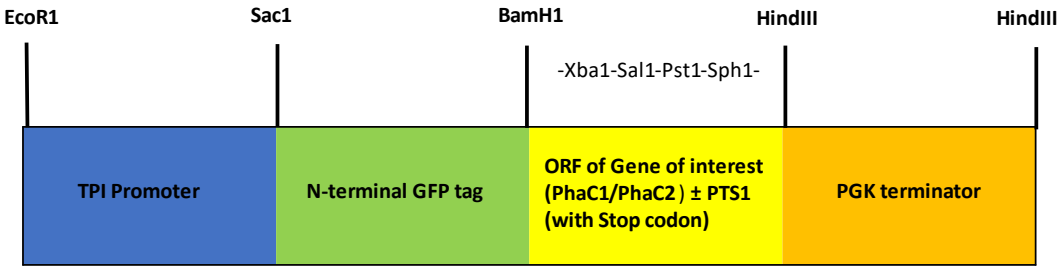

Figure 3.3: Diagrammatic representation of the gene expression cassette containing TPI promoter, N-terminal GFP tag, ORF of PhaC1/PhaC2 from *P. mendocina* with and without PTS1 recombined with vector plasmid pEW355, PGK terminator and restriction enzymes.

To target peroxisomes for importing PHA synthase, the *PTS1* sequence (peroxisomal targeting sequence) of a native yeast protein was added to the C-terminus of PhaC1 and PhaC2 (Figure 3.3 and 3.6). To compartmentalise the PHA synthesis procedure within peroxisomes, the PTS1 sequence carries instructions for guiding the protein to these organelles. For cytosolic expression, PhaC1 and PhaC2 genes were inserted directly without the *PTS1* sequence downstream of the TPI promoter. To allow unrestricted interaction with substrates in the cytosol, this configuration promotes the expression of PHA synthase genes in the cytosol. In some cases, the incorporation of the Green Fluorescent Protein (GFP) tag to the N-terminus of the constructs was employed for visualisation and assessment of PHA synthesis.

In this study, the existence of the expected plasmids was confirmed after the development of colonies on the agar plate by implementing a fluorescence microscopic screening technique. The importation of PhaC1 and PhaC2 proteins into peroxisomes was facilitated by the *PTS1* pathway, which was achieved through a distinct C-terminal sequence acquired by PCR. It was anticipated that GFP fused to PhaC1 and PhaC2 resulting in their localisation in peroxisomes, which were readily identifiable by microscopic analysis through their distinct bright green punctate signals (Figures 3.7 and 3.8). Colonies were successfully discovered, and images were preserved through the Volocity software. Once a colony incorporating the targeted plasmid was identified, it was streaked onto a fresh selective plate to facilitate its growth. After reaching a certain stage, the colonies were exploited to isolate their total DNA and introduced into electrocompetent *E. coli* cells.

A few of the resulting colonies were subjected to miniprep in order to purify plasmids and subjected to test digestion utilising corresponding restriction enzymes (Figure 3.4). The successful constructions were confirmed by gel electrophoresis, and subsequent sequencing (Figure 3.5) were conducted to verify the accurate insertion of PHA synthase within the plasmid.

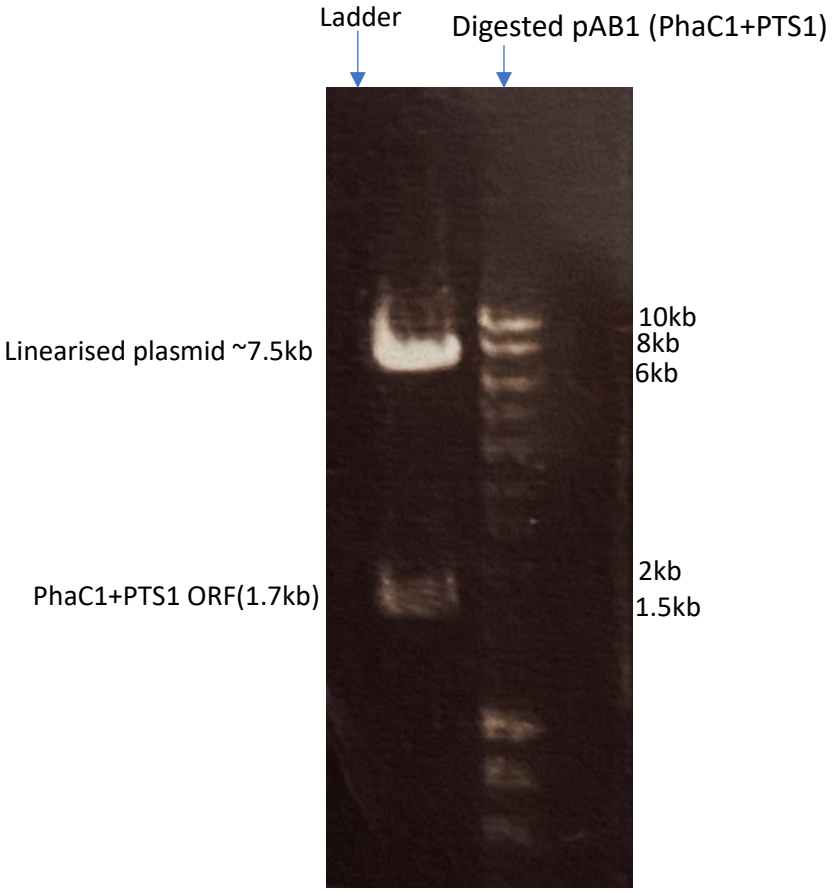

Figure 3.4: The agarose gel image presents the results of a test digest performed on plasmid minipreps derived from the pAB1 construct (PhaC1+PTS1, with GFP). The digestion aimed to assess the presence and integrity of specific restriction sites within the plasmid DNA. BamHI-HF and HindIII-HF enzymes were employed for the digestion. The presence of distinct bands in the digested lanes confirms the successful cleavage of the plasmids at the designated restriction sites.

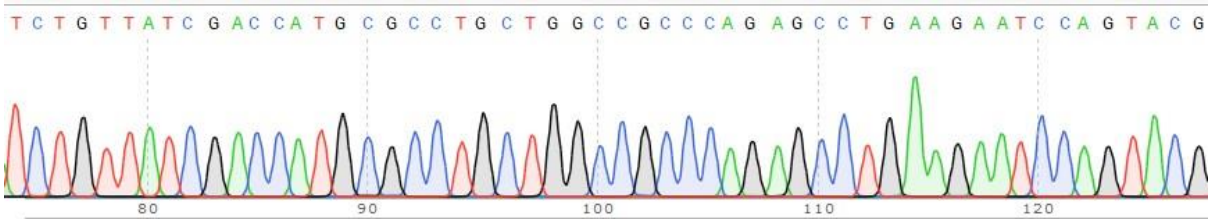

Figure 3.5: The nucleotide sequence chromatogram displays the sequence of nucleotide bases (A, T, G, C) in the DNA sequence of the PHA synthase gene. This chromatogram exhibits distinct and clear peaks that correspond to each of the four nucleotide bases (A = Adenine, C = Cytosine, G = Guanine, T = Thymine). These peaks represent the intensity of the signals detected by the sequencing machine during the Sanger sequencing process. The sequence was compared to the reference genome for verification.

The plasmid map was generated using SnapGene software which serves as a visible potrayal of the construct. It is highlighting important components, and the annotations provide a detailed guide to the functional elements within the vector.

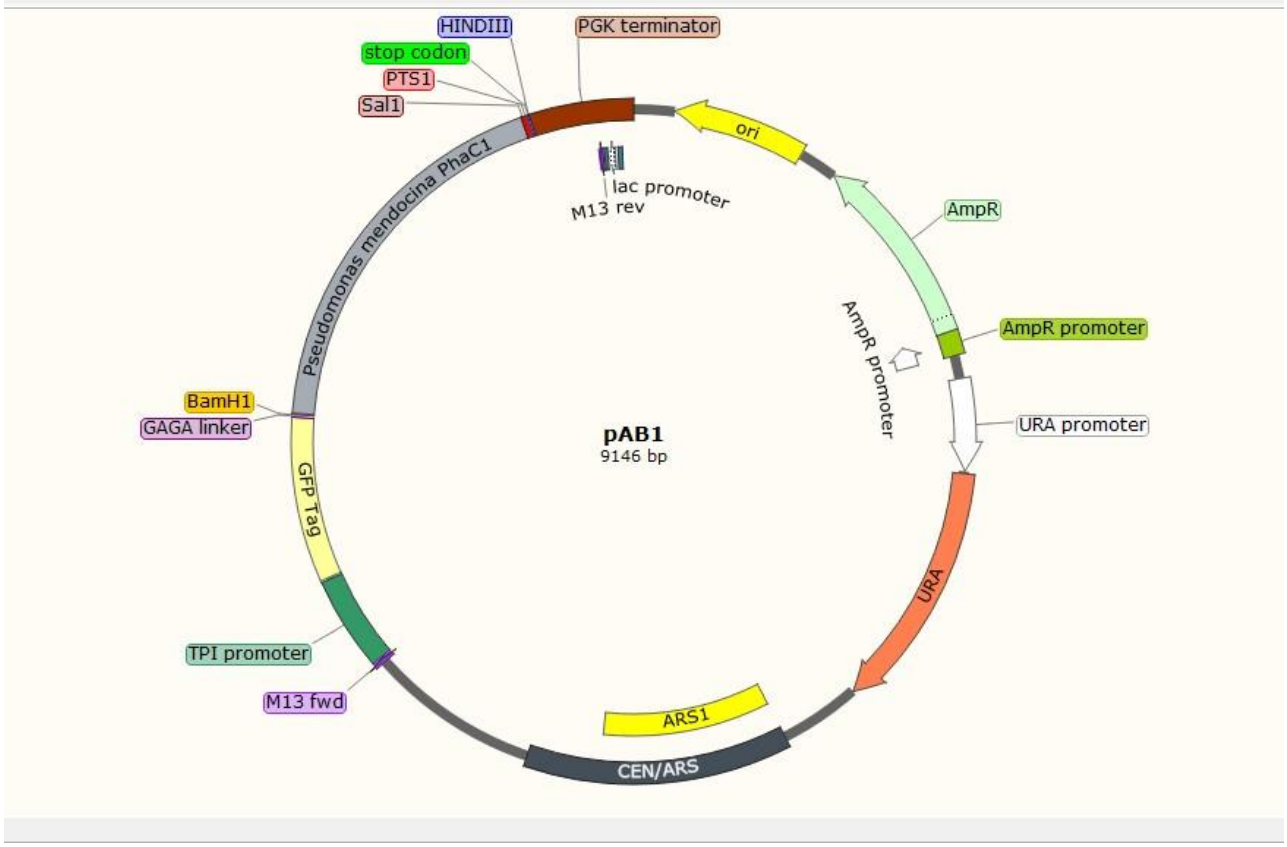

Figure 3.6: A schematic representation of the engineered construct, pAB1, highlighting the integration of the PhaC1Pm ORF with a Peroxisomal Targeting Signal 1 (PTS1). This detailed

map provides a visual representation of the engineered construct, depicting the arrangement of key elements essential for gene expression and plasmid stability.

The yeast cells incorporating the recombinant plasmids were sustained in uracil-deficient media (YM2 Ura-). The selection process to detect successful recombinant cells was enabled by fluorescence microscopy of the N-terminal GFP tag. A similar homologous recombination method was applied to construct other plasmids for this study for example, PhaC1/ PhaC2 without GFP and with PTS1 sequence, PhaC1/PhaC2 without PTS1 and GFP. All the strains containing GFP tags were analysed by microscopy and showed the expected GFP signal (Figures 3.7 and 3.8).

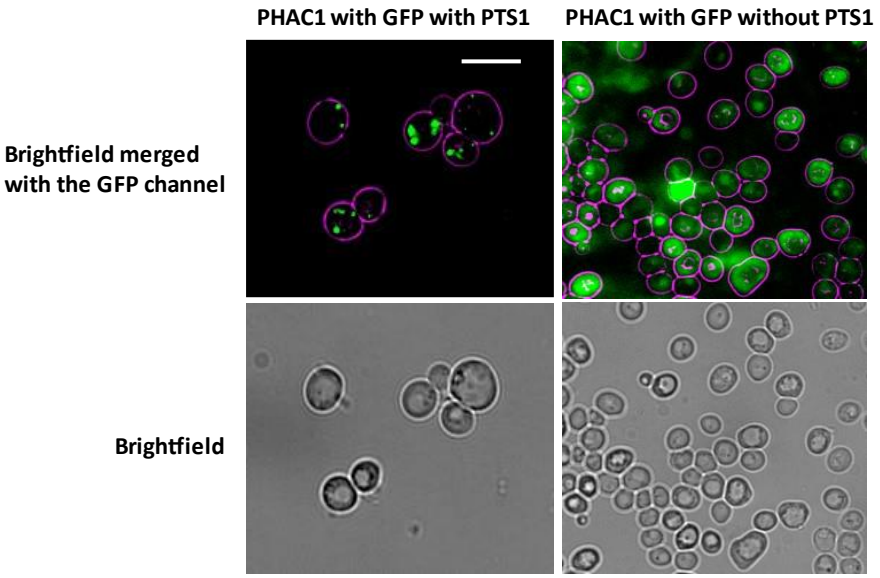

Figure 3.7: Microscopic analysis of GFP fused *P. mendocina* PhaC1 has been identified in peroxisomes and cytosol of *S. cerevisiae*. Scale bar 5µm.

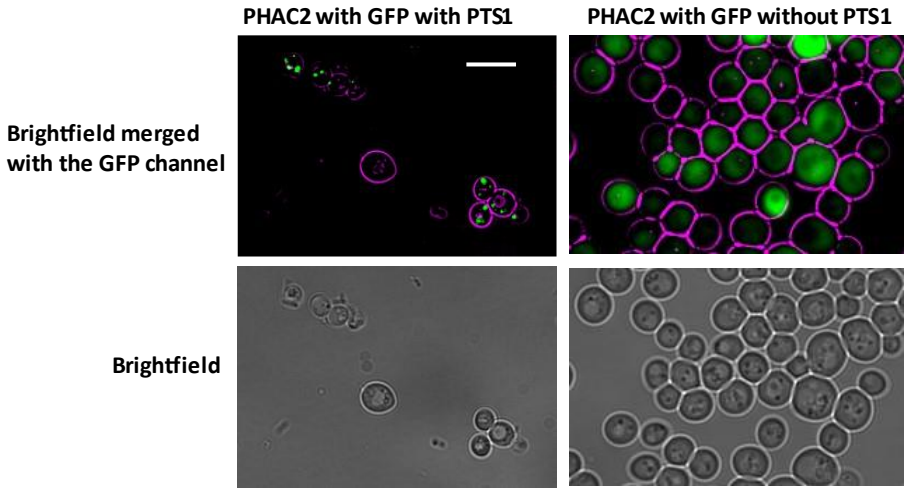

Figure 3.8: Microscopic analysis of GFP fused *P. mendocina* PhaC2 has been identified in peroxisomes and cytosol of *S. cerevisiae*. Scale bar 5µm.

While investigating the localization of PhaC1 and PhaC2 in our study, we acknowledge the importance of various strategies for confirming its presence within peroxisomes and cytosols. It is noteworthy that the primary focus of this study was the production of polyhydroxyalkanoates (PHA) in the engineered yeast strains, and the subsequent experiments were tailored to address questions related to PHA production efficiency and strain engineering. To produce PHA in engineered yeast, alternative approaches were employed to provide insights into the subcellular localization. Specifically, we tested PHA production in recombinant yeast strains exploiting different conditions, including growth on various media, and the use of miscellaneous mutants, details are available in section 3.3.

Growth experiments in oleate media were conducted, aiming to induce peroxisome proliferation, a condition known to influence the localization of proteins associated with peroxisomal functions. Additionally, utilizing mutants like *pex3Δ*, which lacks peroxisomes, is, supported to elucidate the role of these organelles in the observed phenotype. While our study did not directly assess colocalization, these alternative strategies were employed to infer the potential association of the protein with peroxisomes.

3.3 PHA production

S. cerevisiae has been successfully engineered in this study to produce PHA in the lab. Various attempts were made using genetically modified yeast, a non-PHA accumulating microorganism, and several fermentation strategies and growth media were explored to enhance the process of PHA accumulation. While various media were explored in this study for PHA production, we found that oleate and YPO media were the most promising growth media for this experiment. In this study, decanoic acid (C10) and dodecanoic acid (C12) which are medium-chain fatty acids also used in mineral salt media for yeast culture. Both are saturated fatty acids with 10 and 12 carbon atoms in their corresponding chains (Seitz, 2023). Both decanoic acid and dodecanoic acid exhibited toxic effects on yeast cells resulting in cell death. Similarly, nitrogen-deficient media, designed to encourage the accumulation of storage compounds such as PHA, did not produce the expected results. The lack of a nitrogen source was intended to redirect cellular resources towards PHA synthesis. However, the observed outcomes suggested that other factors, such as carbon availability or strain-specific metabolic characteristics, may have influenced the overall performance.

This section of Chapter 3 highlights the production and detection of PHA in recombinant *S. cerevisiae*, incorporating PhaC1 and PhaC2 genes from *P. mendocina.* To investigate PHA synthesis, plasmids containing the PHA synthase gene were introduced into *WT S. cerevisiae* (*BY4742*) and several mutants such as *atg36Δ* (prevents pexophagy, the specific peroxisomal degradation), *pex3Δ* (defective in biogenesis of peroxisome) and *mdh3/gpd1Δ* (double mutant, where peroxisomal level of 3-hydroxyacyl-CoA is increased) by one-step transformation. Transformants exhibited successful uptake of corresponding plasmids and an elevated number of recombinant cells showed the ability to grow on YM2 Ura- plates. PHA production was evaluated in several growth media to assess their overall impact on cellular growth and accumulation of PHA. Cultures were incubated at 30°C and shaken at 200 rpm. Samples were collected at numerous time points to analyse cell growth, visualisation, PHA content, and protein expression patterns.

Oleate media: Oleic acid is a monounsaturated fatty acid and is used as a carbon source for yeast growth. This media induces lipid accumulation in conventional yeast *S. cerevisiae*. This context can activate metabolic pathways that lead to the generation of PHA precursor which breaks down the oleate by fatty acid β-oxidation and therefore has increased the production of suitable β-hydroxyacyl metabolites. The expression of the PHA synthase gene originating from *P. mendocina* can channel the carbon flux towards the synthesis of PHA. Exploitation of oleate media has the potential to produce PHA by harnessing lipid metabolism in *S. cerevisiae*.

YPO media: This media supplies a balanced composition of nutrients with oleate as a carbon source, peptone as a nitrogen source, and yeast extract providing essential vitamins. This media composition potentially induces a lipid accumulation pathway to culminate in PHA synthesis. By adopting genetic modification along with finely tuning the components of this media, it is foreseeable to exploit *S. cerevisiae* for PHA production.

3.3.1 Western blot analysis

This study aimed to validate the expression of GFP-tagged PhaC1 and PhaC2 in recombinant yeast. Protein samples were collected from the PHA production experiment. Western blot analysis was performed utilising an anti-GFP antibody to determine the presence of fusion proteins. Western blot analysis displayed bands between 100 kDa and 75 kDa in most samples, corresponding to the expected size of GFP-PhaC1 and GFP-PhaC2 fusion proteins (around 90 kDa) (Figures 3.9 and 3.10). The negative control strains (WT with control plasmid, YCplac33 and *atg36Δ* with control plasmid, YCplac33) showed no protein expression at all, as expected (Figures 3.9 and 3.10). Proteolytic cleavage of GFP was observed in some samples, yielding breakdown products around the 25 kDa marker. The *Δpex3*+pAB4 (GFP+PhaC2 without PTS1) strain exhibited a breakdown product likely representing cleaved GFP from PhaC2 (27.3 kDa) (Figures 3.10). Differences in band intensities were noted, with weaker bands observed for *Δpex3* + pAB3 (GFP+PhaC2+PTS1), but no breakdown product (Figure 3.10).

The presence of bands in the 75-100 kDa range confirmed the successful expression of GFP-tagged PhaC1 and PhaC2 fusion proteins in recombinant yeast cells during PHA production. Importantly, the absence of protein expression in negative control strains validated the specificity of the antibody detection (Figures 3.9 and 3.10).

The proteolytic cleavage of GFP observed in some samples at different stages suggests intracellular dynamics. Specifically, the breakdown product around 25 kDa likely corresponds to cleaved GFP from PhaC2. The occurrence of proteolytic cleavage of GFP is indicative of pexophagy-mediated degradation. This suggests that GFP-PhaC1 and GFP-PhaC2 fusion proteins, initially synthesized in peroxisomes, undergo proteolytic cleavage and potential relocation during PHA production. The differences in band intensities between strains may be attributed to variations in the degree of proteolysis or expression levels. pAB1 and pAB2 indicate GFP+PhaC1+PTS1 and GFP+PhaC1 without PTS1 respectively in this study.

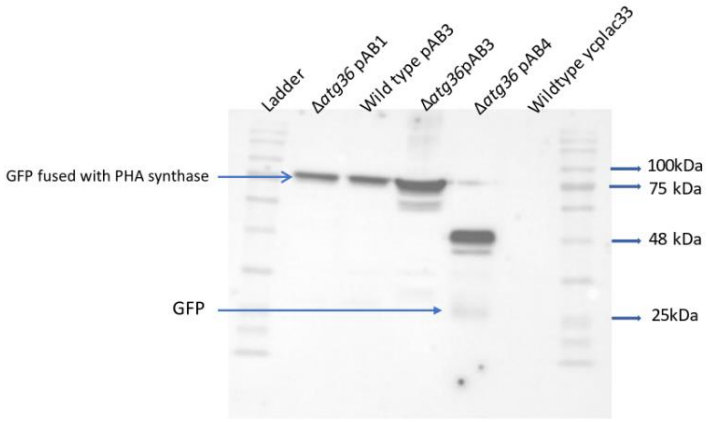

Figure 3.9: To determine the expression of PhaC1 and PhaC2, a Western blot analysis was performed during the PHA production experiment using the anti-GFP primary antibody, secondary antibody (goat anti-mouse), the CSL-BBL pre-stained protein ladder as reference for protein size. An initial analysis was conducted on a pre-culture and the resulting detected bands depicted insight into the protein expression of the inoculated cells which had undergone overnight growth in selective media with 0.12% oleate and 0.3% glucose. The resulting detected bands provided valuable insight into the protein expression of the inoculated cells. The bands depicted the protein size and thus provided a clearer understanding of the expression of PhaC1 during the PHA production experiment.

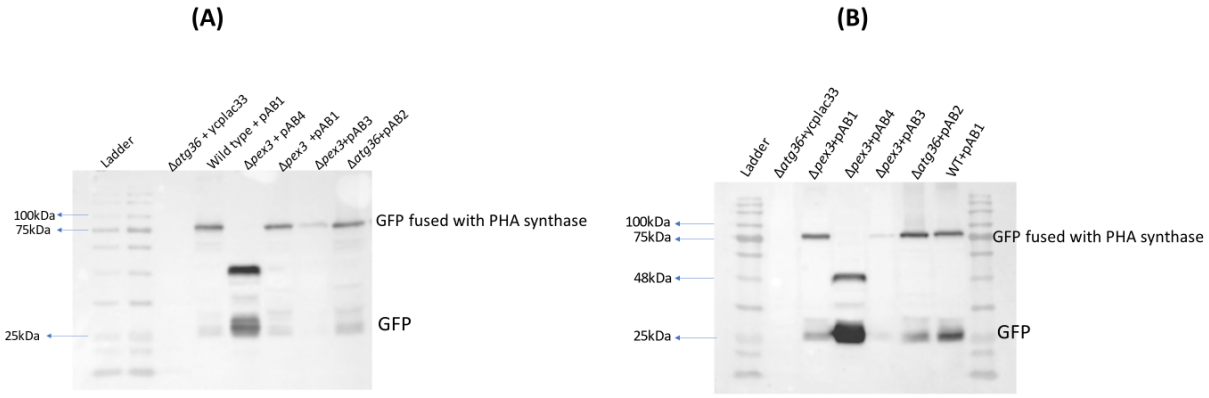

Figure 3.10: (A) To determine the expression of PhaC1 and PhaC2, a Western blot analysis was performed during the PHA production experiment using the anti-GFP primary antibody, secondary antibody (goat anti-mouse), the CSL-BBL pre-stained protein ladder as reference for protein size. An analysis was conducted after 24 hours, and the resulting detected bands depicted insight into the protein expression of the inoculated cells which had undergone 24 hours of growth in selective media with 0.12% oleate and 0.3% glucose. The anti-GFP primary antibody was used to detect the PHA synthase protein, and the CSL-BBL pre-stained protein ladder was used to determine the protein size. The goat anti-mouse secondary antibody was used to bind the primary antibody and facilitate detection. The resulting detected bands provided valuable insight into the protein expression of the inoculated cells. **(B)** To determine the expression of PHA synthase, a Western blot analysis was performed after 96 hours during the PHA production experiment using the anti-GFP primary antibody, secondary antibody (goat anti-mouse), the CSL-BBL pre-stained protein ladder as a reference for protein size. The resulting detected bands depicted insight into the protein expression of the cells that had undergone 96 hours of growth in selective media with 0.12% oleate and 0.3% glucose. After 96 hours, the resulting detected bands depicted insight into the protein expression of the cells including more cleavage of GFP.

3.3.2 Nile red analysis

Nile red is a fluorescent dye commonly employed for the staining and visualisation of intracellular lipid droplets and PHA granules (Zuriani *et al*., 2013). Nile red assay was carried out in this study to serve as an independent and qualitative indicator of intracellular PHA content in engineered yeast strains using oleate media. Nile red exhibits strong fluorescence while binding with hydrophobic regions. PHA granules are surrounded by a lipid membrane, hence featuring as bright fluorescent red granules, therefore making it suitable for detecting and studying PHA granules in the cells (Zuriani *et al*., 2013).

In this study, atg36Δ, *mdh3/gpd1Δ* and WT cells were grown in oleate media with the plasmid containing the PHA synthase gene, PhaC1 with PTS1, and GFP until the late stationary phase. Cells were also grown with control plasmid Ycplac33, in oleate media for 72 hours. Cells were then harvested and stained with Nile red and imaged with a fluorescence microscope after 72 hours of culture. Nile red-stained recombinant *S. cerevisiae* in the stationary phase of growth were viewed with filter set EGFP (Ex 488 nm/ Em 509 nm) and Ds Red (Ex 545/ Em 572 nm). The image was acquired at 63x magnification with a scale bar indicating 5µm for reference. The images (Figures 3.10) exhibited the bright red puncta in the cells which correspond to the Nile red stained PHA granules. The fluorescence signals from Nile red-stained cells were notably intense and associated with bright and well-defined puncta. The observed fluorescence signals are suggestive of intracellular PHA granules, consistent with previous studies (Zuriani *et al*., 2013). On the other hand, cells with a control plasmid did not exhibit bright fluorescent red signals (Figures 3.11), indicative of the absence of PHA.

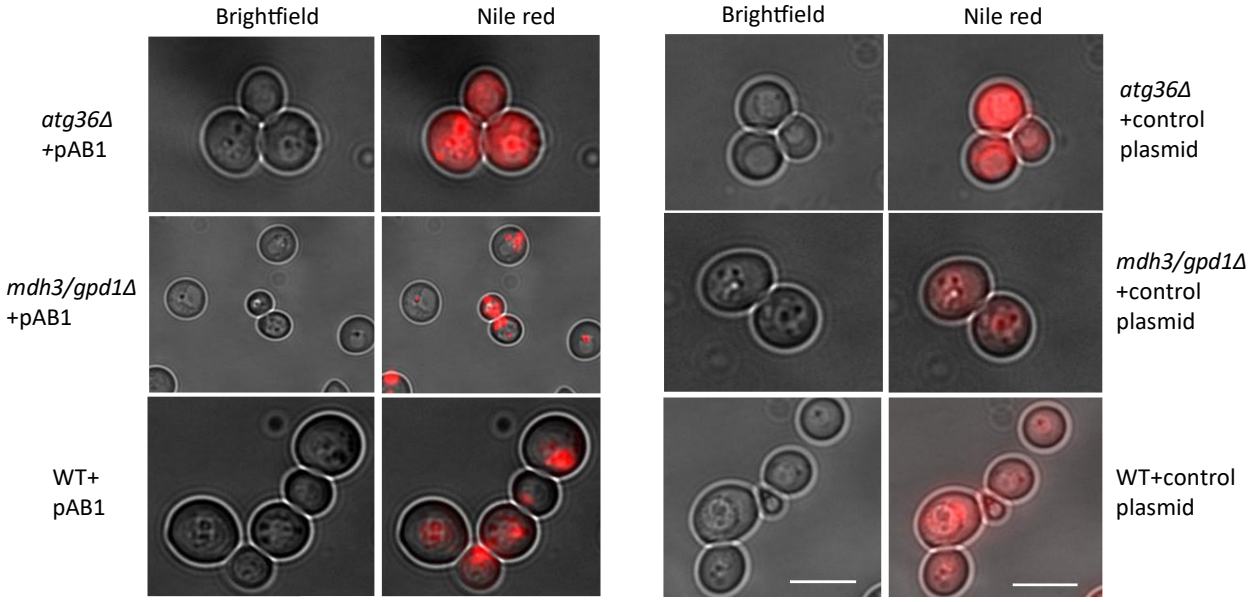

Figure 3.11: Fluorescence microscopy images of *atg36Δ*, *mdh3/gpd1Δ and* WT cells with pAB1 (GFP+PhaC1+PTS1) after 72 hrs of PHA production phase stained with Nile red (left 2 panels) Fluorescence microscopy images of *atg36Δ*, *mdh3/gpd1Δ and* WT cells with control plasmid (YCplac33) after 72 hrs of PHA production phase stained with Nile red (right 2 panels). Bar 5 µm.

Fluorescence was also measured by means of 96 well plates using a multilabel plate reader to have a rapid qualitative measurement of PHAs. Fluorescence intensity was measured using an excitation wavelength of 535 nm and an emission wavelength of 605 nm for recombinant yeast. This analysis was carried out to determine the significance of fluorescence intensity differences between the test [*mdh3/gpd1Δ* cells with pAB1 (GFP+PhaC1+PTS1) and WT cells with pAB1 (GFP+PhaC1+PTS1)] and control [*mdh3/gpd1Δ* cells with control (YCplac33), WT cells with control (YCplac33) and water (stained and unstained)] samples (Figure 3.12). It showed significant fluorescent intensity differences produced between test and control samples. Significance is indicated here between test and control samples as **** $p<0.0001$ (Figure 3.12).

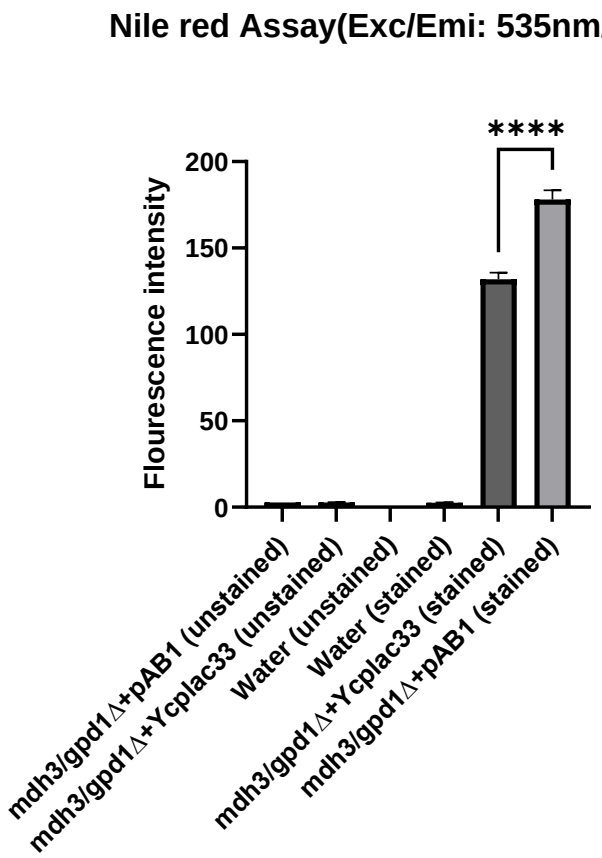

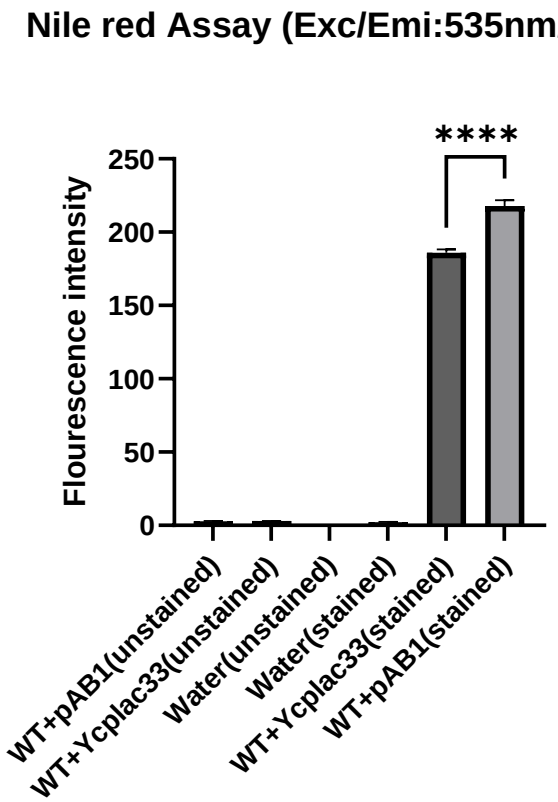

Figure 3.12: The effect of Nile red on fluorescence intensity differences between the test samples [*mdh3/gpd1Δ* cells with pAB1 (GFP+PhaC1+PTS1) and WT cells with pAB1

(GFP+PhaC1+PTS1)] and the control samples [*mdh3/gpd1Δ* cells with control (YCplac33), WT cells with control (YCplac33) and water]. Data expressed here were the mean values and standard deviations of five replicates.

3.4 Detection of PHA By Nuclear Magnetic resonance (NMR) and Gas Chromatography (GC)

NMR and GC techniques were applied in detecting the PHA polymers synthesized by numerous recombinant *S. cerevisiae* strains cultivated in various media. NMR offered information regarding the monomer composition in PHA polymer, while GC quantified the precise amount of the monomer content present in samples. Both techniques were crucial in this study for the comprehensive characterisation of PHA polymers.

3.4.1 NMR analysis: NMR spectroscopy is a powerful technique employed for the analysis of chemical compounds including PHAs. NMR delivered insights into the structure and makeup of PHA polymers, providing useful information regarding monomer composition in recombinant samples. To proceed with the NMR technique, lyophilised samples were dissolved in a deuterated solvent appropriate for analysis, for instance, deuterated chloroform ($CDCl_3$) in this experiment. Sodium hypochlorite solution and deuterated chloroform ($CDCl_3$) were added to each sample of freeze-dried cells. The mixture was vortexed and incubated on a shaker at 200rpm for two hours to overnight at 30°C. After extraction, samples were centrifuged at 1500xg for 10 minutes to induce phase separation, and the bottom organic layer of $CDCl_3$ was removed and transferred to a 5mm NMR tube (Hahn *et al*., 1993). ^1H, HSQC and TOCSY spectra were recorded utilising a Bruker DRX-600 spectrometer to analyse the composition and structure of the polymer. Monomer composition was deduced from the chemical shifts in the spectra.

A combination of 1-dimensional and 2-dimensional NMR experiments was needed for complete confidence in chemical structure. The chemical structure of the synthesised polymer was determined by ^1H NMR with $CDCl_3$-NaOCl extracts from recombinant yeast and revealed three groups of distinct signals of the polymer. The chemical shifts on the X-axis (in ppm) suggest the specific environment of the protons. Methyl (CH_3), methylene (CH_2), and methine (CH) protons of polymer units were detected by ^1H NMR. Peaks assigned for the methyl group (CH_3 at 1.22 ppm), methylene (CH_2 at 2.4 ppm), and methine (CH at 5.2 ppm) were detected, suggestive of the presence of polyhydroxybutyrate (PHB) in Figures 3.13 and 3.14.

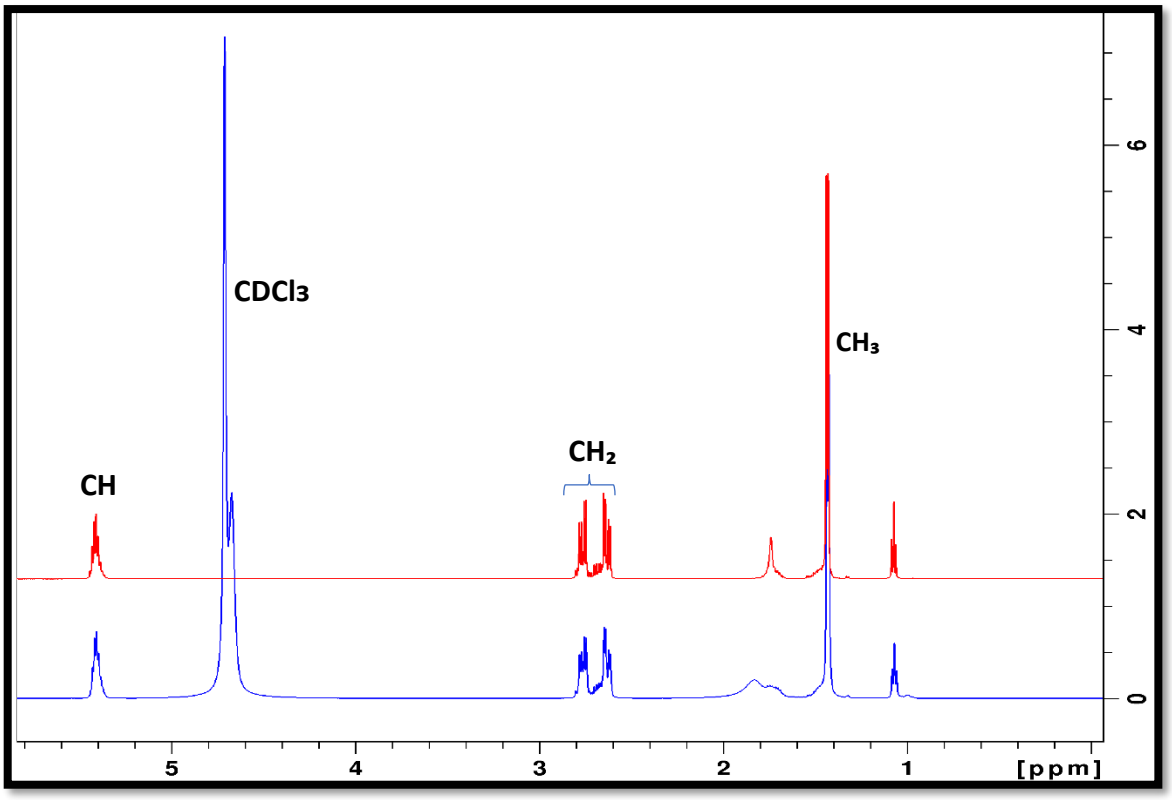

Figure 3.13: ^{1}H-NMR spectra analysis of polymer provided from Sigma-Aldrich (blue spectrum) and pure PHAs (red) extracted through deuterated chloroform-sodium hypochlorite dispersion method as a standard in this analysis.

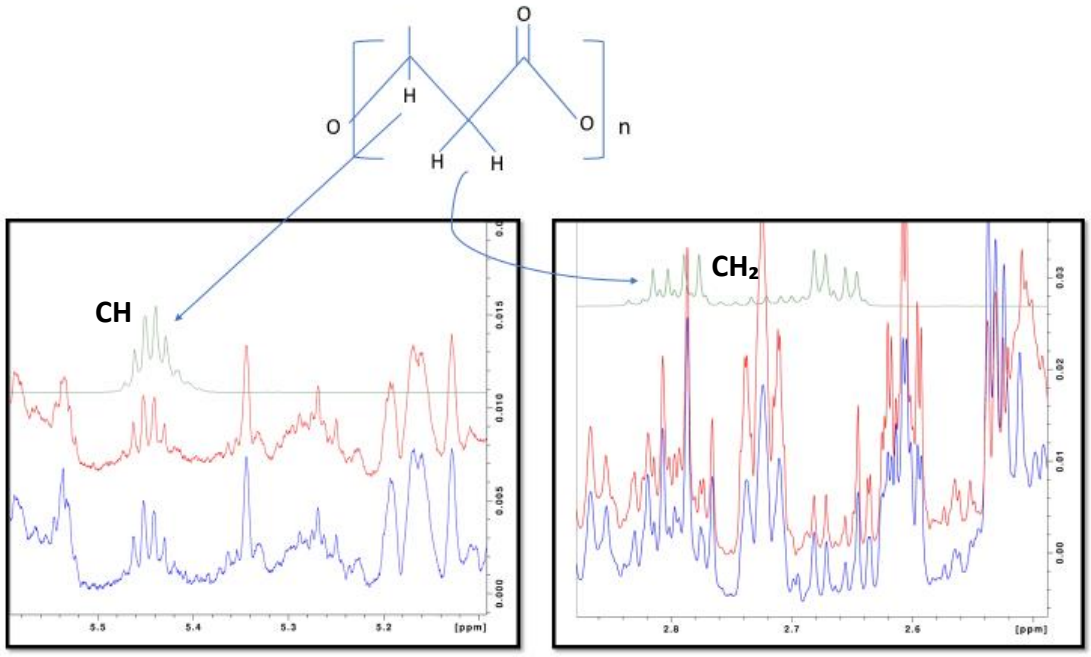

Figure 3.14: Polymer structure on top indicating peaks arising from the protons of the corresponding structure acquired in ^{1}H NMR, suggesting the presence of Polyhydroxybutyrate

(PHB) in recombinant yeast strains cultured in oleate media, WT+pAB5 (PhaC1+PTS1 and without GFP) in red and *atg36Δ*+pAB5 (PhaC1+PTS1 and without GFP) in blue. Pure PHA (green) is also shown as a standard in $CDCl_3$. The other signals are from yeast background metabolites.

TOCSY analysis provided detailed information about the connectivity between the protons. Figure 3. 15 shows the cross-peak between CH (5.45 ppm) and CH_2 protons (the proton signals shown in Figure 3.14 at about 2.7 ppm), indicating they are coupled to each other in the PHB unit. In the TOCSY spectrum, we observed cross-peaks between the methylene group, CH_2 protons, and nearby protons, suggesting that CH_2 protons are coupled to each other to make PHB unit. We observed cross peaks between the methine (CH) group at 5.45 ppm with the neighbouring protons. By examining the cross peaks in the TOCSY spectra, we can deduce the connectivity of all three types of protons in the polymer structure. Cross peaks connecting CH_3 to CH_2, as well as CH_2 to CH in the polymer units, affirming the connectivity of these protons. This result establishes the connectivity between the protons, aiding in the structural elucidation of PHB to confirm the presence in the recombinant yeast samples. Our findings from 1-D and 2-D NMR data showed that recombinant yeast cells produce PHB. Analysis collectively confirmed the molecular composition of the polymer to be PHB.

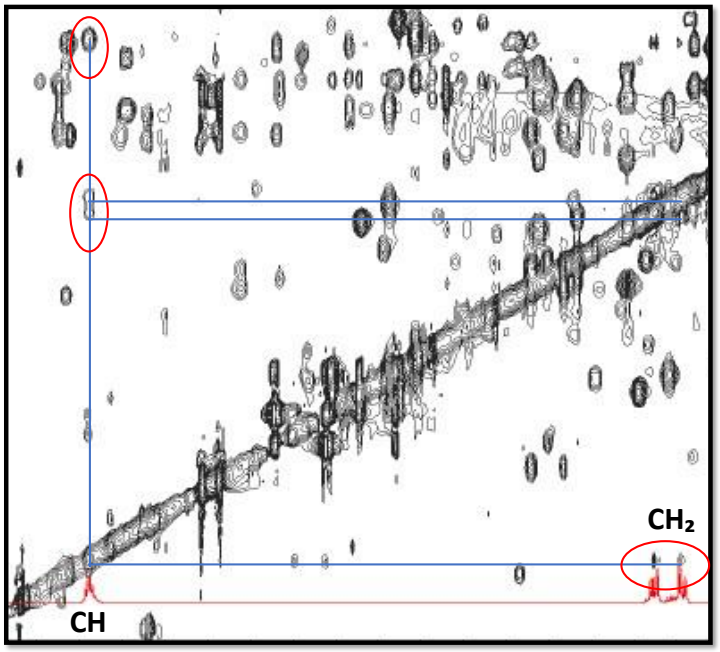

Figure 3.15: 2D TOCSY spectrum in deuterated chloroform measured at 600 MHz reveals the cross-peaks between the protons present in the Polyhydroxy-butyrate molecule. The red

spectrum indicates 1D of pure (Sigma) Polyhydroxy-butyrate. The vertical and horizontal lines connect together the coupled protons of PHA.

However, we also investigated plasmid constructs containing the PHA synthase gene with GFP, and PTS1. GFP was for visualisation while PTS1 was introduced to promote peroxisomal localisation of PHA synthase to produce PHA efficiently. GFP expression was confirmed with fluorescence microscopy and GFP fluorescence was detected in cells incorporating the plasmid construct, suggesting successful GFP expression. Western blot analysis confirmed the presence of GFP in plasmid-bearing cells, even though the presence of GFP did not affect the expression of PHA synthase. Unexpectedly, although there was successful expression of GFP, PHA production was inhibited in recombinant yeast containing plasmid constructs with GFP. A previous study found GFP consumes cellular resources (energy and precursors) for synthesis and maturation (Deng *et al*., 2021). This competition for resources probably leads to decreased availability of substrates and eventually hinders PHA production in this study.

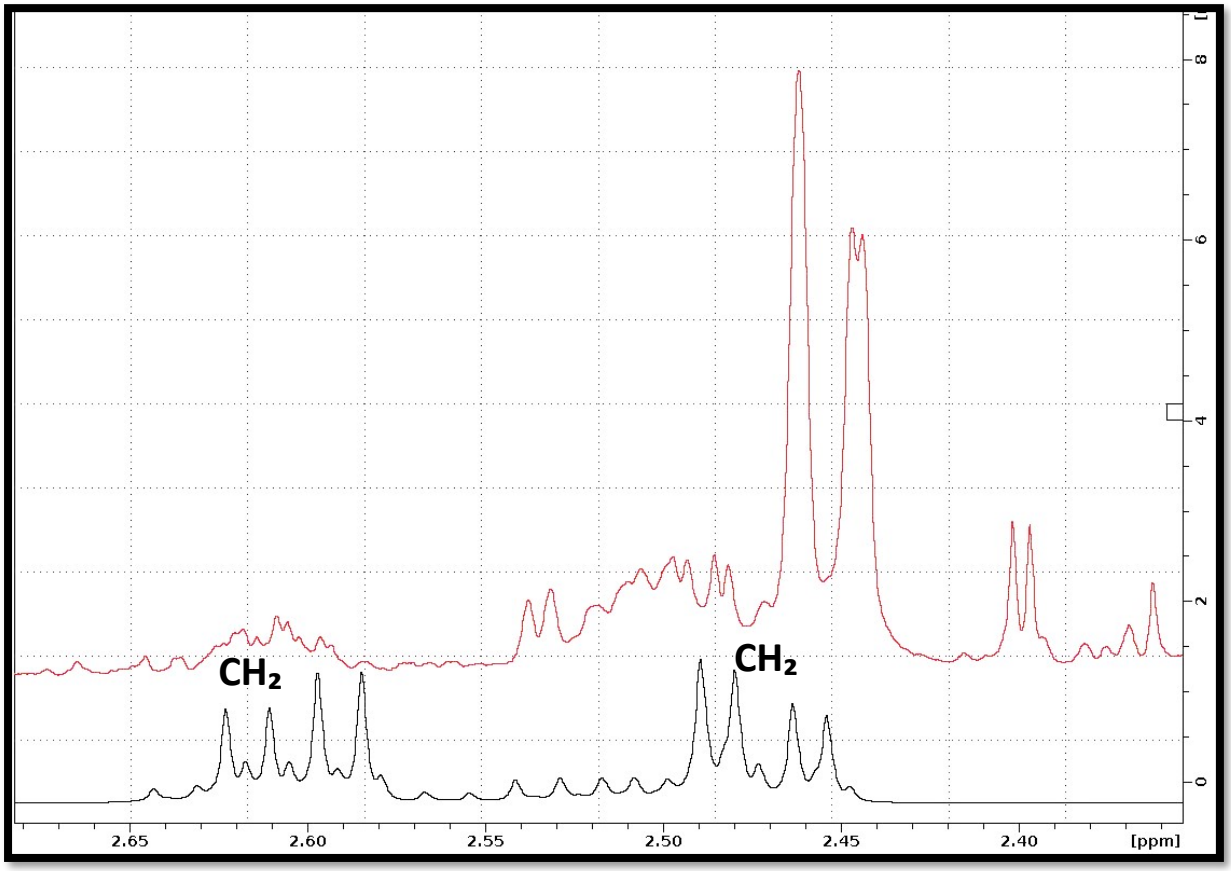

Figure 3.16: ^{1}H-NMR spectra analysis of recombinant yeast [*atg36Δ*+pAB1(GFP+PhaC1+PTS1)] grown in oleate media did not reveal characteristic peaks for CH_2 at 2.4-2.6 ppm (red), while standard peaks (black) from pure PHA showed respective peaks for CH_2.

This study reveals the analysis of control samples comprising WT-type strain with the control plasmid (YCplac33) and WT strain only (without plasmid). Both samples were cultivated under identical conditions to the recombinant *S. cerevisiae* to produce PHA. NMR analysis of lyophilised cells from control samples comprising WT-type strain with the control plasmid (YCplac33) and WT strain only (without plasmid) displayed the absence of PHB compounds. There were no detectable peaks corresponding to PHB monomers were observed (Figures 3.17 and 3.18). These findings served as a crucial baseline to assess PHA production in engineered *S. cerevisiae* and spotlighted the success of the genetic engineering effort in enabling polymer synthesis in eukaryotic systems. The results also indicate the absence of PHA accumulation in the WT-type strain, confirming that this strain does not naturally produce PHA. The absence of characteristic PHA peaks in NMR (Figures 3.19 and 3.20) validates this observation.

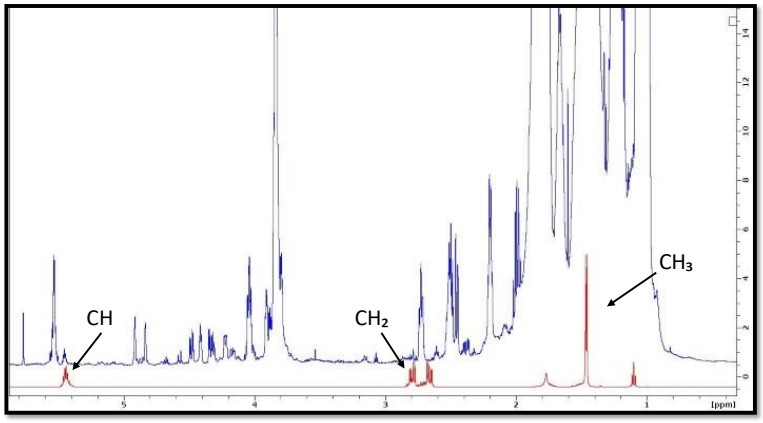

Figure 3.17: ^{1}H-NMR spectra analysis of the control sample (WT+YCplac33) grown in oleate media did not reveal characteristic peaks for PHB (blue), while standard peaks (red) from pure PHA showed respective peaks for PHB.

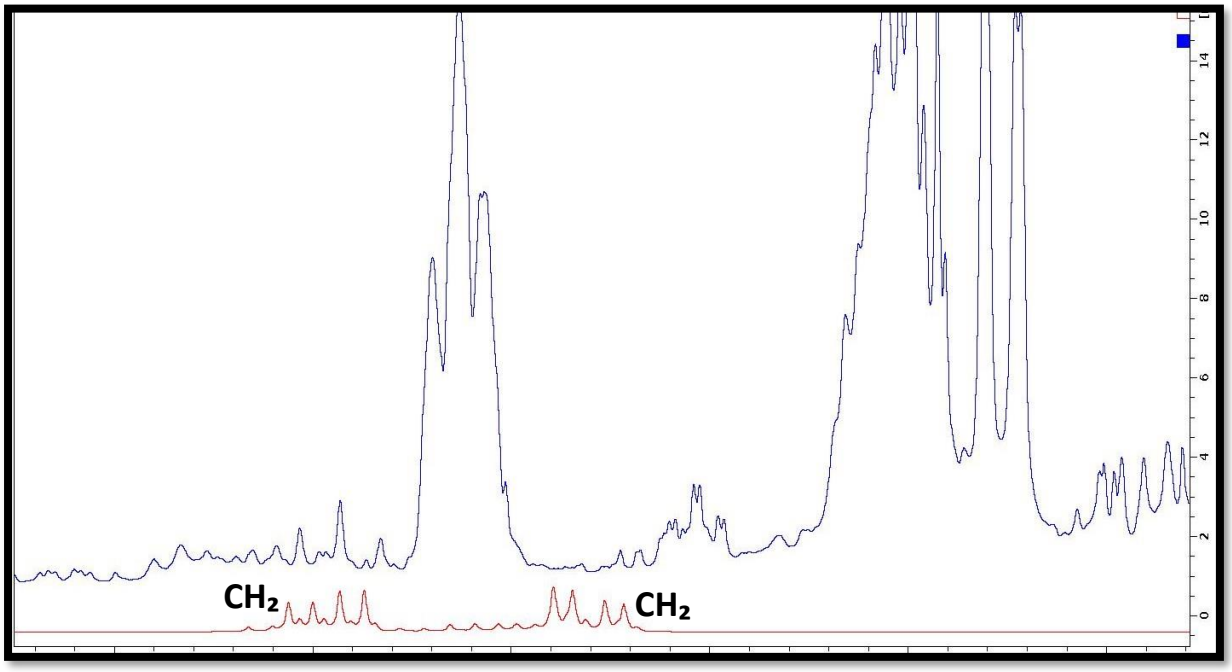

Figure 3.18: ^{1}H-NMR spectra analysis of the control sample (WT+YCplac33) grown in oleate media did not reveal characteristic peaks for CH_2 at 2.4-2.6 ppm (blue), while standard peaks (red) from pure PHA showed respective peaks for CH_2.

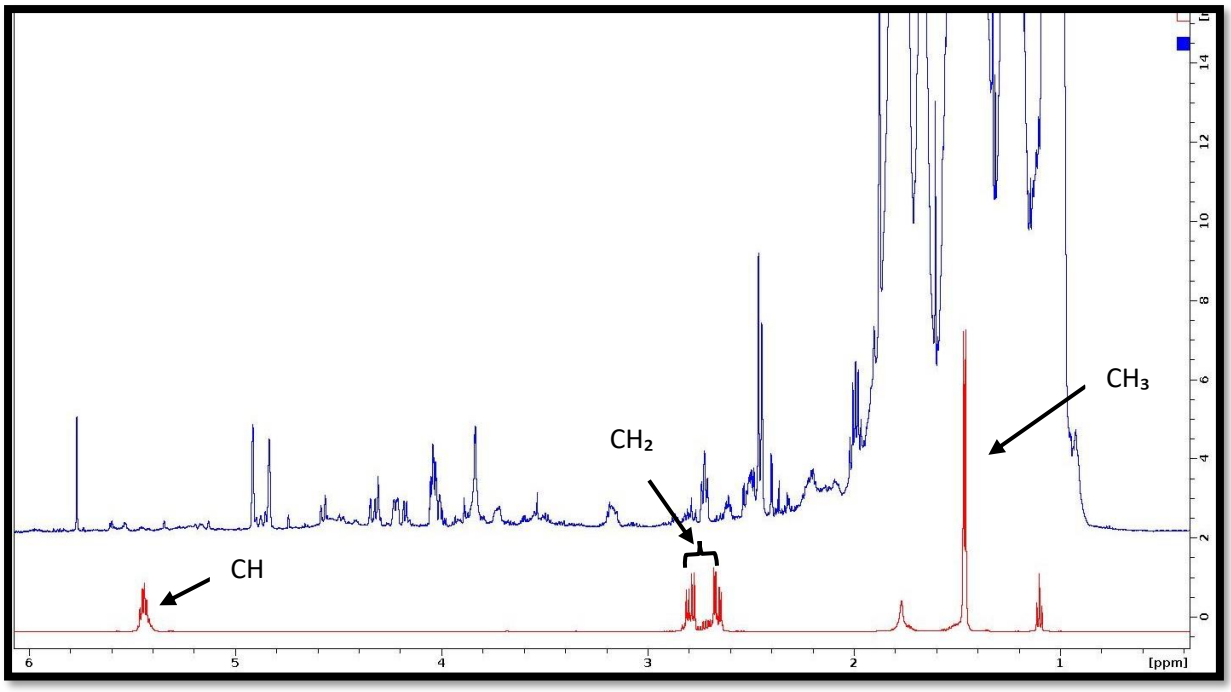

Figure 3.19: ^{1}H-NMR spectra analysis of the control sample, WT only (without plasmid) did not reveal characteristic peaks for PHB (blue), while standard peaks (red) from pure PHA showed respective peaks for PHB.

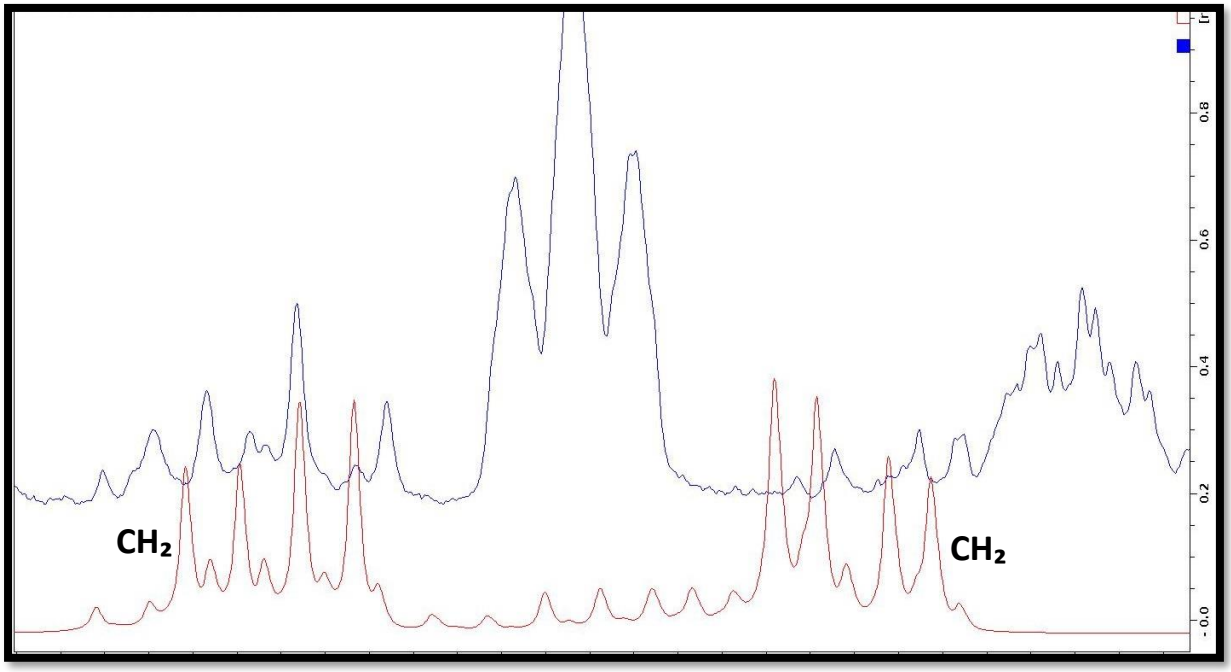

Figure 3.20: ^{1}H-NMR spectra analysis of the control sample, WT only (without plasmid) did not reveal characteristic peaks for CH_2 at 2.4-2.6 ppm (blue), while standard peaks (red) from pure PHA showed respective peaks for CH_2.

We gained a detailed understanding of the structural composition of the polymer by linking the carbon chain length information to the observation and analysis of peaks in NMR analysis. In the context of polymer production in recombinant yeast, the NMR spectra provide a fingerprint that reflects the structural characteristics of the polymer. The CH peaks represent methine groups within the polymer chain, while CH_2 peaks indicate methylene groups and CH_3 peaks signify terminal methyl groups. In the NMR spectrum (Figures 3.13 and 3.14), the observed peaks at chemical shifts 2.4 ppm and 5.2 ppm correspond to the methylene (CH2) and methine (CH) groups in the polymer backbone, while the peaks at chemical shifts 1.22 ppm indicate the presence of methyl (CH3) groups in the 3-hydroxybutyrate units. The analysis conducted confirmed that the molecular composition of the polymer is polyhydroxybutyrate (PHB).

The multiplicity and chemical shift of these signals further contributes to the detailed analysis of the carbon chain structure. CH Peaks in the NMR spectrum correspond to the hydrogen atoms in the CH2 in the polymer chain. In PHB, the methylene groups are part of the butyrate side chains. CH3 Peaks correspond to the hydrogen atoms in the methyl groups attached to the carbon backbone. The methyl groups are part of the 3-hydroxybutyrate units in PHB. The carbon chain length is determined by the number of carbon atoms in the 3HB monomers, typically four carbon atoms. For PHB, the carbon chain length is homogenous, with each repeating unit containing the same number of carbon atoms. There are no other signals in the NMR spectrum in the same spin system (such as, *J* coupled to these spins). If the sample contains any monomers with chain length longer than hydroxybutyrate, then there will be additional cross peaks in the TOCSY spectrum. No such peaks can be seen, allowing us to deduce that the only monomer present is hydroxybutyrate, and thus that the molecular composition of the polymer is pure polyhydroxybutyrate (PHB).

3.4.2 GC analysis: This is a widely adopted analytical technique for the determination of low concentrations of polymers and is superior to other methods (Braunegg *et al.,* 1978). GC is employed in this study as a quantitative means of determining the type and amount of monomer present in recombinant yeast samples. The first step involved subjecting lyophilised samples to methanolysis, a procedure that splits the polymer into its constituent monomers. This was performed with heating at 100°C in the fume hood in the presence of methanol with catalyst, sulphuric acid. To promote the hydrolysis of ester bonds in PHA, sulphuric acid was used as a catalyst resulting in the release of monomeric units. Following methanolysis, the resulting monomers were derivatised as methyl esters to form volatile derivatives suitable for GC analysis. The derivatised samples were then injected into a gas chromatograph equipped with the appropriate column. The monomer derivatives were separated depending on their volatility by the column. A flame ionisation detector (FID) was employed to quantify the separated monomers. The FID is a commonly used analytical instrument in gas chromatography (GC) for detecting and quantifying the concentration of organic compounds. It operates on the principle of ionization of carbon-containing compounds in a hydrogen flame. When these compounds pass through the flame, they are ionized, and the resulting

ions generate a current that can be measured. The strength of the current is directly proportional to the concentration of the analyte in the sample. The FID data presented here as peak heights and areas, provide quantitative information about the concentration of each compound.

Confidence in assigning a peak to PHB in GC analysis relies on a combination of factors, such as retention time specificity along with the results of calibration experiments. Retention time in GC is a critical parameter for compound identification. Each compound has a characteristic retention time under specific chromatographic conditions. If the peak aligns with the expected retention time of PHB, it provides preliminary evidence supporting the assignment (Ansari and Fatma, 2016). Running standards of known compounds, for instance, PHB, under identical conditions allowed for the comparison of retention times. The retention time of the small peak matched that of the PHB standard, it strengthened the confidence in the assignment. Additionally, calibration curves generated using known concentrations of PHB standards provided a quantitative aspect to the analysis. The small peak's area corresponded to a concentration within the linear range of the calibration curve, it supported the assignment. The systematic evaluation of these elements ensured in this study a rigorous and reliable interpretation of the data and the quantification of the monomers present in the samples.

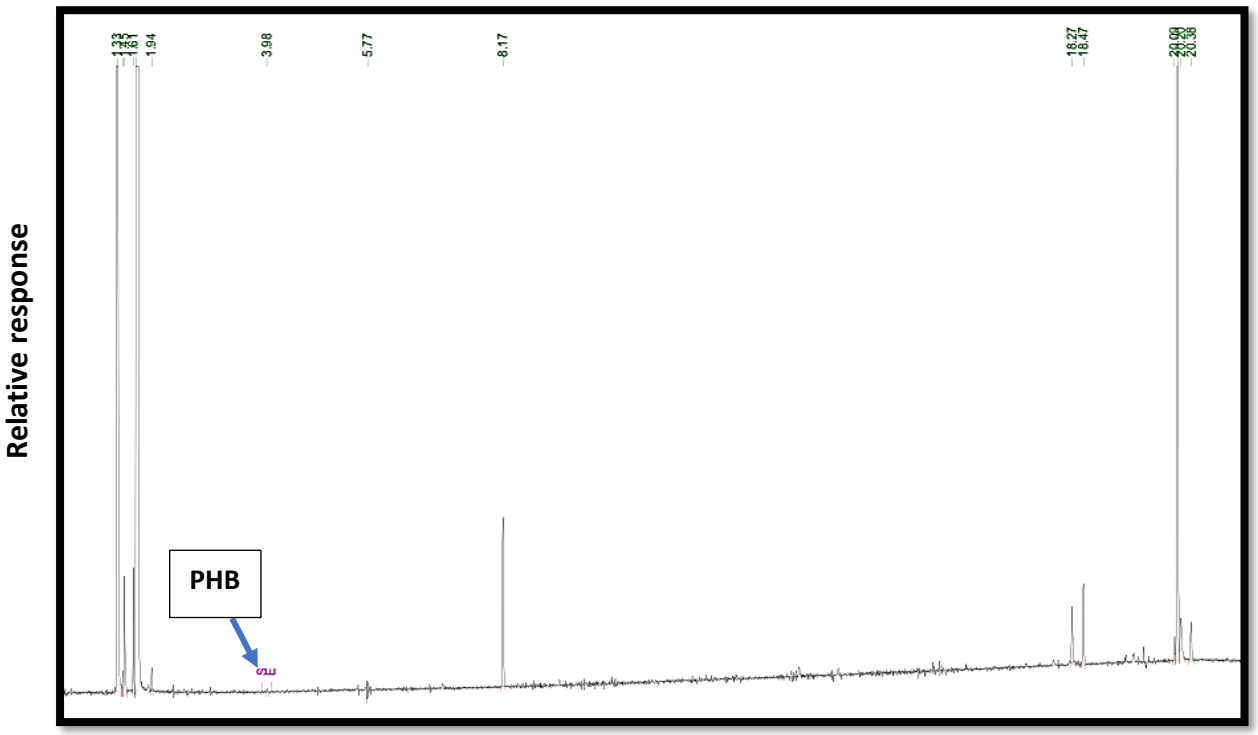

Figure 3.21: GC analysis of 3-hydroxybutyric acid produced in WT yeast transformed with plasmid pAB5 (PhaC1+PTS1, without GFP). Cells were harvested after 48 hrs of culture in 600ml oleate media in a 3L flask. In the chromatogram, the retention time for PHB is marked with an arrow. The retention time of the target PHB is 3.98 minutes.

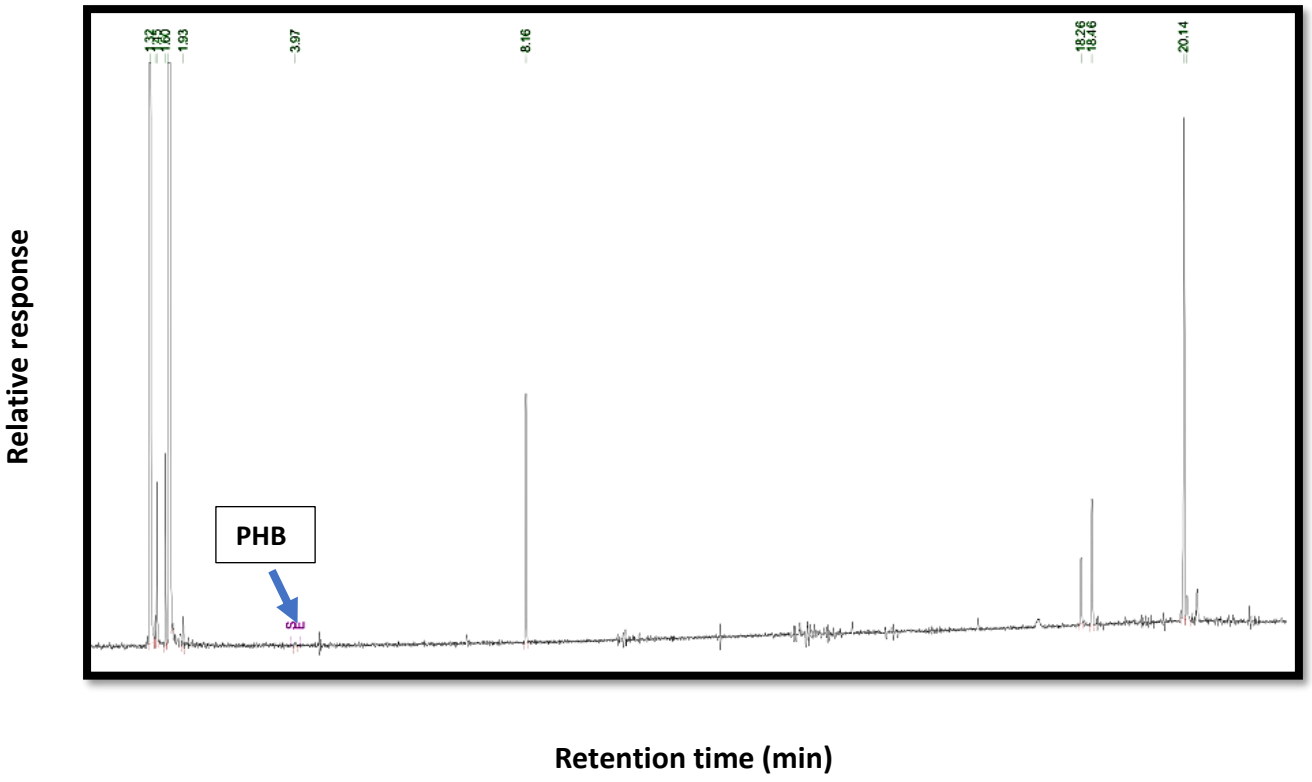

Figure 3.22: GC analysis of 3-hydroxybutyric acid produced in *atg36Δ* transformed with plasmid pAB5 (PhaC1+PTS1, without GFP). Cells were harvested after 48 hrs of culture in 600ml oleate media in a 3L flask. In the chromatogram, the retention time for PHB is marked with an arrow. The retention time of the target PHB is 3.97 minutes.

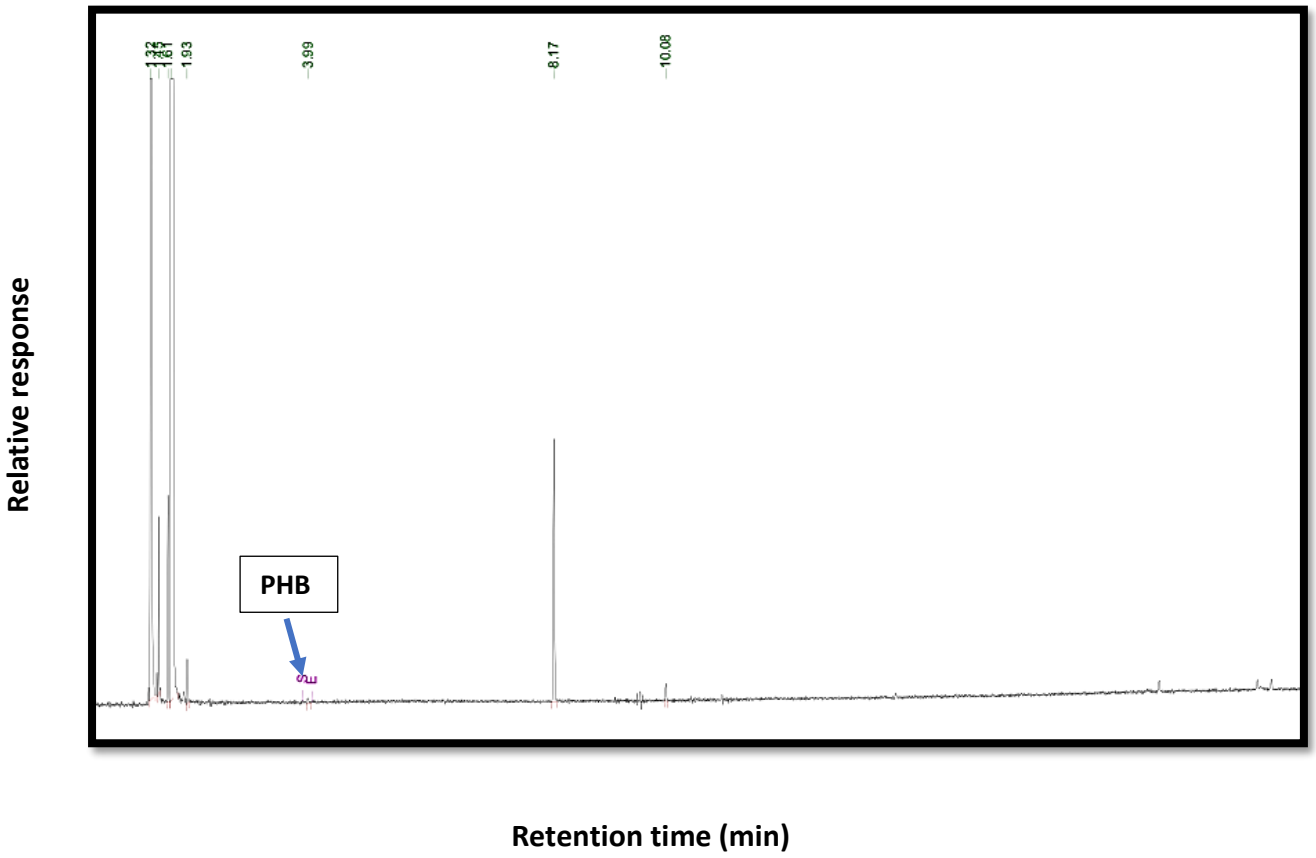

Figure 3.23: GC analysis of 3-hydroxybutyric acid produced in *atg36Δ* transformed with plasmid pAB5 (PhaC1+PTS1, without GFP). Cells were harvested after 48 hrs of culture in 50ml oleate media in a 250ml flask. In the chromatogram, the retention time for PHB is marked with an arrow. The retention time of the target PHB is 3.99 minutes.

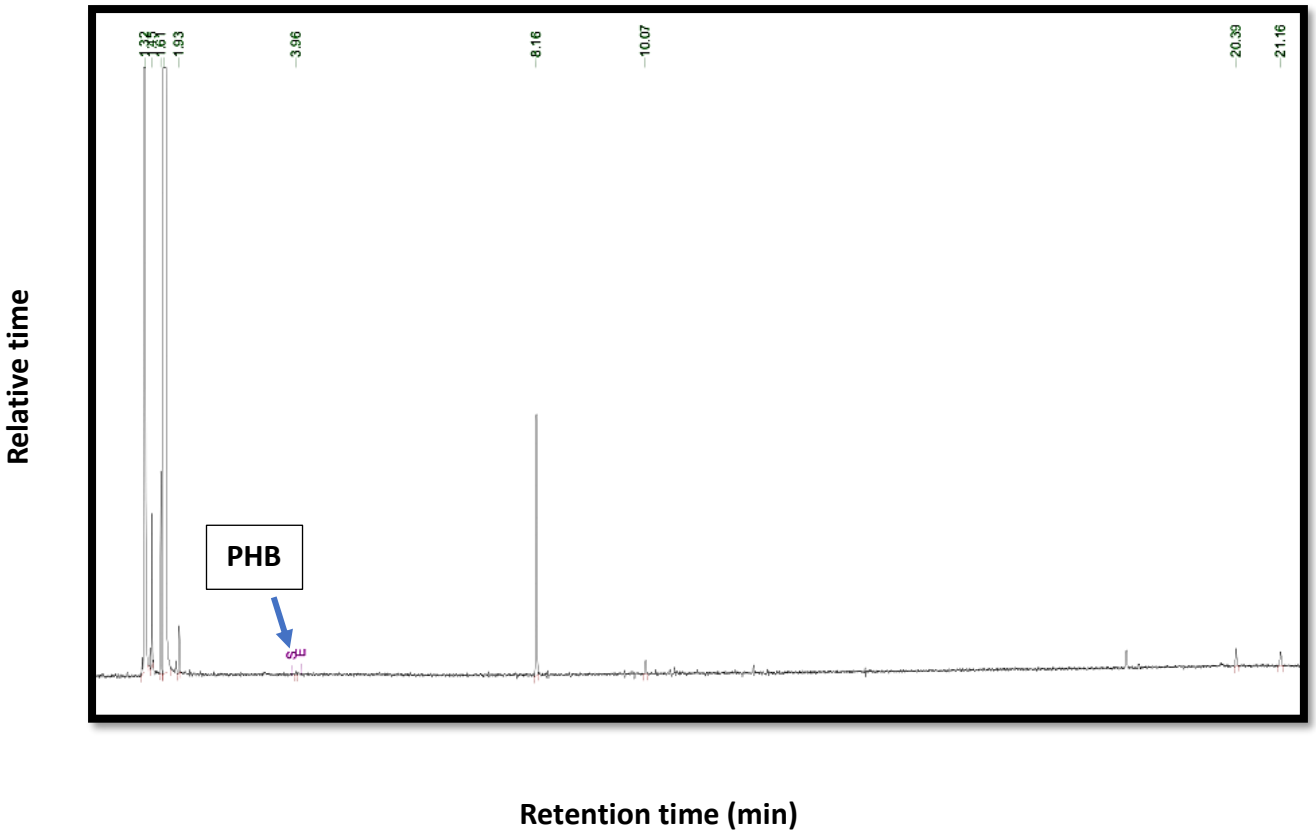

Figure 3.24: GC analysis of 3-hydroxybutyric acid produced in WT yeast transformed with plasmid pAB5 (PhaC1+PTS1, without GFP). Cells were harvested after 48 hrs of culture in 50ml oleate media of a 250ml flask. In the chromatogram, the retention time for PHB is marked with an arrow. The retention time of the target PHB is 3.96 minutes.

Table 3.1: This table represents the quantification of polymer synthesised by recombinant *S. cerevisiae* strains **[**WT+pAB5 (PhaC1+PTS1, without GFP and *atg36*Δ+pAB5 (PhaC1+PTS1, without GFP)] grown in oleate media utilising Gas Chromatography (GC). This analysis was performed with methanolysis derivatives, and the results are expressed as weight percent. (It is crucial to note that this study represents a single experimental run. Due to covid restrictions, did not get enough access to conduct further experiments to Roy's lab).

Samples	DCW in CHCl3 (g/L)	Peak area (Y-axis)	Concentration (g/L) (X-axis)	Polymer content (%)
WT+pAB5 (PhaC1+PTS1, without GFP) cultured in 600 ml of oleate media	8.45000	11.66	0.009383173	0.11 %

*atg36*Δ+pAB5 (PhaC1+PTS1, without GFP) cultured in 600 ml of oleate media	7.60000	21.35	0.017181024	0.23%
*atg36*Δ+pAB5 (PhaC1+PTS1, without GFP) cultured in 50 ml of oleate media	0.15000	19.43	0.015635939	0.104%
WT+pAB5 (PhaC1+PTS1, without GFP) cultured in 50 ml of oleate media	2.30000	10.57	0.008506015	0.37%

The study aimed to determine the polymer content in recombinant yeast using chloroform ($CHCl_3$) as a solvent. The analysis was conducted by weighing a known volume of each sample, extracted polymer utilising $CHCl_3$. The peak area for each sample was measured with GC and it corresponds to the presence of polymer in the sample. The concentration of polymers was calculated based on the peak area values. This step involved the conversion of peak area to concentration using appropriate calibration factors. The polymer content (%) was determined by comparing the concentration of polymers in the sample to the initial sample mass or volume. The formula used was, Polymer Content (%) = (Concentration of Polymers / Initial Sample Mass or Volume) x 100. The results displayed variations in polymer content between samples, with the *atg36Δ*+pAB5 samples showing higher polymer content compared to the WT+pAB5.

This analysis also aimed to detect polymer content in recombinant cells grown in YPO media. The results revealed variations in polymer content between the two sample sets, with *atg36Δ*+ pAB9 having a higher PHB content compared to the *mdh3/gpd1*Δ+ pAB5 sample. PHB concentration was determined by measuring the peak area in samples. The result was used to calculate the concentration of PHB in the samples.

In the investigation of polyhydroxyalkanoates (PHAs) production in yeast, the obtained PHA content of 0.37% serves as a pivotal metric to be evaluated in the context of existing literature. In a previous study, a genetically modified strain of *Yarrowia lipolytica* was created by introducing the PhaC1 gene from *Pseudomonas aeruginosa* PAO1 with a PTS1 peroxisomal

signal. The study found that when the codon optimized PhaC1 was present in a single copy, it enabled the synthesis of 0.205% DCW of PHA after 72 hours of cultivation in a YNBD medium containing 0.1% oleic acid. However, employing a multi-copy integration approach resulted in an increase of PHA content to 2.84% DCW when the YNBD concentration of oleic acid was raised to 1.0%. Additionally, when the recombinant yeast was grown in a medium containing triolein, PHA production increased to 5.0% DCW with as much as 21.9 g/L DCW, equivalent to 1.11 g/L in the culture (Gao *et al*., 2015). This variability necessitated a detailed examination of the methodologies employed, highlighting the role of factors such as carbon source selection, fermentation parameters, and genetic modifications in influencing PHA accumulation.

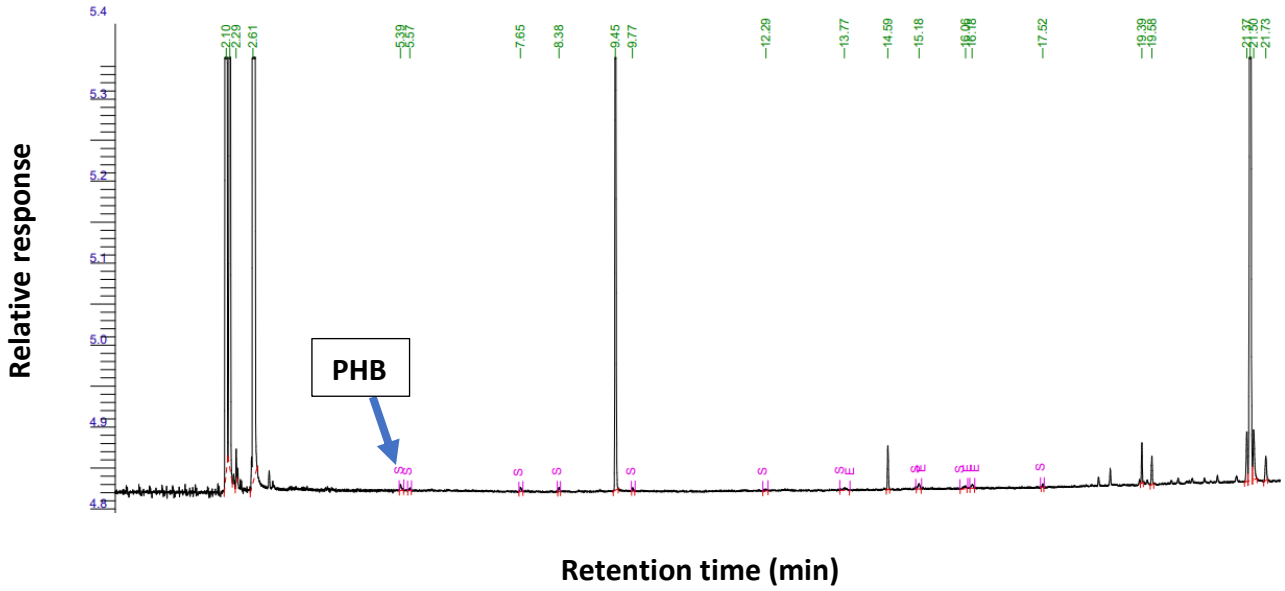

Figure 3.25: GC analysis of 3-hydroxybutyric acid produced in *atg36*Δ yeast strain transformed with plasmid pAB9 (synthetic PHA synthase, PhaC1+PTS1, without GFP). Cells were harvested after 48 hrs of culture in 50ml YPO media in a 250ml conical flask. In the chromatogram, the retention time for PHB is marked with an arrow. The retention time of the target PHB is 5.39 minutes.

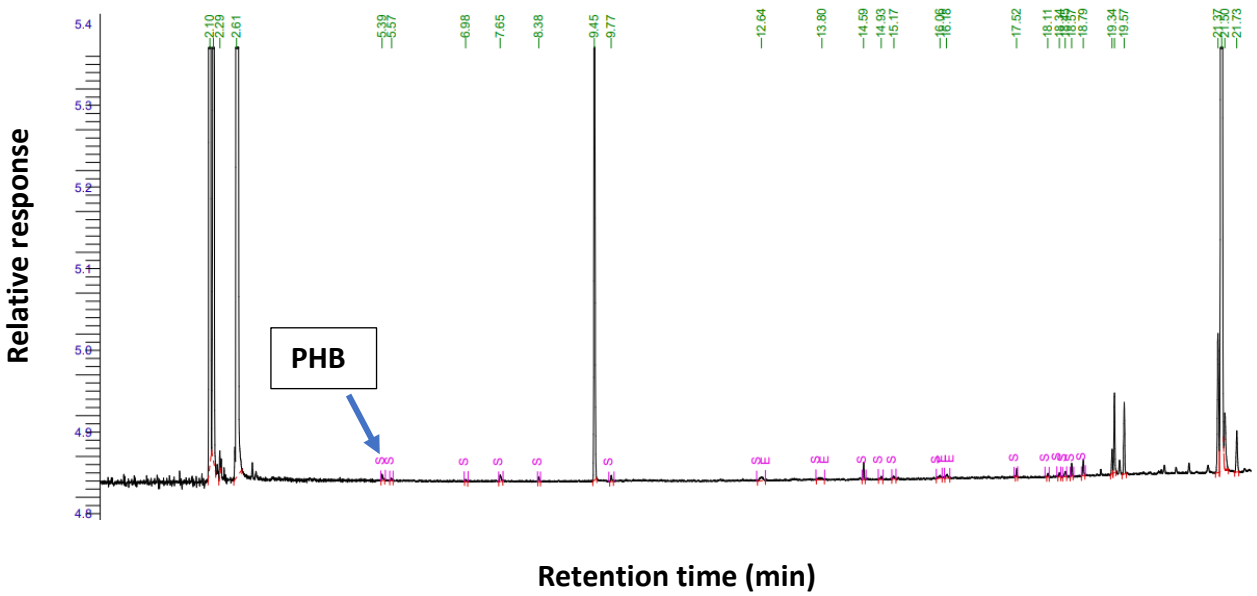

Figure 3.26: GC analysis of 3-hydroxybutyric acid produced in *mdh3/gpd1Δ* yeast strain transformed with plasmid pAB5 (PhaC1+PTS1, without GFP). Cells were harvested after 48 hrs of culture in 50ml YPO media in a 250ml conical flask. In the chromatogram, the retention time for PHB is marked with an arrow. The retention time of the target PHB is 5.39 minutes.

Table 3.2: This table represents the quantification of polymer synthesised by recombinant *S. cerevisiae* strains *atg36Δ* with plasmid pAB9 (synthetic PHA synthase, PhaC1+PTS1, without GFP) and *mdh3/gpd1Δ* with plasmid pAB5 (PhaC1+PTS1, without GFP) grown in YPO media utilising Gas Chromatography (GC). This analysis was performed with methanolysis derivatives, and the results are expressed as weight percent.

Samples	DCW in $CHCl_3$			HB					[PHA]	
	DCW(g)	$CHCl_3$ g/mL	$CHCl_3$ g/L	Peak Area	$CHCl_3$ mg/l	Real mg/L	g/L $CHCl_3$	M	%	g/L
atg36Δ + pAB9(synthetic PHA synthase, PhaC1+PTS1 without GFP)	0.0160	0.00400	4.000	14.42	5.08	10.16	0.01	0.0024	0.3%	0.010
mdh3/gpd1Δ + pAB5 (PhaC1+PTS1, without GFP)	0.0282	0.00705	7.050	12.90	4.54	9.09	0.01	0.0021	0.1%	0.009

In summary, NMR and GC are two distinct analyses used in this study for detecting and characterising polymers in recombinant yeast. NMR spectroscopy manifests detailed information regarding polymer structure but might have some limitations about sensitivity. On the other hand, GC is highly sensitive and suitable to quantify polymer content but is primarily focused on the quantification of monomers, and does not offer structural insights. NMR and GC analysis combinedly validate the characterisation of PHA, providing a comprehensive analysis of polymer composition. The assignment of peaks at 1.22 ppm, 2.4 ppm, and 5.2 ppm in the proton NMR spectrum strongly suggests the presence of polyhydroxybutyrate (PHB), a short-chain length polymer. The chemical shifts are in accordance with the expected resonances for the methyl, methylene, and methine protons within the PHB polymer observed in Figures 3.13 and 3.14, providing valuable information about the molecular composition and confirming the presence of this biopolymer in the analysed samples (WT+pAB5 and *atg36Δ*+pAB5). In examining PHB production, distinct patterns emerged based on yeast strain selection. For instance, *atg36Δ* with plasmid containing PHA synthase gene with PTS1, without GFP exhibited a higher overall PHB content compared to *mdh3/gpd1Δ,* with plasmid containing PHA synthase gene with PTS1, without GFP using oleate media suggesting inherent differences in the strains' metabolic capabilities or regulatory pathways influencing PHA synthesis. In essence, both of these analyses simultaneously affirm the effective incorporation of the PHA synthase gene (PhaC1/PhaC2) from *P. mendocina* into *S. cerevisiae* for the production of PHA.

3.5 Discussion

Production of PHA utilising the PHA synthase gene from *P. mendocina* in various locations of *S. cerevisiae* exhibited a promising avenue for sustainable bio-based polymer synthesis. This study highlighted the potential of exploiting microbial cell factories to produce bioplastic as an alternative to traditional plastics. This section spotlights the implications of our findings, the potential challenges, and benefits incorporated with this approach along with new avenues for future research.

The target localisation of genes plays a vital role in evaluating the efficiency of metabolic pathways. We investigated in this study, the impact of targeting PhaC1 and PhaC2 to different compartments such as peroxisomes and cytosol of *S. cerevisiae.* By using specific localisation sequences, PTS1, we successfully drove PhaC1 and PhaC2 to the distinct compartment, peroxisomes. The results from this study indicated that compartmental localisation significantly influenced PHA production by influencing the availability of substrates and co-factors to that compartment.

Targeting PhaC1 and PhaC2 to peroxisomes, organelles that are involved in lipid metabolism can facilitate PHA production. Localising to peroxisomes exploited the capability of compartmentalising reactions by these organelles to prevent appalling metabolic crosstalk. This outcome aligns with the concept of channelling of metabolism, where the proximity of enzymes involved in a particular pathway amplifies the substrate flow and ultimately end-product formation. Peroxisomes play a crucial role in fatty acid metabolism and this study suggests that targeting the PHA synthase gene to peroxisomes can promote the efficient conversion of intermediates to PHA precursors through the presence of relevant enzymes in this compartment.

The implementation of this strategy still provides some challenges. Corroborating the transport of intermediates along with substrates to the expected compartments demands a comprehensive understanding of the transport mechanism in cells and possible setbacks. Moreover, achieving an equitable expression of PHA synthase involved in PHA biosynthesis is pivotal to preventing disparity in metabolic pathways, that might lead to suboptimal or no PHA production.

This study revealed that PHA production is inhibited due to the presence of GFP (Figure 3.16). We investigated a number of plasmids containing PHA synthase gene with GFP and PTS1, transformed with WT and *atg36Δ* strains of *S. cerevisiae*. Surprisingly the recombinant organisms did not accumulate polymer, despite functional GFP expression along with PTS1 localisation. The concrete mechanism behind this phenomenon remains to be unravelled and mandates further investigation. This finding spotlights the significance of considering potential interactions between metabolic pathways and heterologous genes while engineering microbes for polymer production. Future research is required to elucidate the intricate interplay between PHA synthesis and GFP expression in recombinant yeast.

To achieve maximum yield and efficiency, it is essential to optimise the fermentation conditions. Several factors play a crucial role in the optimisation strategy, including the availability of carbon sources, temperature, pH, and aeration. The potential impact of targeting a specific organelle on overall cell physiology requires careful assessment, considering the potential repercussions of some factors such as growth rate, yield of biomass, and use of energy. Furthermore, downstream processing for extraction of PHA and isolation would require to be adapted and deployed on the compartmental localisation of PHA accumulation.

Looking ahead, this study provides valuable insights, but several avenues remain for further development and research. Exploring other cellular compartments, optimising production levels, and unravelling the regulatory mechanisms that maintain localisation could collectively furnish our comprehensive understanding of PHA biosynthesis in *S. cerevisiae*. Moreover,

evaluating the performance of engineered strains under unconventional growth media such as rice wastewater and in larger fermentation scales will be decisive for the assessment of the viability of PHA production following this strategy.

Rice wastewater is a plentiful and underused asset produced from the parboiling process of paddy. The use of rice wastewater as a growth media for conventional yeast, *S. cerevisiae,* offers a cost-effective alternative and substitute for regular synthetic media to reduce the production cost related to PHA bioprocessing. This would certainly make PHA production more competitive and economically viable in Biotechnology. Therefore, we aim to establish the organic content and nutrient composition of rice waste effluent from Bangladesh, the fourth-largest producer of rice in the world (Muthayya *et al*., 2014) to contribute to the sustainable production of polymer by using the rice waste stream. Chapter 4 explores the constituents of rice wastewater from rice mills in Bangladesh to justify its suitability as a potential candidate for microbial growth and bioproduction application.

In conclusion, this research underscores the significance of protein localisation for modulating PHA production in peroxisomes of *S. cerevisiae* cells. By targeting different cellular compartments for PhaC1 and PhaC2, this study demonstrated the potential of PHA yield by facilitating substrate flow and enhancing cofactor availability. These outcomes add value to the metabolic engineering domain and pave the way for the development of environmentally friendly and sustainable production by utilising waste streams of rice mills from the targeted place.

Chapter 4: The constituents of rice wastewater from rice mills in Bangladesh

4.1 Introduction

Pollution has appeared as a major global threat in recent years and is impacting the ecosystem significantly. The exponential growth of the population of humans is the prime reason contributing to pollution, resulting in various forms of contamination, for instance, water, soil, air including groundwater. Human beings are the key contributors to pollution on this planet (Hammer and Hammer Jr, 2013). Notably, water pollution is a vital issue now, due to the release of untreated industrial effluent into the water bodies such as lakes, rivers, and streams (Rajaram and Das, 2008). Approximately two million tons of waste effluents are discharged into surface water bodies every day around the world. The situation is even more critical in developing countries where 70% of untreated industrial wastewater and more than 90% of raw sewage are released into water bodies (Azizullah *et al*., 2011).

Bangladesh has been experiencing an indistinguishable situation as a developing nation with its growing population and sanitation facilities. Bangladesh has a population of 173 million people (worldometer, 2023) and the People's Republic of Bangladesh Country Overview (2020) reported that 98% of people have access to water and only 56% have proper sanitation facilities. However, WHO estimated that a staggering 60% of people have no access to safe drinking water and that the overall system of wastewater management is ineffective (Arefin and Mallik, 2017). The population in Bangladesh is continually increasing and leading to a rise in industries to meet the growing demand including agro industries, catering to the rising demand for food. Rice mills are an indispensable part of the expanding industry.

Rice has immense significance as a staple food for many countries including Bangladesh and oversees the bulk of the world's rice production (Muthayya *et al*., 2014). Several methods are available to produce edible rice in Bangladesh, but parboiling is the most used method. Parboiling typically follows two simple steps. In the beginning, the grains are soaked in water for several hours followed by steaming for 20 to 30 minutes (Kumar and Deswal, 2021). A substantial amount of wastewater is originated throughout the parboiling process amounting to 1.5 to 2 litres per kilogram of paddy depending on the moisture content of the paddy, the amount and type of paddy, and the capability of the boilers (Islam *et al.*, 2020). Most of the rice mills discharge wastewater and other by-products on land or nearby waterbodies which holds a high amount of organic and inorganic component (Islam *et al*., 2020). Throughout the

milling process, numerous components from the paddy such as starch, lipids, proteins, and other organic elements are released in waste effluent. Moreover, inorganic components for example, metals, minerals, and chemical residues may also be available in the effluent (Kumar and Deswal, 2021).

The chemical composition of the waste effluent produced by the rice mills may vary from one to another mill. A range of factors could be responsible for these differences like the type and quality of paddy being processed, the specific milling process employed, and the quality and quantity of incoming water (Kumar and Deswal, 2021). However, there has been a lack of scientific research regarding organic and inorganic constituents of rice wastewater generated in Bangladesh. One of the objectives of this study is to evaluate the water quality parameters of the waste effluent from rice mills in Bangladesh to determine the constituents and to assess the methodology of conversion of rice wastewater to biomass and bioplastics. Rice waste effluent produced during the process of parboiled rice in Bangladesh is simply discharged on land or into the surface water every year leading to eutrophication and foul odour generation which ultimately create a negative impact on the environment and public health (Kumar *et al.,* 2017). The prime aim of this study is to utilise nutrient-rich waste effluent to grow conventional yeast along with the production of high-value products, Polyhydroxyalkanoates (PHAs), and biomass. This approach not only contributes to environmental sustainability by repurposing agricultural waste streams but also offers a valuable strategy for the eco-friendly production of biopolymer and biomass. Chapter 4 focuses on the results of the analysis conducted on rice wastewater collected from Bangladesh in two distinct stages from two different rice mills to assess the suitability of the rice waste stream as a substrate for yeast culture (relevant data are available in Chapter 5, Section 5.3).

4.2 Rationality of elemental analysis of rice wastewater

The primary objective of this project was to investigate the composition of rice waste effluent from Bangladesh's rice mills. The study was, therefore, aimed to assess the pollutant concentration in waste effluent to gain insights into the characteristics and potential impact on the environment. The concentration of various components in rice wastewater is a critical aspect to understand, particularly in the context of water quality assessment. The impact of these components on water quality can be substantial to employ the waste effluent for the cultivation of yeast.

Rice wastewater samples were collected by one of our collaborators from Bangladesh, Professor Morsaline Billah (Biotechnology and Genetic Engineering, Khulna University, Bangladesh) from two rice mills namely Soha auto-rice mill and Zia auto-rice mill situated in Dinajpur district, the region known for its significant rice production in Bangladesh. We

received the samples for the required analysis, from another collaborator, Professor Ipsita Roy (Material Science and Engineering, University of Sheffield) who first received the samples from Professor Morsaline. Water samples were taken in two different stages, known as before boiling (the paddy was soaked in water for several hours) and after boiling, the final step of the milling process, representing two key points in wastewater production.

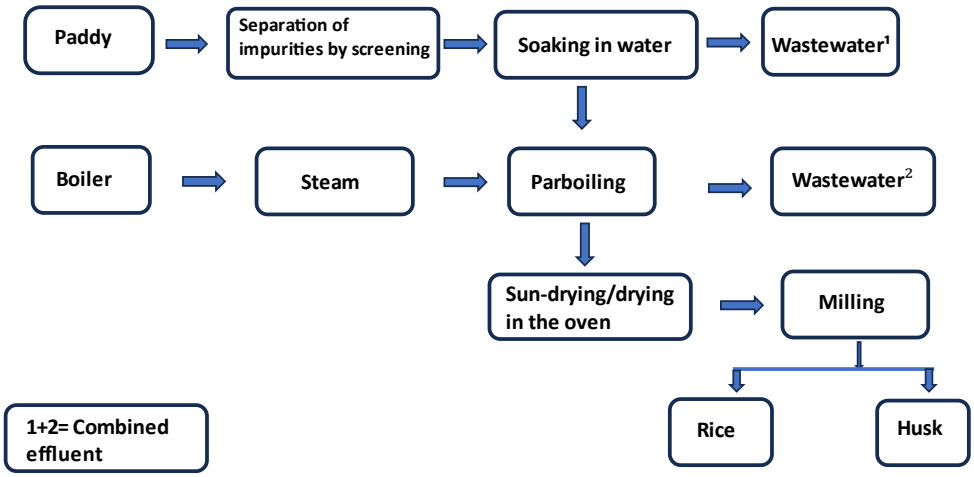

Figure 4.1: Flow chart shows the procedure of rice parboiling in a rice mill. Wastewaters 1 and 2 generate combined effluent in a rice mill. Modified and reproduced from (Pradhan and Sahu, 2004).

To establish the composition of rice wastewater samples delivered from Bangladesh for this study were analyzed by Inductively Coupled Plasma spectroscopy. Samples were analyzed by Inductively coupled Plasma-Mass Spectrometry (ICP-MS) to assess element concentrations. This technique uses a high ionization energy (argon-plasma) to produce elemental ions from liquid samples, then positive ions are separated and quantified based on their mass-to-charge ratio as described in the website of the University of Sheffield (https://www.sheffield.ac.uk/mass-spectrometry/chemms/inductively-coupled-plasma spectroscopy). This chapter represents the outcomes obtained from ICP-MS and NMR experiments and provides a brief analysis and discussion of the findings. The following isotopes were measured through this analysis: ^{24}Mg, ^{31}P, ^{34}S, ^{43}Ca, ^{53}Cr, ^{54}Fe, ^{63}Cu, ^{66}Zn, ^{75}As, ^{111}Cd, ^{202}Hg, and ^{208}Pb. The careful selection of these elements reflects a strategic approach aimed at comprehensively characterizing the nutritional content of rice wastewater for yeast culture while simultaneously evaluating the potential impact of heavy metal

contaminants. This analytical strategy aligns with the dual objectives of understanding the suitability of rice waste effluent for yeast-based processes and ensuring its safety in broader contexts. A study in Sambalpur (Orissa) revealed the physicochemical properties of parboiled rice effluent including the highest permissible limits as per Indian Standard Institution guidelines which are presented below (Sayanthan and Thusyanthy, 2018).

Table 4.1: Recommended limits on wastewater effluent published by the Indian Standard Institution (Sayanthan and Thusyanthy, 2018).

Physico-chemical characteristics of the effluent of a rice mill at Sambalpur, Orissa with their maximum permissible limits as recommended by Indian Standard Institution

Parameters	Range	Mean ±SD	ISI limit of discharge of industrial effluents	
			On land for Irrigation (ISI, 1977)	Into inland surface waters (ISI, 1974)
Colour		Brown	-	-
Odour		Unpleasant	-	-
Temperature (^{0}C)	35.0-48.0	38.0±5.09	-	40
Conductivity (µho/cm)	0.46-0.86	0.66±0.15	-	-
pH	7.2-8.8	8.0±0.54	5.5-9.0	5.5-9
Total Solids (mg/L)	998.1-1459.1	1200.0±189.48	-	-
TSS (mg/L)	432.5-576.0	530.0±53.00	100	100
TDS (mg/L)	522.1-833.1	670.0±1.49.2	2100	2100
Dissolved Oxygen (mg/L)	0.2-1.6	0.9±0.52	-	-
BOD at 20^{0}C(mg/L)	312.1-540.1	450.0±76.61	100	30
COD (mg/L)	400.2-892.1	630.0±183.03	-	-
Total Alkalinity (mg/L)	180.7-340.1	272.0±58.29	-	-
Total hardness (mg/L)	98.3-256.4	182.0±59.84	-	-
Ca hardness (mg/L)	38.4-98.3	78.0±22.22	-	-
Mg hardness (mg/L)	14.1-24.3	21.0±3.68	-	-
Chloride (mg/L)	95.1-170.3	140.0±28.06	600	1000
Sulphate (mg/L)	28.4-70.1	40.0±15.66	1000	1000
Phosphate (mg/L)	10.1-35.2	21.0±11.11	-	-
Nitrate (mg/L)	0.3-0.8	0.5±0.15	-	-
Sodium (mg/L)	213.4-263.7	235.0±20.34	60%	-
Potassium (mg/L)	14.1-32.1	20±7.12	-	-
Phenols (mg/L)	13.3-50.4	35.0±13.98	-	1.0
SiO_2 (mg/L)	35.4-75.1	58.0±15.5	-	-

This study investigated and compared the concentrations of various components present in rice wastewater collected from both Zia and Soha rice mills before and after boiling samples.

Table 4.2. Concentration of different components present in rice wastewater (before boiling, and after boiling samples) collected from Zia rice mill and Soha rice mill, Dinajpur, Bangladesh.

	Before-boiling (Zia rice mill)	After-boiling (Zia rice mill)	Before-boiling (Soha rice mill)	After-boiling (Soha rice mill)
Elements	Concentration (mg/L)	Concentration (mg/L)	Concentration (mg/L)	Concentration (mg/L)
Calcium (Ca)	14.109	22.33	6.46	10.44
Magnesium (Mg)	11.71	27.28	5.34	14.13
Phosphorus (P)	27.241	109.46	17.99	37.95
Sulphur (S)	15.33	27.36	23.72	19.8
Potassium (K)	98.96	154.7	131.1	138
Copper (Cu)	0.0278	0.101	0.016	0.059
Chlorine (Cl)	30.17	93.77	104.84	42.33
Manganese (Mn)	2.03	6.74	1.30	2.86
Aluminium (Al)	0.0024	0.236	0.01	0.027
Iron (Fe)	2.17	3.38	0.96	2.56
Zinc (Zn)	0.131	0.363	0.079	0.184
Chromium (Cr)	0.0034	0.007	0.004	0.007

Arsenic (As)	0.01048	0.054	0.024	0.0319
Cadmium (Cd)	0.000178	0.000782	0.00007	0.000272
Mercury (Hg)	0.000049	0.000086	0.000068	0.000134
Lead (Pb)	0.002	0.0085	0.004	0.0073

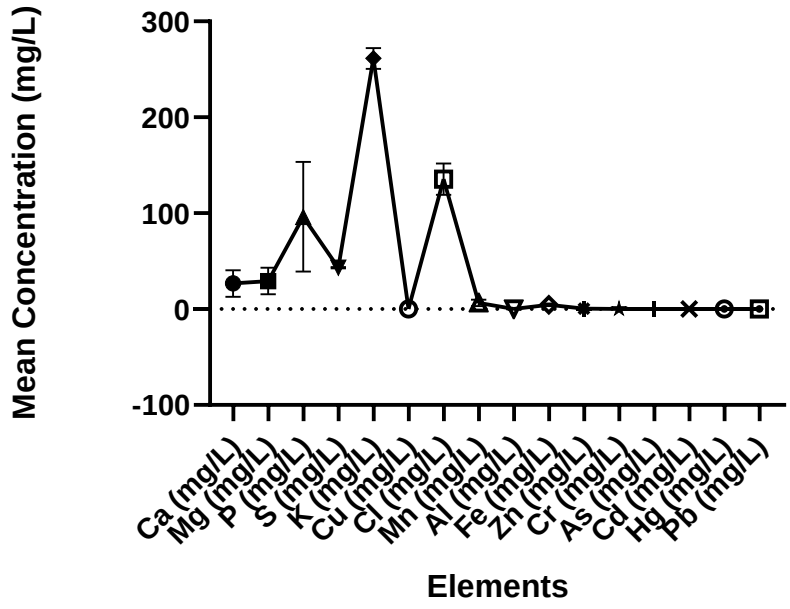

Figure 4.2: Mean concentration of inorganic elements (Ca: 26.67 mg/L, Mg: 29.24 mg/L, P: 96.32 mg/L, S: 43.11 mg/L, K: 261.38 mg/L, Cu: 0.102 mg/L, Cl: 135.55 mg/L, Mn: 6.465 mg/L, Al: 0.137 mg/L, Fe: 4.53 mg/L, Zn: 0.37 mg/L, Cr: 0.01mg/L, As: 0.05 mg/L, Cd: 0.00027 mg/L, Hg: 0.00016 mg/L, Pb: 0.01 mg/L) present in rice wastewater samples obtained from Bangladesh.

All the above findings (mentioned in section 4.2) are discussed in detail in the following sections 4.3 and 4.4.

4.3 Analysis of inorganic compounds

It is pivotal to determine the physicochemical constituents available in the waste effluent following the cultivation of rice. A comprehensive list of elements and properties was detected in the samples, as detailed below.

4.3.1 Colour: The colour of waste effluent depends on several factors such as the presence of organic and inorganic matters, microbiological matters, as well as industrial wastes. In this case, a visual inspection was conducted utilizing the eyes as a method of analysis to determine the hue of rice wastewater. Before boiling rice wastewater from both Soha and Zia rice mills appeared light brown whereas after boiling water from both mills was dark brown in colour.

4.3.2 Odour: The smell of the rice wastewater from both mills was detected when the samples were brought in proximity to the nose and found unpleasant. This might be attributed to the presence of organic matter and microorganisms in the sample. The offensive odour affects the quality of the water and can trigger nausea and vomiting in sensitive individuals.

4.3.3 pH: The pH value indicates the concentration of hydrogen ions and provides an alkalinity level present in effluent or water. pH values of both before and after boiling samples from both mills ranged from 5.5 to 6. pH plays a critical role in biological and chemical reactions, as these functions are optimal within specific pH ranges. Based on the pH value of the analyzed samples, it was determined that all the samples were slightly acidic. According to the Indian Standard Institution (ISI), the recommended limit of pH (Table 4.1) for the release of industrial effluents on land for irrigation and into inland surface water is between 5.5 to 9.0 (Sayanthan and Thusyanthy, 2018). A previous study found that the pH value of groundwater samples collected from Dinajpur, Bangladesh ranged from 5.32 to 7.00 (Uddin, 2004; Islam *et al*., 2020).

4.3.4 Total dissolved solids (TDS): Both organic and inorganic soluble compounds found in wastewater are referred to as total dissolved solids. To determine TDS, a measured amount of waste effluent was centrifuged, harvested the pellets followed by freeze-drying for 24 hours. Samples were measured before and after freeze-drying. Upon analysis of the studied samples, it was found that total dissolved solids ranged between 140,000 to 200,000 mg/L. The obtained mean value for the total dissolved solid was 170,000 mg/L. The concentration value of dissolved solids in effluents was found to be much higher than the acceptable limit (Table 4.1) recommended by ISI (2100 mg/L) for discharging industrial effluent on land or inland water (Sayanthan and Thusyanthy, 2018). TDS concentration of groundwater in

Dinajpur district, Bangladesh was reported to be between 52.02 to 422.51 mg/L (Uddin, 2004).

4.3.5 Calcium (Ca): The analyzed samples exhibited a diverse range of calcium concentrations**.** The concentration of calcium in before, after, and combined boiling samples from the Zia rice mill was 14.109, 22.33, and 36.44 mg/L respectively (Table 4.2), while samples from the Soha rice mill had 6.46, 10.44, and 16.9 mg/L of calcium in before, after and combined boiling effluents (Table 4.2). Calcium concentration in water is heavily influenced by the solubility of $CaSO_4$, $CaCO_3$, and occasionally by $CaCl_2$ (Karanth, 1994). The mean value of calcium in this study was 26.67 mg/L (Figure 4.2). Uddin (2004) discovered that in Dinajpur, Bangladesh, the concentration of calcium in groundwater ranged from 4.21 to 72.54 mg/L.

4.3.6 Magnesium (Mg): The concentration of Mg in before, after, and total boiling samples from the Zia rice mill was 11.71, 27.28, and 39 mg/L (Table 4.2), whereas 5.34, 14.13, and 19.48 mg/L of Mg concentrations were detected in before, after and combined boiling samples from the Soha rice mill (Table 4.2). In this study, the mean value of magnesium was 29.24 mg/L (Figure 4.2). According to Uddin (2004), Mg concentration in the groundwater of Dinajpur, Bangladesh ranged from 0.85-18.60 mg/L. Interestingly, it was discovered that the concentration of Mg in the samples was higher than that reported in Dinajpur's groundwater.

4.3.7 Phosphorus (P): Zia samples, before boiling, after boiling, and combined waste effluent showed a phosphorus content ranging from 27.241, 109.46, and 136.7 mg/respectively (Table 4.2). In contrast, samples from Soha rice mills showed 17.99, 37.95, and 55.94 mg/L before, after, and combined boiling effluents (Table 4.2). The analysis revealed the mean concentration of phosphorus was 96.32 mg/L (Figure 4.2). The reported phosphorus content in the Dinajpur area, Bangladesh groundwater varies from 0.001-1.08 mg/L (Hossain, 2014). It is worth noting that the concentration of phosphorus in all the studied samples was significantly higher than the reported range of groundwater in Dinajpur.

4.3.8 Sulphur (S): In the wastewater sample, the concentration of sulphate was set by ISI as 1000 mg/L for discharging on land and as well as surface water (Table 4.1). The gained mean value for sulfur found in this experiment was 43.11 mg/L as shown in figure 4.2, which suggested the level was within the acceptable limit.

4.3.9 Potassium (K): A natural element, potassium, is present in the solution but does not form any precipitation. As demonstrated in Tables 4.2, the concentration of potassium levels observed in both before and after samples from the Zia rice mill was 98.96, 154.7, and 253.67 mg/L (Table 4.2), whilst samples from another mill namely the Soha rice mill represented the concentration of potassium in before, after and total effluent was 131.1, 138 and 269.1 mg/L

respectively (Table 4.2). The mean value for potassium was found to be 261.385 mg/L in this study. This finding is noteworthy as it can be compared to the concentration of potassium in the groundwater of the same Dinajpur area, which was significantly lower, varying from 0.39 to 57.08 mg/L, when compared to the concentration observed in studied samples (Uddin, 2004).

4.3.10 Copper (Cu): To maintain good health, a small quantity of copper is required in our diet as it is a vital element for living organisms. However, excessive uptake of Cu could lead to serious health concerns including death (Awual *et al*., 2014). To safeguard public health, WHO and USEPA suggested a maximum permissible limit of copper ions in drinking water at 1.5 mg/L and 1.3 mg/L respectively (World Health Organization, 2004; Griffiths *et al*., 2012). The copper content in before, after, and total effluents of both Zia and Soha (Table 4.2) rice mills were 0.0278, 0.101, 0.129, 0.016, 0.059, 0.075 mg/L respectively, and within the limit. Figure 4.2 portrayed the mean concentration of copper analysed in this study as 0.102 mg/L.

4.3.11 Chloride (Cl^-): Chloride is a natural mineral that is present in all types of water. However, chloride concentration is relatively low in natural fresh water. While domestic sewage and industrial effluent are released into waterbodies, the chloride level tends to rise remarkably. In the case of wastewater from the Zia rice mill, the chloride concentration was 30.17, 93.77, and 123.94 mg/L in before, after, and combined boiling samples, as shown in Table 4.2. On the other hand, the chloride level was 104.84, 42.33, and 147.17 mg/L in before, after, and total boiling samples from the Soha rice mill, mentioned in Table 4.2. This investigation reported the mean concentration of chloride was 135.55 mg/L (Figure 4.2). The chloride concentration of groundwater in Dinajpur, Bangladesh varied from 5.67-63.46 mg/L (Uddin, 2004; Islam *et al*., 2020). Interestingly, samples from both rice mills showed a notable amount of chloride content compared to Dinajpur's groundwater. However, the concentration of chloride in the wastewater samples was within the maximum tolerance limit set by the Indian Standard Institution in terms of discharging effluent on land (600 mg/L) or into surface water (1000 mg/L) as reported in Table 4.1.

4.3.12 Manganese (Mn): One of the most common metals found in soil, water, air, or on the earth's surface is manganese. It can be available on both surface and groundwater either from natural sources or as a result of industrial discharges along with mining. Even though manganese is a basic nutrient at minor doses, it could create health concerns at high doses. At present, there is no mandatory maximum contaminant level for manganese in drinking water (Water Quality Association, 2023). The mean concentration of manganese in this study was found to be 6.465 mg/L in wastewater (Figure 4.2).

4.3.13 Aluminium (Al): There are several aluminium forms that exist in nature as hydroxides, silicates, aluminium oxide, and combined with different elements. The common ways for

aluminium to get into the water are through soil seepage, surface runoff, and acid rain due to industrial activity (Shallcross, 2022). While water flows over the rocks or soil accompanied by a dense concentration of aluminium, traces of it could dissolve in water. WHO (0.1- 0.2 mg/L) and USEPA (secondary maximum contaminant level: 0.05- 0.2 mg/L) have got guidelines for this metal in drinking water (Shallcross, 2022). The mean value for aluminium in rice wastewater samples was 0.137 mg/L, found to be within the limit for waste effluent (Figure 4.2).

4.3.14 Iron (Fe): Iron plays a vital role in our biological system as it is an essential mineral for human beings. Anaemia can develop due to insufficient intake of iron, a condition that leads to a reduction of red blood cell production and capacity of oxygen-carrying. On the other hand, excessive iron intake can be toxic to human health, leading to a condition called haemochromatosis, characterized by iron overload in tissues and organs resulting in tissue and organ damage (Singh *et al*., 1988). In stream water, the suggested iron content is 0.3 mg/L, higher than that might cause nausea, and vomiting (Vasu, 2008). The wastewater samples investigated in this research revealed the mean concentration of iron was found to be 4.535 mg/L, depicted in Figure 4.2.

4.3.15 Zinc (Zn): To maintain enzymatic processes, organisms require trace amounts of a few metal ions, for instance, copper (Cu), cobalt (Co), and zinc (Zn) as essential co-factor as they play crucial roles in biochemical reactions (Zhang *et al.*, 2014; Kozlowski *et al*., 2009). However, the presence of excessive amounts of these metals in living organisms could lead to complications due to their potential carcinogenicity, higher toxicity, and bioaccumulation capacity. Therefore, zinc-containing solid and liquid wastes are regarded as hazardous waste due to their non-biodegradability and toxicity (Zhang *et al.,* 2014; Kozlowski *et al*., 2009). WHO and USEPA recommended the maximum permissible concentration of zinc in drinking water is 5.0 mg/L (World Health Organization, 2004; Griffiths *et al.,* 2012). The mean value of zinc in the wastewater samples in this analysis manifested a low level (0.3765 mg/L) which is depicted in Figure 4.2.

4.3.16 Chromium (Cr): Hexavalent chromium, known for its toxicity, could disrupt human physiology and bioaccumulate in the food chain. This could lead to severe health issues varying from skin rashes and irritation to lung cancer (Chiha *et al.,* 2006). The acceptable limit for Cr (VI) for industrial effluents discharged into surface water is 0.1 mg/L, whereas, for drinking water, the acceptable limit is 0.05 mg/L (World Health Organization, 2004; Chiha *et al.,* 2006). The sample from the Zia rice mill showed 0.0034, 0.007 and 0.01 mg/L chromium was present in before, after, and combined effluent (Table 4.2). Similarly, before, after, and combined effluent had 0.004, 0.007, and 0.01 mg/L of chromium in Soha samples (Table 4.2). Both samples in different conditions including the mean value of 0.01 mg/L (figure 4.2) were within the permissible limits for chromium according to WHO guidelines.

4.3.17 Arsenic (As): Arsenic is a natural metalloid and commonly found in the earth's crust but its contamination in surface and groundwater is a serious concern (Singh *et al*., 2015). The major concern regarding arsenic is chronic exposure may lead to arsenic poisoning, even at low concentrations (Singh *et al.*, 2015). Arsenic poisoning could lead to severe health issues such as broncho-pulmonary disorder, chromosomal abnormalities, and lung, skin, or bladder cancer, predominant in Vietnam, India, Thailand, Bangladesh, Cambodia, Chile, Canada, and the southwest USA (Vadahanambi *et al*., 2013; Singh *et al.,* 2015). Therefore, As has been classified as the top toxic element and carcinogen by World Health Organization (WHO) and US Environmental Protection Agency (USEPA) (Gautam *et al.,* 2016). According to WHO, USEPA, and the Bureau of Indian Standards (BIS), the maximum permissible limit of arsenic should not exceed 0.05 mg/L in drinking water (Kouras *et al*., 2007; Sharma and Shon, 2009).

4.3.18 Cadmium (Cd): This heavy metal is naturally distributed in the earth's crust with an average concentration of 0.1-0.2 mg/kg and is often found incorporated with zinc (Masih *et al.*, 2009). Cd can substitute Zn in a few enzymes which may lead to alteration in the stereo structure of enzymes and make a defect in the catalytic activity of the enzymes (Jarup *et al.,* 2000). Cadmium has been classified as a probable human carcinogen by USEPA due to its potential health risks. The permissible limit for cadmium in drinking water has been set by both WHO and USEPA as 0.005 mg/L while 0.01 mg/L for wastewater (World Health Organization, 2004; Griffiths et al., 2012). Table 4.2 represents the amount of Cd in before, after, and combined effluents of the Zia rice mill were 0.000178, 0.000782, and 0.002 mg/L which indicates the level is within the limit. Samples from the Soha rice mill correspondingly contained 0.00007, 0.0000272, 0.000342 mg/L of cadmium in before, after, and combined effluents, which is also within the acceptable limit (Table 4.2). The mean value for cadmium showed an extremely low level (0.000271 mg/L) in this study (Figure 4.2).

4.3.19 Mercury (Hg): It is widely acknowledged that mercury is one of the most toxic metals found in the environment. The high toxicity of mercury poses a substantial amount of risk to both human health and as well as the ecosystem (Nickens *et al.,* 2010). Based on significant risks associated with mercury, WHO and USEPA set a strict upper limit of 0.001mg/L and 0.002 mg/L for Hg (II), the iconic state of mercury, for drinking water respectively (World Health Organization, 2004; Griffiths *et al.,* 2012).

4.3.20 Lead (Pb): USEPA has categorized lead as a major pollutant. Therefore, the maximum contaminant level of Pb ions for drinking water has been established by USEPA and WHO as 0.015 mg/L, an extremely low concentration and 0.05 mg/L respectively (Griffiths *et al*., 2012; World Health Organization, 2004). On the other hand, the maximum limit of Pb in wastewater should not exceed 5.0 mg/L, as recommended by WHO (Chopra and Pathak, 2015). Table 4.2 indicates 0.002, 0.0085, and 0.01 mg/L lead present in before, after, and combined effluent

of Zia rice wastewater and did not exceed the limit set by WHO. Likewise, rice wastewater from the Soha rice mill had an acceptable level of lead content with 0.004, 0.0073, and 0.011 mg/L in before, after, and total effluents (Table 4.2). Additionally, the mean value (0.0105 mg/L) was detected to be within the limits of USEPA and WHO (Figure 4.2).

4.4 Detection of major elements in the wastewater samples

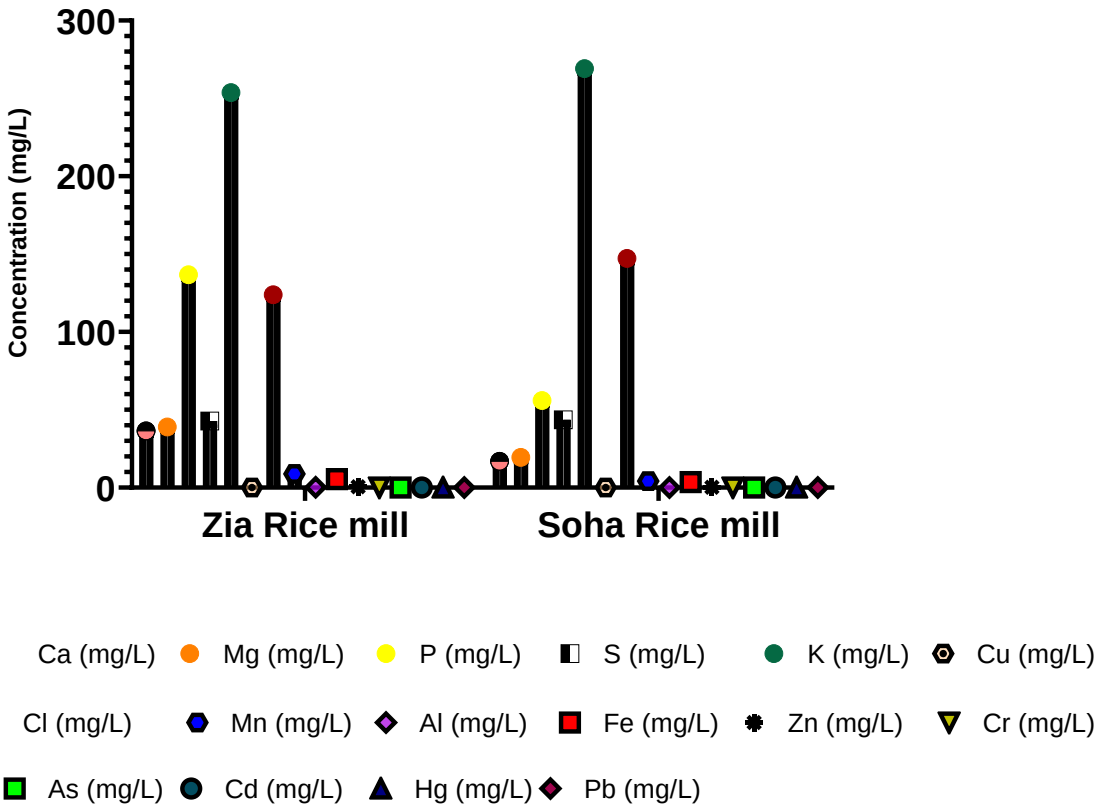

Figure 4.3: Comparative analysis of the constituents that were present in both samples of rice wastewater collected from Bangladesh.

This analysis aims to compare the contents of waste effluents from two different rice mills to understand any potential variations existed in them. Zia rice mill exhibited the presence of major elements in the order of K (253.67 mg/L)>P (136.7mg/L)>Cl (123.94 mg/L)>S (42.7

mg/L)>Mg (39 mg/L)>Ca (36.44 mg/L)>Mn (8.77 mg/L). In contrast, the order of elements in Soha sample was K (269.1 mg/L)>Cl (123.94 mg/L)>P (55.94 mg/L)>S (43.53 mg/L)>Mg (19.48 mg/L)>Ca (16.9 mg/L)>Mn (4.16 mg/L). The analysed samples in this study displayed a common order of metals present regarding their relative concentrations, albeit with differences in actual values. Potassium persistently remains with the highest value, followed by chlorine, phosphorus, sulphur, magnesium, calcium, and manganese. This order indicates a potential trend present in the elemental concentration of studied rice wastewater samples.

4.5 Characterization of organic compounds using Nuclear Magnetic Resonance (NMR) spectroscopy

Nuclear Magnetic Resonance (NMR) spectroscopy is one of the most powerful analytical techniques that present detailed and elaborate insights into the molecular content of organic substances. This section of Chapter 4 reveals, NMR findings of organic components in rice waste effluent samples of Zia and Soha rice mills (both before and after boiling samples) obtained from Dinajpur, Bangladesh.

Interpretation of NMR results

Rice wastewater is generated from different stages of rice processing, including soaking and parboiling (Figure 4.1). Samples from both stages were analysed by NMR. All samples were processed simply by addition of 10% deuterium oxide (D_2O) to provide a field/frequency lock. Trimethylsilyl Propionate (TSP) was used as an internal reference to provide a 0 ppm for aqueous solvents as well as the concentration standard and subjected to NMR analysis. Particularly, this analysis focused on the identification and quantification of organic content in rice waste effluent samples.

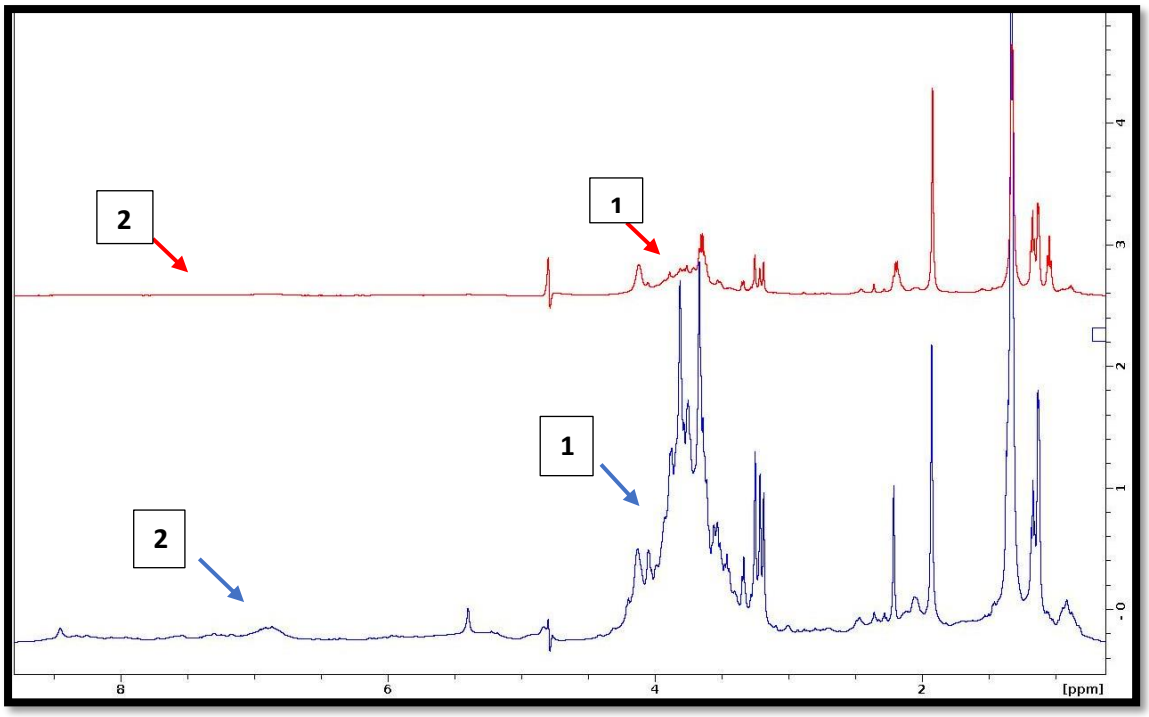

Figure 4.4: ^{1}H-NMR spectra of rice wastewater from Zia rice mill displayed the chemical shifts of proton in water suppression. After boiling spectrum is shown in blue and before boiling spectrum is overlaid in red. The increased concentrations of both sugars and protein in after boiling are clear. Peaks are labelled with 1, indicating the presence of complex sugars in the samples, whereas label 2 suggests the existence of protein content. The residual water signal after suppression is at 4.7 ppm.

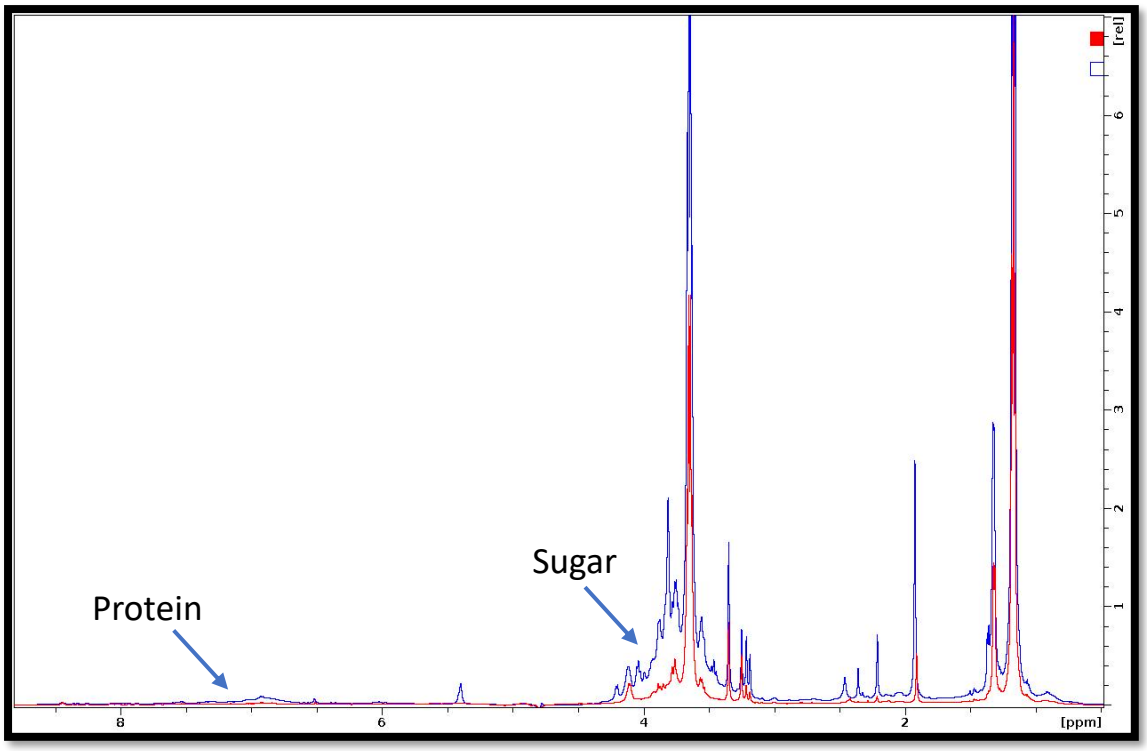

Figure 4.5: NMR spectra from before boiling (red) and after boiling (blue) samples of Soha rice mill. The spectra are set to the same intensity of the TSP signal (0 ppm), meaning that changes in intensity between the two spectra are proportional to changes in concentration. The spectra illustrate the changes in intensities of peaks between 3.38 to 4.3 ppm for carbohydrate molecules, also between 6.6 to 9.2 ppm for protein content. The spectra highlight the differences in organic content amounts present in the samples, aiding and identifying variation between those samples.

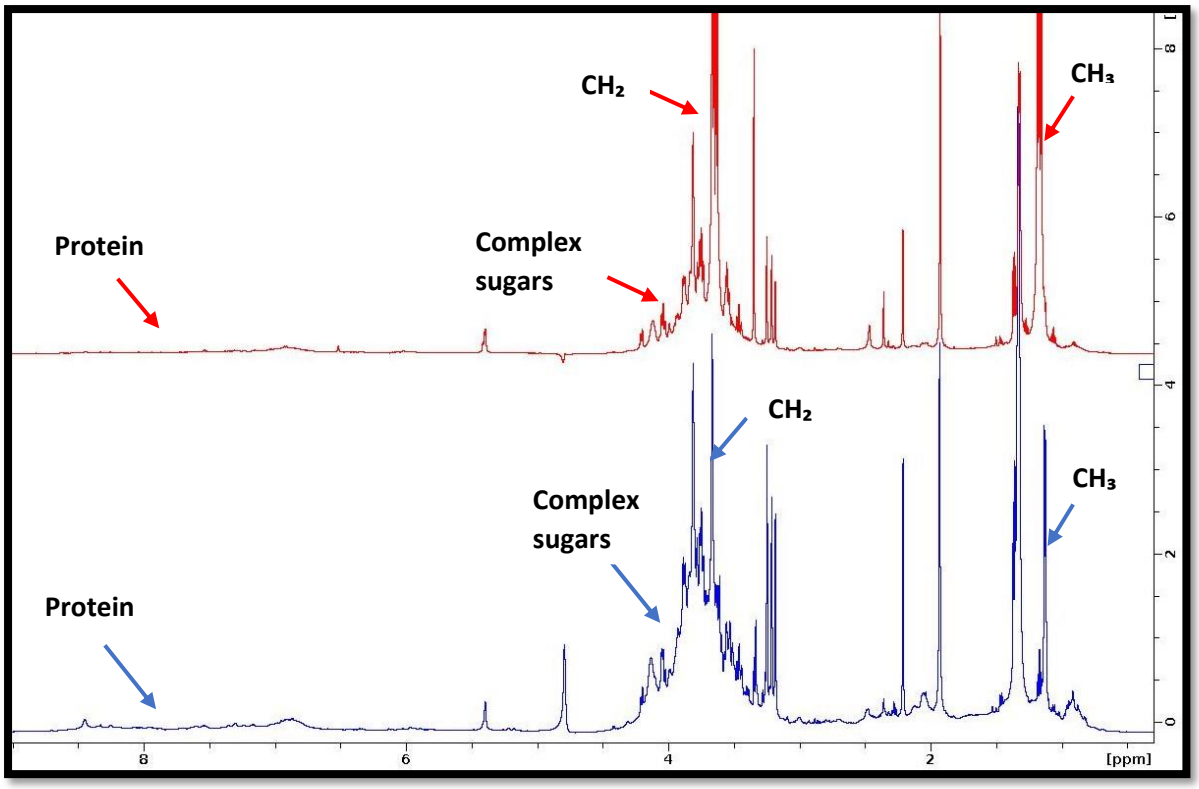

Figure 4.6: Comparison of NMR spectra between two after-boiling rice wastewater samples from Bangladesh. Blue peaks were acquired from the Zia rice mill while the red peaks were from the Soha rice mill. Peaks are labelled with corresponding functional molecules.

^{1}H-NMR spectra of rice wastewater from both rice mills of different stages (Figures 4.4, 4.5, 4.6) showed several distinct signals corresponding to different organic compounds present in the samples. A broad and intense set of peaks at 3.38 to 4.3 ppm was observed (Figure 4.4, 4.5, 4.6), suggesting the presence of complex sugar moieties. This peak might arise from starch and other carbohydrates, for instance, glucose or other polysaccharides present in the samples. The complex peak shape indicates that multiple overlapping signals are contributing to this region.

The triplet peak at 1.191 ppm is attributed to the presence of methyl (CH_3) protons of ethanol. In aqueous solutions, the presence of chemical shift to this region is a notable identifier of methyl protons in ethanol (CH_3CH_2OH). Additionally, a sharp quartet peak at 3.66 ppm corresponds to the presence of the methylene (CH_2) group of ethanol. This peak reinforces the recognition of ethanol in samples (Figure 4.4, 4.5, 4.6) since it is a characteristic signal of CH_2 protons in ethanol molecules.

Peaks between 6.6 to 9.2 ppm are attributed to amino acid residues. The signals in this region arise from amide and aromatic protons in amino acids, indicating the heterogeneous criteria of protein material in the samples. The signal at 8.4 ppm indicates the presence of organic acid such as formic acid and it shows distinct patterns due to the number of protons along with neighbouring groups.

4.6 Determination of concentration of organic components in rice wastewater

Integration values were obtained in the ^{1}H-NMR spectra, from the peak areas of individual signals. To know about the relative number of protons that are contributing to each peak, we need to do a quantitative measurement, known as integration. NMR tools were used to integrate the area under every peak of interest in the spectra to get insights into the relative abundance of organic contents of the sample. Integration values were used to determine the concentration of sugar, protein, and ethanol present in samples. The integration technique requires assigning a numerical (integration) value to every peak (Figure 4.7) that represents the relative area under the corresponding peak. In this study, TSP served as an internal standard for quantification and did not interfere with the signals of organic constituents of interest.

In this study, TSP served as an internal standard for quantification and did not interfere with the signals of organic constituents of interest. Concentrations of sugars and amino acids were calculated as follows. The non-anomeric protons of sugars (2’ to 6’) give rise to the signals in the range 3.38 to 4.3 ppm. In a typical hexose there are 6 of these. Thus, each sugar monomer in a polymeric carbohydrate such as starch contributes 6 protons in this range, and has a mass of 162 Da. This allows a calculation of the concentration of sugars in the sample, in mg/L. Similarly, the signals in the range 6.6 to 9.2 ppm are produced by amide and aromatic protons in amino acids. This averages roughly 1.2 protons per amino acid, with an average mass of 110 Da, allowing us to calculate the approximate protein concentration in mg/L.

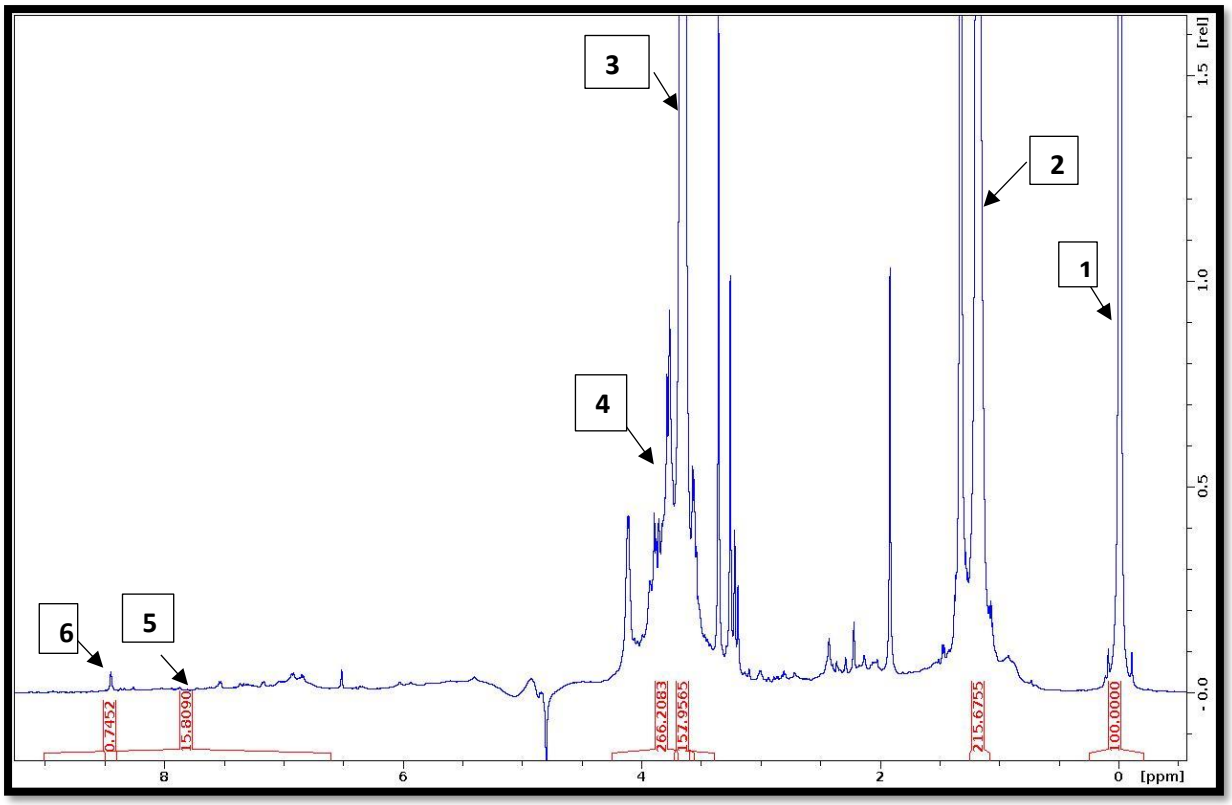

Figure 4.7: The integration spectra of the before boiling sample from the Soha rice mill showed the integration value of some peaks indicated with arrows 1, 2, 3, 4, 5, 6 to represent the relative area of TSP, EtOH-CH3, EtOH-CH2, sugar + EtOH CH_2, protein + formate, and formate respectively under the peak.

The concentrations of major constituents in rice wastewater were measured from the NMR spectra by integration of peak areas, which are proportional to concentration. TSP was added at a known concentration, and therefore approximate concentrations of ethanol, protein and sugars were determined by comparison of integrals with the integral of TSP. The Topspin program on the Bruker NMR spectrometer was used to measure integrals for ethanol and sugar, and for the range 3.38 to 4.3 ppm which contains the sugar 2' to 6' protons and the ethanol CH_2, and the region 6.6 to 9.2 ppm which contains amide and aromatic protein signals and formate.

Table 4.3: The following table represents the concentration of sugar, protein, and ethanol in rice waste effluent obtained from Zia and Soha rice mills (before and after boiling).

Samples	Sugar (mg/L)	Protein (mg/L)	EtOH (mM)
After boiling (Zia rice mill)	1.33	0.62	0.95
Before boiling (Zia rice mill)	0.22	0.09	0.33
After boiling (Soha rice mill)	0.81	0.35	8.28
Before boiling (Soha rice mill)	0.25	0.1	5.4

Sugar:

The concentration of sugar in the samples differs among the various conditions and the rice mills. The maximum sugar concentration was observed in the after-boiling sample from the Zia rice mill with 1.33 mg/L, followed by after boiling sample from the Soha rice mill with 0.81 mg/L (Table 4.3). Before boiling samples from both rice mills show significantly lower sugar concentrations, with 0.22 mg/L in the Zia rice mill and 0.25 mg/L in the Soha rice mill samples (Table 4.4).

Protein:

Protein concentration in the samples also manifested the variations between different conditions and rice mills. After boiling wastewater sample from the Zia rice mill had a higher concentration of protein (0.62 mg/L) compared to after boiling sample from the Soha rice mill (0.35 mg/L). Protein concentration was found to be lower in the before-boiling samples from both rice mills, with the Soha sample having 0.1 mg/L and the Zia sample having 0.1 mg/L (Table 4.3).

Ethanol:

Interestingly, rice waste effluents displayed the presence of ethanol in all samples but with differing concentrations depending on the treatment conditions and the rice mill. Rice wastewater from the Zia rice mill, both before (0.33 mM) and after boiling (0.95 mM) revealed

insights into the chemical composition along with the presence of ethanol in both samples (Table 4.3). Rice wastewater samples obtained from the Soha rice mill showed strong and distinct peaks which were consistent with ethanol signals and the identification of these peaks affirms the notable concentration of ethanol in Soha samples with 5.4 and 8.28 mM in before and after boiling rice waste stream samples respectively (Table 4.3).

In the analysis of post-boiled rice wastewater, a notable increase in ethanol content was observed compared to the pre-boiling stage. This phenomenon can be attributed to the boiling process which may have facilitated the breakdown of complex organic compounds present in the rice wastewater, leading to the release of fermentable sugars. Subsequently, during the fermentation process, microorganisms present in the wastewater metabolize these sugars, producing ethanol as a byproduct.

4.7 Discussion

The analysis of rice waste effluent disseminated a wide range of essential nutrients, trace metals, and heavy metals as presented in this result chapter. The constituents of rice waste effluent are impacted by numerous factors such as water source, agricultural practice, soil characteristics, and industrial activities. The concentration of major elements like magnesium, sulphur, phosphorus, potassium, and chlorine was found to be exceeding the anticipated range of local groundwater. These elements can be assigned to the utilization of irrigation water, fertilizer, and soil leaching during the production phase.

In addition, the existence of trace metals, for example, manganese, aluminium, copper, zinc, and iron in wastewater might be attributed to several sources like soil contamination, industrial discharge, untreated wastewater, and urban runoff. While few of these metals are necessary micronutrients for crops, accumulation in the environment could lead to adverse effects on both human health and the environment.

Along with metals, this study also found chlorine in waste effluent, which could be a residue from the disinfection process of the water used for the milling process. The identification of potentially toxic heavy metals, for instance, arsenic, chromium, cadmium, mercury, and lead in wastewater samples raise considerable health and environmental concerns. Although detected heavy metals were found to be within the safe limit, these toxic metals could accumulate, enter the ecosystem, and pose potential health complications along with environmental pollution. The detection of these metals in rice waste effluent highlights the requirement for strict regulatory measures to safeguard both public health and the environment.

The implementation of Nuclear Magnetic Resonance (NMR) spectroscopy to establish the organic compounds that exist in rice waste effluent delivered valuable insights into the complex mixture of organic matter. NMR spectra exhibited a number of organic compounds including carbohydrates, amino acids, ethanol, and formate in the samples (Figure 4.7).

The presence of carbohydrates in waste effluent can be attributed to the breakdown of organic constituents like rice husk during paddy processing and also from the decomposition of other plant materials. Carbohydrates play a vital role in biogeochemical processes as they can supply a major carbon source for microorganisms (Holesh *et al.,* 2022). NMR peaks corresponding to amino acids were observed in the spectra which indicates the existence of organic nitrogen compounds. Nitrogen-containing compounds might be derived from rice residues and fertilizers utilized for cultivation purposes. For microorganisms, amino acids are essential for their growth (Holesh *et al*., 2022), and it plays a crucial role in the breakdown of organic compound in waste effluent.

The detection of ethanol, interestingly, in rice wastewater with NMR analysis brings a fascinating aspect to the overall constituents of waste effluent (Figures 4.6, 4.7). Identification of ethanol in the samples could emanate from various sources. It could derive from fermentation processes incorporated with grain proceeding where microbes might become active and convert sugar into ethanol. Additionally, the breakdown of starches or carbohydrates present in samples could emit ethanol and might contribute to the presence of ethanol in waste effluents.

NMR peaks corresponding to formate (Figure 4.7) were detected in the spectra which might originate from the decomposition of organic matter present in wastewater or from microbial activity during transport from Bangladesh to the United Kingdom.

The affiliated understanding of rice waste effluent constituents along with NMR findings of organic contents has various implications and guide directions for future research. Essential nutrients and trace metals in waste samples emphasize the importance of wastewater management to prevent water pollution, maintain soil fertility, and long-term sustainability of the rice cultivation program. A holistic approach to rice wastewater supervision, considering both organic and inorganic compounds, is necessary for protecting the environment, safeguarding water bodies, and ensuring the sustainability of agricultural practices. Therefore, further research into the transformation of organic content into a valuable resource during wastewater treatment will definitely enhance the understanding of the environmental impact and eventually will facilitate the expansion of biotechnological approaches.

Establishing the constituents of rice waste effluent is a critical first step in understanding its composition along with its suitability for yeast growth. This investigation suggests that agricultural waste streams can serve as a sustainable and cost-effective media for yeast-based bioprocesses. Rice waste effluent contains a diverse range of nutrients, and the heavy metals found in the samples are within safe limits, as discussed in this Chapter. This indicates it is a potentially rich nutrient and an acceptable source for the cultivation of *S. cerevisiae*. Overall, using agricultural wastewater as a growth media for engineered yeast offers a dual advantage, it promotes a cost-effective means of wastewater management and simultaneously facilitates the synthesis of valuable bioproducts like PHA and biomass. This approach aligns with the principles of sustainable bioprocessing, where waste streams are converted into valuable resources, contributing to both environmental protection and biotechnological advancements.

Chapter 5: Rice parboiling wastewater as a promising source of biotechnology and future perspectives

5.1 Introduction

The innovative concept which is acquiring momentum in the industrial sector is the utilisation of waste material from one industry for another as a raw material. This collaborative approach is manifesting to be an eminent tool for revamping the industrial zone (Dixit *et al*., 2015). This perspective is environmentally sustainable because it reduces waste disposal and minimises the requirement of extracting new resources. The liquid effluent released in the rice industry proves to be an outstanding source of raw material for other industries. Recycling rice wastewater is a critical task and converting it into value-added products is a key undertaking that involves assessing, identifying, and quantifying major components present in waste products before using them in the respective industry through conventional or novel methods (Dixit *et al*., 2015). The constituents of rice wastewater have been discussed in Chapter 4, which suggests the potential of their utilisation as an auxiliary source for producing valuable products.

Rice is consumed worldwide as a staple food and has become the centre of discussion in terms of waste management and sustainable production. A significant amount of waste effluent is produced during the processing of rice, characterized by the presence of organic matter, inorganic components, and several byproducts as summarised in Chapter 4. Systematic use of rice waste effluent provides an opportunity for us to handle major challenges simultaneously which include wastewater management along with microbial cultivation for generating biomass and biopolymer.

Yeasts stand out as one of the most adaptable and versatile microorganisms among all microbial candidates, which can thrive in a wide range of environments and substrates and could generate value-added compounds. Among yeasts, *Saccharomyces cerevisiae* has been studied extensively and considered as a model system for genetic engineering leading to the development of strains with optimised features (Badotti *et al*., 2008). Previous studies investigated the feasibility of using *Saccharomyces boulardii* and *Pichia pastoris* in parboiled rice effluent supplemented with additional carbon sources, with the dual objectives of production of value-added cellular biomass to be used as a probiotic for animals and reduction of environmental impact (Schneid *et al*., 2004; Gaboardi *et al.,* 2018; Santos *et al*., 2018). The results from those studies demonstrated that yeasts are a highly promising candidate for biotechnological application as they can convert the complex carbon source in rice waste effluent into probiotics along with a positive environmental impact. Thus, the

present study is based on the preceding research highlighting the potential of *S. cerevisiae* for biotechnology by utilizing parboiled rice effluent as feedstock. Nonetheless, there is very little information available on the use of *S. cerevisiae* in the bioprocessing of rice wastewater. Therefore, the study aims to evaluate the viability of using parboiled rice waste effluent with various additives as a substrate for *S. cerevisiae* and determine its impact on generating cellular biomass and PHAs. In the upcoming sections of this chapter, a rigorous assessment of the outcomes gained through experimentation will be presented. This is going to highlight the kinetics of yeast growth, accumulation of biomass, and production of PHAs along with the impact of constituents of parboiled rice effluent during these critical processes.

5.2 Preparation and characterisation of rice wastewater

This chapter investigates the yeast growth and PHA production using rice wastewater prepared in Sheffield, where the tap water composition is known and amounts available for study are greater than using the samples brought from Bangladesh, reported in Chapter 4. Parboiled rice effluent was prepared here following the steps described in Chapter 2, Section 2.11 for the cultivation of *Saccharomyces cerevisiae* as a growth medium, aiming to generate biomass and potential PHAs. The process involved generating before and after boiled wastewater, sterilization, characterization, and optimization of the composition for subsequent experiments. This procedure assures that parboiled effluent is befitted for the utilization of biological studies, encouraging valid and consistent results.

5.2.1 Characterisation of parboiled wastewater

To determine insights into the composition of prepared rice wastewater, we characterized its physicochemical properties. Several parameters, for instance, pH, colour, odour, organic compounds, and inorganic constituents were established. The organic content of the waste effluent was analysed using NMR spectroscopy and inorganic composition was determined with ICP-MS, providing an understanding of the nutrient availability for yeast cultivation.

5.2.2 Physical characteristics

Parboiled rice wastewater exhibited apparent physical criteria that define its composition and potentiality. Typically, rice waste effluent is distinguished by its light to dark brown colour, which might result from organic particles and rice husks. In addition, it possessed an unpleasant odour, which may be due to the decomposition process of husk and organic matter. The pH of rice wastewater was measured and found to be acidic with a value of 5.8, which may result from the presence of organic acids produced during the degradation of organic matter. The physical criteria of rice wastewater are critical determinants for exploring different applications as a growth media for conventional yeast and bioprocessing experiments.

5.2.3 Determination of organic compounds

NMR spectroscopy was employed to unravel the organic compounds of parboiled rice wastewater, a byproduct of rice processing to get valuable insights for potential applications. ^{1}H-NMR experiments were conducted utilising a 600 MHz spectrometer and calibrated with a known concentration of TSP which acts as a reference material for the chemical shift. To yield interpretable data, baseline correction, phasing, and reference calibration were performed after obtaining the NMR spectrum. Identification of organic compounds was acquired by comparing the chemical shifts with reference spectra and chemical databases. A set of peaks was observed at 3.38 to 4.3 ppm (Figure 5.1) indicating the presence of carbohydrates and peaks between 6.6 to 9.2 ppm suggesting the presence of amino acid residues. Interestingly, triplet and quartet peaks at 1.191 and 3.66 ppm were detected suggesting the presence of CH_3 and CH_2 group of ethanol respectively. The signal at 8.4 ppm indicates the presence of formate in the wastewater sample.

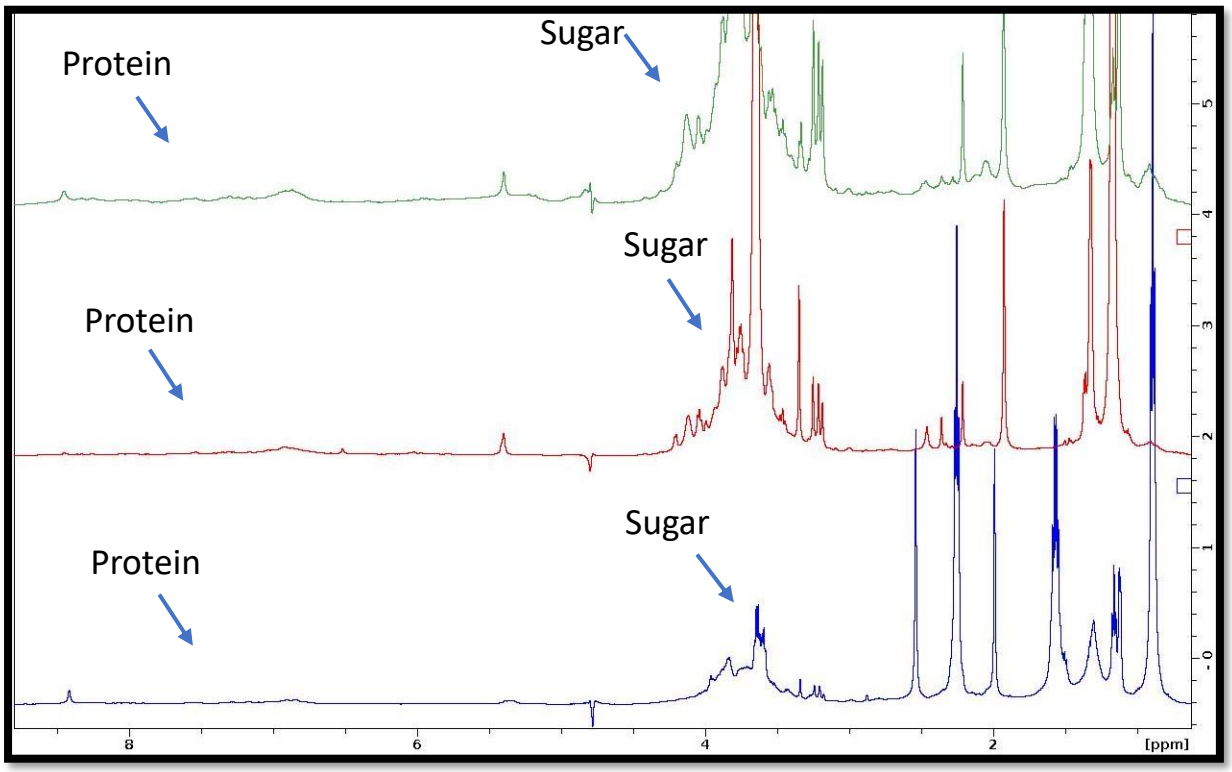

Figure 5.1: Comparison of ^{1}H-NMR spectra of three after-boiled rice waste effluent samples. Green and red peaks were acquired from the sample of the Zia and Soha rice mill, in Bangladesh, while the blue peaks were from after boiled rice wastewater prepared here. The spectra illustrate the changes in intensities of broad peaks between 3.38 to 4.3 ppm for carbohydrate molecules, and also between 6.6 to 9.2 ppm for protein content between samples.

To quantify the concentration of sugar, protein, and as well as by-product ethanol, peak integration was executed. Integration values were obtained in the ^{1}H-NMR spectra from the peak areas of the individual signal as this is proportional to the concentration. We calculated 0.32mg/ml of sugar, 0.21 mg/ml of protein, and 0.76 mM of ethanol present in the after-boiled rice wastewater sample that was prepared here. The calculation follows a similar way as described in Chapter 4, Section 4.7.

5.2.4 Identification of inorganic compounds

Rice wastewater was prepared here with the supplied tap water, and it served as the initial reference point to compare tap water, with before and after boiling wastewater samples. Tap

water dispensed the guideline from which alteration in the properties of water can be estimated.

Tap water: The chemical composition of tap water is mostly dependent on local water sources along with the regional treatment process. With regard to parboiled rice waste effluent preparation, tap water acts as the primary medium for rice grains soaking. Analysed tap water samples exhibited concentrations of Ca, Mg, P, S, Cl and Cu are 15, 3, 1, 14, 17, and 0.01 mg/L respectively (Table 5.1, Figure 5.2).

Before boiling waste effluent: This sample was obtained after the soaking step of paddy processing and the composition differs from the tap water in order to leach several compounds from the rice husk and grain. The soaking process might allow water-soluble components to diffuse to the liquid step and contribute to its overall contents. The analysis revealed the levels of Ca, Mg, P, S, Cl, and As are 11, 3, 5, 25, 61, and 0.02 respectively present in the un-boiled rice wastewater sample (Table 5.1, Figure 5.2).

After boiling waste effluent: The boiled sample is likely to manifest an elevated level of nutrients compared to tap water due to the release of complex compounds from the husk and grains. The boiling process led to the concentration of Ca, Mg, P, S, Cl, Zn, and As are 10, 4, 26, 22, 79, 0.1, and 0.05 respectively in the parboiled sample (Table 5.1, Figure 5.2).

Both before and after-boiled samples showed altered physical and chemical properties compared to tap water because of the dissolution of constituents of rice as expected. Understanding these alterations is vital for evaluating the impact of parboiled water for exploring as growth media for microorganisms, taking into account the advantage of nutrient components.

Table 5.1: Concentration of different components present in local tap water, rice wastewater prepared here (both before and after boiling wastewater).

	Tap water	Before boiling	After Boiling
Elements	Concentration (mg/L)	Concentration (mg/L)	Concentration (mg/L)
Calcium (Ca)	15	11	10
Magnesium (Mg)	3	3	4
Phosphorus (P)	1	5	26
Sulphur (S)	14	25	22
Copper (Cu)	0.01	0.0	0.0
Chlorine (Cl)	17	61	79
Iron (Fe)	0.0	0.0	0.0
Zinc (Zn)	0.0	0.0	0.1
Chromium (Cr)	0.0	0.0	0.0
Arsenic (As)	0.00	0.02	0.05
Cadmium (Cd)	0.0	0.0	0.0
Mercury (Hg)	0.0	0.0	0.0
Lead (Pb)	0.0	0.0	0.0

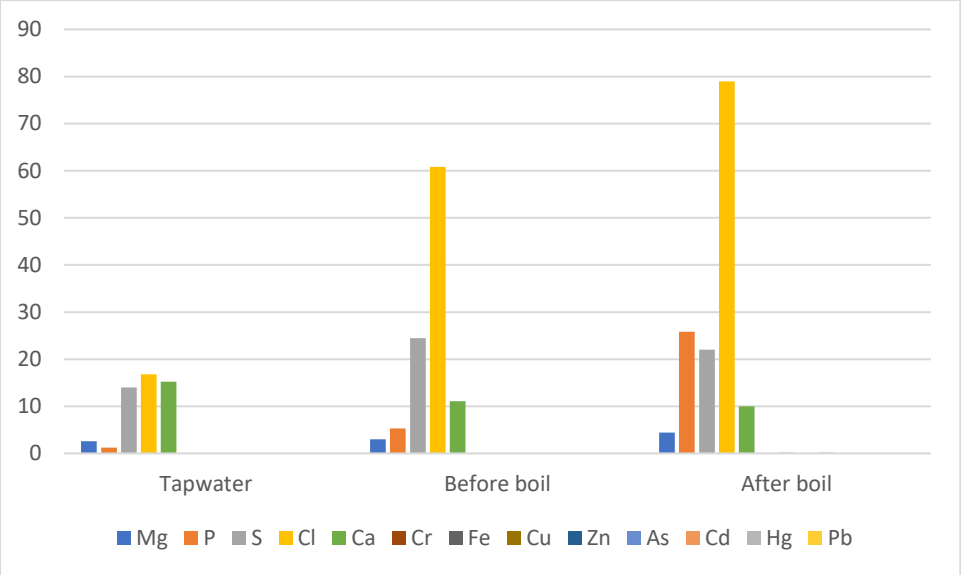

Figure 5.2: The column chart illustrates a comparison of the elements found in local tap water, both before and after boiling rice wastewater prepared here.

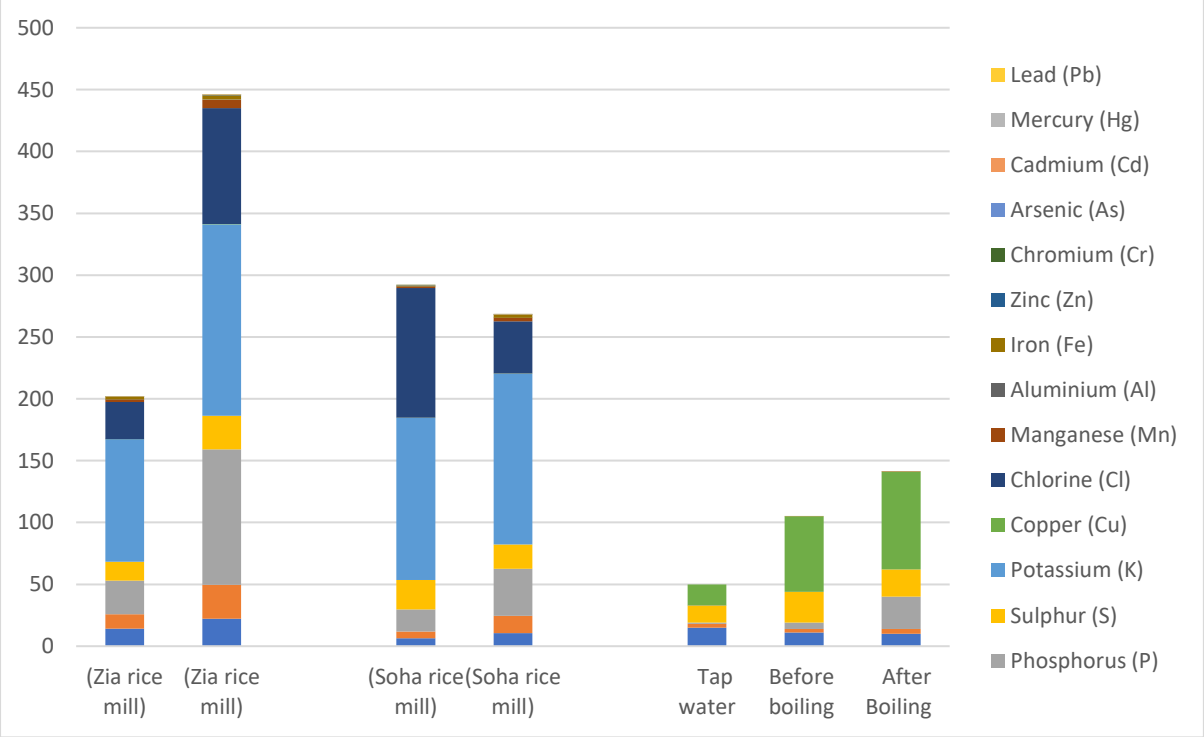

Figure 5.3: The column chart depicts a comparative analysis of elemental concentrations in various water sources, including Zia Rice Mill (pre-boiling and post-boiling), Soha Rice Mill (pre-boiling and post-boiling), local tap water, and rice wastewater prepared in this study before and after boiling.

The provided data (Figure 5.3) presents a comparative analysis of elemental concentrations in water sourced from two rice mills (Zia and Soha) before and after boiling rice wastewater, as well as tap water, before and after boiling rice waste effluent prepared for experiments. Both Zia and Soha rice mill wastewaters exhibited an increase in calcium concentration after boiling. Tap water, in contrast, displayed a decrease in calcium levels post-boiling. A substantial increase in magnesium is observed after boiling in both rice mill waters. Tap water showed a modest increase in magnesium levels after boiling.

Both rice mill waters experienced a significant rise in phosphorus concentrations post-boiling. Tap water, interestingly, registered a decrease in phosphorus levels after boiling. While Zia rice mill water shown an increase in sulfur content after boiling, Soha rice mill water witnessed a decrease. Tap water exhibited an increase in sulfur concentration after boiling. A notable increase in potassium concentrations is noted after boiling in both rice mill waters. Tap water recorded a substantial increase in potassium after boiling. Zia rice mill water demonstrated a slight increase in copper after boiling, while Soha rice mill water showed a decrease. Tap water, interestingly exhibited a significant rise in copper levels after boiling. Both rice mill waters witnessed fluctuations in chlorine concentrations after boiling, with Zia water experienced a decline and Soha water an increase. Tap water demonstrated a substantial increase in chlorine after boiling. Both rice mill waters show a decrease in iron concentrations after boiling. Tap water exhibits an increase in iron after boiling. The variations observed in elemental concentrations post-boiling can be attributed to factors such as water source characteristics, boiling temperature, and the solubility of different elements. Differences between rice mill waters and tap water highlight the influence of local water composition and treatment methods. The concentrations of elements in rice mill water, especially after boiling, often surpass those in tap water.

5.3 Yeast growth

To understand the impact of various additives in rice waste effluent as described in Chapter 2 (Section 2.11, Table 2.14) on yeast proliferation, biomass, and potential PHA production, a number of experiments were executed utilizing wastewater from the rice parboiling process. Five media compositions were assessed, such as 1) waste effluent supplemented with 1% yeast extract, 2) effluent with 1% glucose, 3) wastewater with 0.02% amylase, 4) wastewater with 1% yeast extract+ 1% glucose, and 5) only rice wastewater, no additive. The modified waste effluent was subjected to autoclaving for sterilization, to eliminate the potential contaminants. To conduct the experiment, a double mutant strain of *S. cerevisiae, mdh3/gpd1Δ* was transformed with plasmid pAB7 (PhaC2 with PTS1 and without GFP) and pAB9 (synthetic PHA synthase, PhaC1 with PTS1 and without GFP) using One step transformation method. After two days, cells were inoculated in YM2 Ura- media supplemented with 2% glucose for pre-culture media and shaken at 200 rpm overnight at

30°C. 4% of cells (v/v) from overnight cultures were inoculated in all rice wastewater media (Rice wastewater only, Rice wastewater + Glucose, Rice wastewater + Yeast extract, Rice wastewater + Glucose + Yeast extract, Rice wastewater + Amylase) in 250 ml conical flasks and agitated for 48 hours at 200 rpm. Cultures were monitored over time to facilitate the construction of growth curves, enabling the analysis of growth dynamics to perceive the effects of added supplements on yeast growth.

The progress of the culture was observed by calculating the optical density (OD) at 600nm using a spectrophotometer as an indicator of biomass. A growth curve was constructed by plotting the OD values (Y-axis) of the samples over time (X-axis) to determine the effect of different supplements on the growth kinetics of *S. cerevisiae*. Growth was studied until 48 hours of culture, as Fehrenbach *et al.* (2022) mentioned longer treatments than 48 hours are considered inviable.

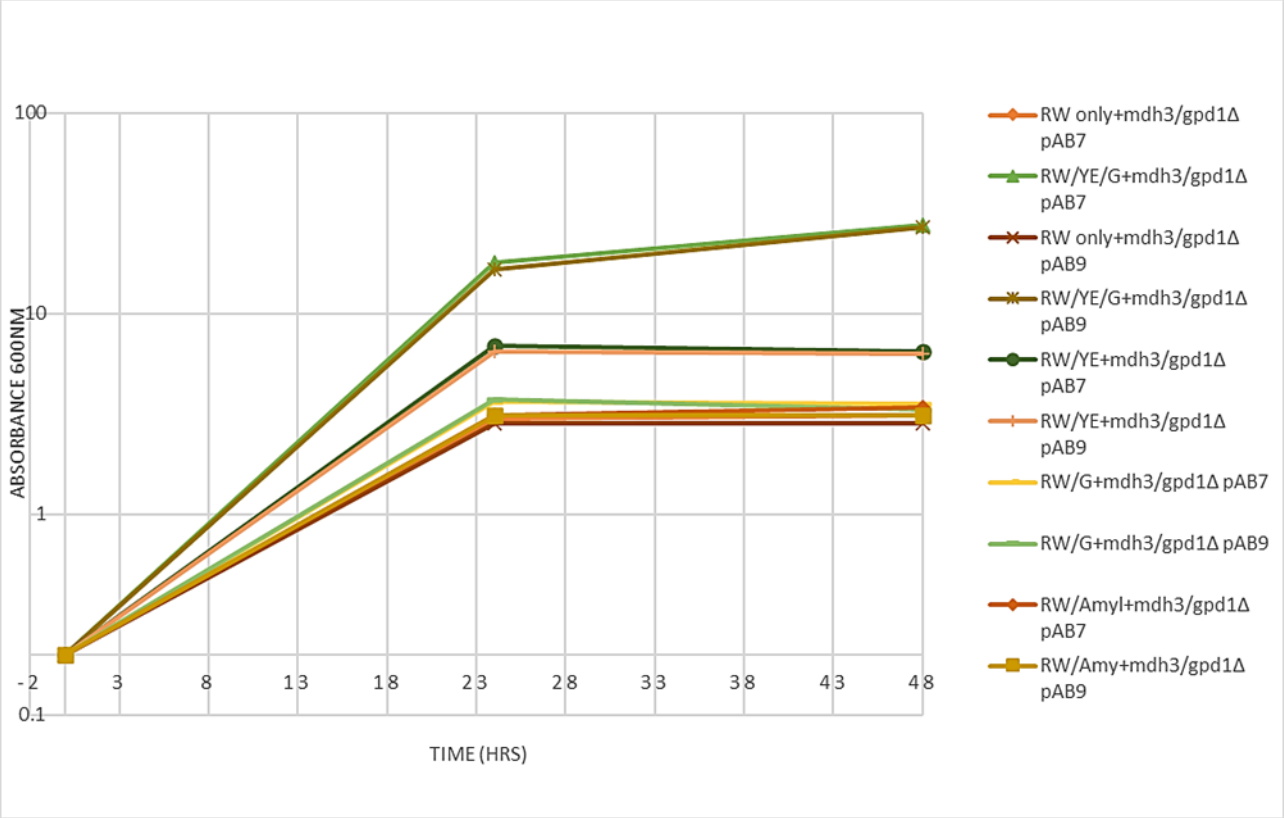

Figure 5.4: The presented graph based on optical density values at 600 nm recorded using a spectrophotometer at preculture (0hour), at 24 hours, and at 48 hours while a double mutant strain of *S. cerevisiae, mdh3/gpd1Δ* transformed with pAB7 (PhaC2+PTS1, without GFP) and pAB9 (synthetic PHA synthase, PhaC1 with PTS1 and without GFP) were cultivated at 30°C in rice wastewater. The experiment included supplements, for instance, glucose, yeast extract,

amylase, and combined glucose + yeast extract as well as only wastewater without any supplements**.** This data indicates the cell viability of the strain over the 48-hour culture period.

While *S. cerevisiae* was cultivated in rice wastewater solely without any external supplements, modest growth and biomass yields were observed demonstrating the capability of parboiled rice effluent to sustain its metabolism to some extent. According to the current protocol in the case of *S. cerevisiae*, OD600 of 1.0 is roughly $3x10^7$ cells/ml (Hutch, 2012). At the end of the experimental period (after 48 hours), OD600 was 3.1 and 2.85, and dry weight from the harvested cells was observed to be 0.90 g and 0.88 g from 50ml of cultures with *mdh3/gpd1Δ +*pAB7 and *mdh3/gpd1Δ*+pAB9 respectively while grown in waste stream without additives (Table 5.2, Figure 5.4).

The moderate impact of supplementation with amylase (the enzyme that breaks down the starch into simple sugar) on growth kinetics suggested that the enzyme has the potential to facilitate the discharge of carbon sources from complex carbohydrates present in rice waste effluent. At the end of the experimental period, OD600 was 3.4 and 3.1 and dry weight from the harvested cells was observed to be 0.99 g and 0.97 g from 50ml of cultures with *mdh3/gpd1Δ* +pAB7 and *mdh3/gpd1Δ*+pAB9 respectively while grown in waste stream with amylase (Table 5.2, Figure 5.4). Albeit the amylase effect on growth was less pronounced compared to other explored additives. Therefore, the potential for amylase to increase the growth rate by carbohydrate hydrolysis warrants further investigation.

As a readily available carbon source, glucose supplementation seemed to fuel increased yeast metabolism, leading to accelerated growth and biomass generation. At the end of the experimental period, OD600 was 3.55 and 3.3 and dry weight from the harvested cells was observed to be 0.90 g and 0.88 g from 50ml of cultures with *mdh3/gpd1Δ* +pAB7 and *mdh3/gpd1Δ*+pAB9 respectively while grown in the waste stream with glucose (Table 5.2, Figure 5.4).

Accelerated growth rate and biomass yield due to supplemented with yeast extract highlighted the crucial role of nitrogen source (Hakobyan *et al*., 2012) along with a variety of nutrients to promote yeast proliferation. At the end of the experimental period, OD600 was 6.45 and 6.3 and dry weight from the harvested cells was observed to be 1.06g and 0.97 g from 50ml of cultures with *mdh3/gpd1Δ* +pAB7 and *mdh3/gpd1Δ+*pAB9 respectively while grown in waste stream with yeast extract (Table 5.2, Figure 5.4). The significant effect of yeast extract validates the view that a wide range of nutrients, vitamins, and growth factors available in yeast extract contribute to the vitality and proliferation of *S. cerevisiae*.

The highest growth rate and biomass production were observed until 48 hrs in waste stream media supplemented with glucose and yeast extract and remained in the stationary phase until the end of the experiment (48 hours). At the end of the experimental period, OD600 was 27.5 and 26.75 and dry weight from the harvested cells was observed to be 1.24g and 1.20 g from 50ml of cultures with *mdh3/gpd1Δ* +pAB7 and *mdh3/gpd1Δ*+pAB9 respectively while grown in waste stream with both glucose and yeast extract (Table 5.2, Figure 5.4). The synergy was monitored when both supplements were present in waste effluent and highlighted the complexity of nutritional requirements for yeast. The collaborative effects of nutrients and carbon sources appeared to make an optimal growth of *S. cerevisiae*, potentially stimulating cellular pathways to accelerate growth and biomass production.

Table 5.2: Growth rate and biomass production of recombinant *S. cerevisiae* in rice wastewater with different supplements.

Samples	OD 600 nm (48 hrs)	Dry weight (g)
RW only+*mdh3/gpd1Δ* pAB7	3.1	0.90
RW only+*mdh3/gpd1Δ* pAB9	2.85	0.88
RW/Amylase+ *mdh3/gpd1Δ* pAB7	3.4	0.99
RW/Amylase+ *mdh3/gpd1Δ* pAB9	3.1	0.97
RW/Glucose+ *mdh3/gpd1Δ* pAB7	3.55	0.90
RW/Glucose+ *mdh3/gpd1Δ* pAB9	3.3	0.88
RW/Yeast extract+ *mdh3/gpd1Δ* pAB7	6.45	1.06
RW/Yeast extract+ *mdh3/gpd1Δ* pAB9	6.3	0.97
RW/Yeast extract/Glucose + *mdh3/gpd1Δ* pAB7	27.5	1.24
RW/Yeast extract/Glucose + *mdh3/gpd1Δ* pAB9	26.75	1.20

The provided data (Table 5.2) indicate the optical density (OD) at 600 nm and dry weight measurements for different samples after 48 hours of cultivation. The focus is on exploring the correlation between OD yield and dry weight, with particular attention to the last two samples, such as, RW/Yeast-extract/Glucose+*mdh3/gpd1Δ*pAB7 and RW/Yeast-extract/Glucose + *mdh3/gpd1Δ* pAB9, which are identified as outliers. Upon initial examination, it is evident that these two outlier samples exhibit considerably higher OD values relative to their dry weight measurements. The higher OD values in the outlier samples could be attributed to a richer nutrient content in the growth medium. The inclusion of yeast extract and glucose in these particular samples introduces additional nutrients that may enhance microbial growth and metabolism. Yeast extract is a complex mixture of amino acids, peptides, vitamins, and minerals, providing a rich source of nutrients for yeast cells. Glucose, as a readily available carbon source, further supports cellular energy production and biomass accumulation.

The elevated nutrient content in the outlier samples may lead to a more robust growth environment, resulting in increased cell density as reflected in higher OD values. The observed outliers in the correlation between OD yield and dry weight in the last two samples may be attributed to the enriched nutrient content, particularly the inclusion of yeast extract and glucose. However, it is crucial to acknowledge that OD alone does not provide a direct measure of biomass; rather, it indicates light scattering by cells, which can be influenced by factors other than cell density. While the OD values suggest higher microbial growth in the outlier samples, the corresponding dry weight measurements provide a more accurate assessment of actual biomass accumulation. The fact that the dry weight values for the outlier samples are not as proportionally elevated as the OD values indicates about the nature of the biomass produced, whether it includes components other than cells, such as extracellular polymers or debris. In the case of the 48-hour cultivation period, the rapid growth of cells may be followed by cell death, leading to an increase in debris and subsequently an elevated OD reading. In such cases, the increased OD could be a result of the accumulation of cellular debris and dead cells, contributing to light scattering without a proportional increase in dry weight.

Additionally, the freeze-drying process itself may contribute to the smaller dry weight observed as the harvested cells, in this experiment, were freeze dried for 24 hours before analysis. Freeze-drying can cause cell lysis and loss of cellular contents, leading to a reduction in the overall dry weight of the sample. The process of freeze-drying, also known as lyophilization involves freezing a sample and then removing the ice by sublimation under vacuum (Adams, 2007). During this process, ice crystals form and grow, that can cause mechanical damage to cells, ultimately leading to the loss of cellular content. The loss of cellular contents could result in a reduction in the overall dry weight of the samples.

5.4 Microscopic images analysis

In this study, the microscopy images were analysed for observing and comparing the cellular responses of the yeast strain *mdh3/gpd1Δ* with genetic constructs pAB7 and pAB9 under diverse nutritional environments. These observations contribute valuable information to our broader understanding of how the yeast strain responds to variations in growth media composition.

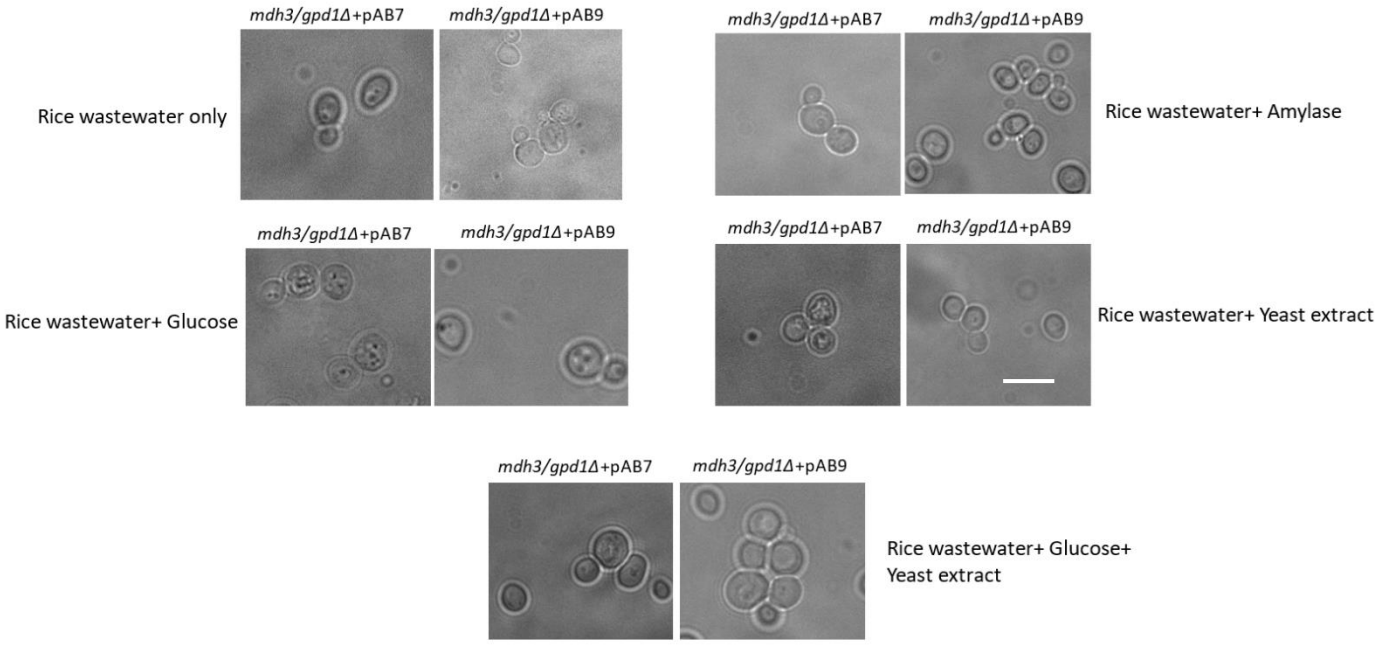

Figure 5.5: Microscopy images of yeast strain *mdh3/gpd1Δ* with pAB7 and pAB9 grown in rice wastewater only (upper panel, left), rice wastewater with the addition of amylase (upper panel, right), rice wastewater with the addition of glucose (middle panel, left), rice wastewater with yeast extract (middle panel, right), rice wastewater with the addition of yeast extract and glucose (lower panel) after 48 hours of cultivation. Bar 5 µm.

Glucose supplementation: The addition of glucose in rice wastewater showed a significant impact on yeast growth, as evidenced by fluorescence microscopy image analysis. The existence of another carbon source that can be metabolized easily by yeast appeared to promote growth rates compared to cultures without any additives. Yeast cultures exhibited densely packed cells suggesting the enhanced growth rate attributable to glucose supplementation (Figure 5.5). Microscopy image analysis portrayed that glucose additives indisputably influenced the metabolism of yeast which ultimately facilitated the efficient conversion of nutrients to biomass.

Yeast extract supplementation: When rice waste effluent was supplemented with yeast extract showed a rising trend of enhanced yeast growth (Figure 5.5). Amino acids and vitamins-enriched yeast extract appeared to supply extra nutrients to complement the present contents of parboiled rice wastewater. This eventually led to increased growth rates and enhanced cellular biomass accumulation. This synergistic action of the yeast extract highlighted its potential to act as an effective supplement for increasing the growth of yeast in parboiled effluents.

Yeast extract and glucose supplementation: Combining both yeast extract and glucose supplementation bestowed a noteworthy synergistic influence on the growth of yeast. Cultures of yeast manifested the highest growth rates compared to other additives and acquired the maximum biomass yields. Microscopy images depicted a robust population of yeast with extensive distribution endorsing the growth increment resulting from combined additives (Figure 5.5). This demonstrates that the complementary behaviour of yeast extract and glucose dispensed a comprehensive range of nutrients in waste effluent that supported the metabolism of yeast optimum and seemed to maximise the use of available sources that led to the robust growth of yeast.

Amylase supplementation: Rice wastewater supplemented with an enzyme called amylase that can hydrolyse complex starch to simple sugars displayed a moderate influence on yeast development. The presence of additional carbohydrates from hydrolysis of starch appeared to contribute to the proliferation of yeast (Figure 5.5). Albeit the impact was not as notable as that perceived with yeast extract, glucose, or combined supplementation. Fluorescence microscopy images displayed less cell density compared to those supplemented with yeast extract, glucose, and combined.

Only rice wastewater (no additive): To evaluate the effect of nutrient addition on yeast proliferation and production of biomass and PHAs in parboiled rice effluent, a comparison was done with yeast cultures that were grown in only rice wastewater without adding any supplements. While yeast growth was observed even in the absence of any supplements, the growth rate and biomass production were comparatively less than those acquired with

supplemented conditions. Microscopy images demonstrated that lower-density yeast cells in the absence of additional nutrients compared to supplemented cultures are in line with the expected growth behaviour, which emphasizes the critical role of adding nutrient supplementation to optimise yeast proliferation in parboiled rice effluent (Figure 5.5).

The microscopy images, offer insights into how the yeast strain *mdh3/gpd1Δ* with different genetic constructs responds to different nutritional conditions. The experiment provides a visual representation of cellular dynamics, aiding in the interpretation of the impact of specific supplements to optimise growth condition.

5.5 Detection of PHB by Gas Chromatography (GC)

We also investigated the potential of PHA accumulation by recombinant *S. cerevisiae* along with the production of biomass. To this end, the samples were harvested from the culture and biomass was recovered by centrifugation and lyophilisation. To extract PHA and further analysis, dried biomass acted as substrate. Biomass samples were subjected to PHA extraction using chloroform and methanol. The extracted PHA was prepared for gas chromatography analysis and samples were derivatised to the methyl esters before analysis. To quantify PHA content, a gas chromatograph was used which was equipped with a flame ionisation detector (GC-FID). Gas Chromatography displayed distinct peaks corresponding to PHA monomers. Integration of the chromatographic peaks enabled us to quantify PHA content in the samples.

This study uncovered insights into PHA production in recombinant *S. cerevisiae* using parboiled rice wastewater as a substrate under various conditions. The area underneath the chromatographic peak corresponds to the PHA monomer and was utilised to calculate the concentration of PHA. A double mutant strain of *S. cerevisiae, mdh3/gpd1Δ,* transformed with plasmid pAB7 (*mdh3/gpd1Δ* +pAB7) was cultivated in rice waste effluent supplemented with glucose and yielded 0.1% PHA, depicting a peak area of 12.10 (Figure 5.7, Table 5.3). Parboiled wastewater without any supplementation was used for cultivation of *mdh3/gpd1Δ* +pAB7 and 0.2% PHA yield was marked, with a corresponding peak area of 12.56 (Figure 5.8, Table 5.3). The waste media was supplemented with yeast extract was also used for the growth of a double mutant, *mdh3/gpd1Δ*+pAB7, which emerged with 0.1% PHA yield, displaying a peak area of 11.32 (Figure 5.6, Table 5.3).

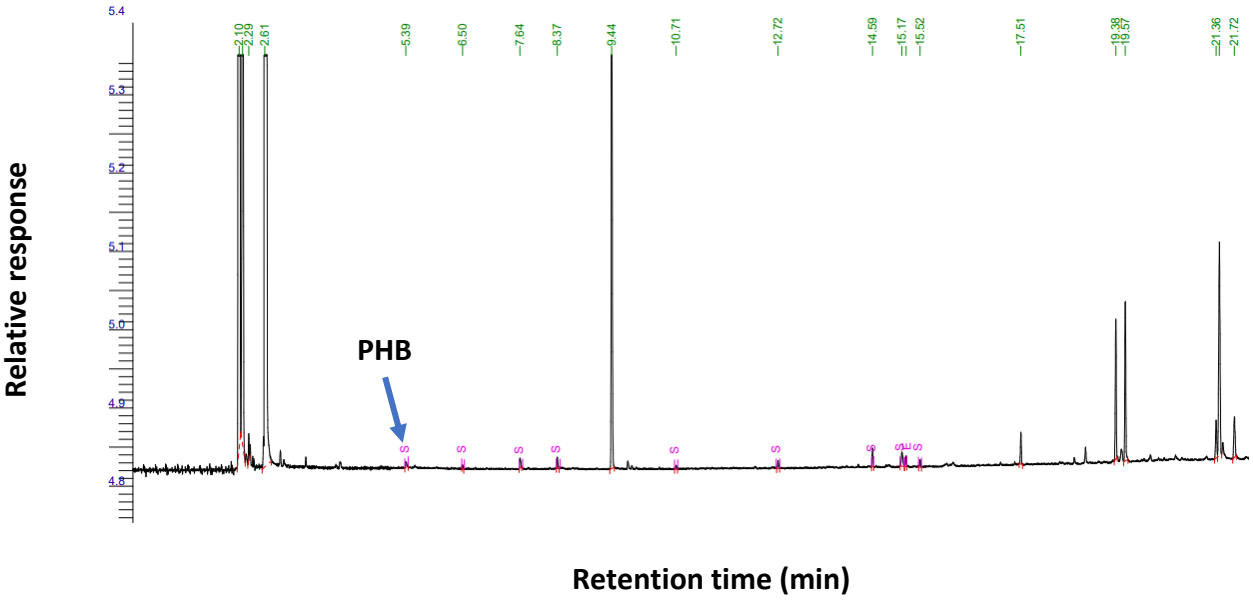

Figure 5.6: Gas Chromatography (GC) analysis of 3-hydroxybutyric acid produced in engineered yeast transformed with a plasmid containing PHA synthase gene*, phaC2* with PTS1 and without GFP (pAB7), cultured in rice wastewater media supplemented with yeast extract. In the chromatogram, the retention time for PHB is marked with an arrow. The retention time of the target PHB is 5.39 minutes.

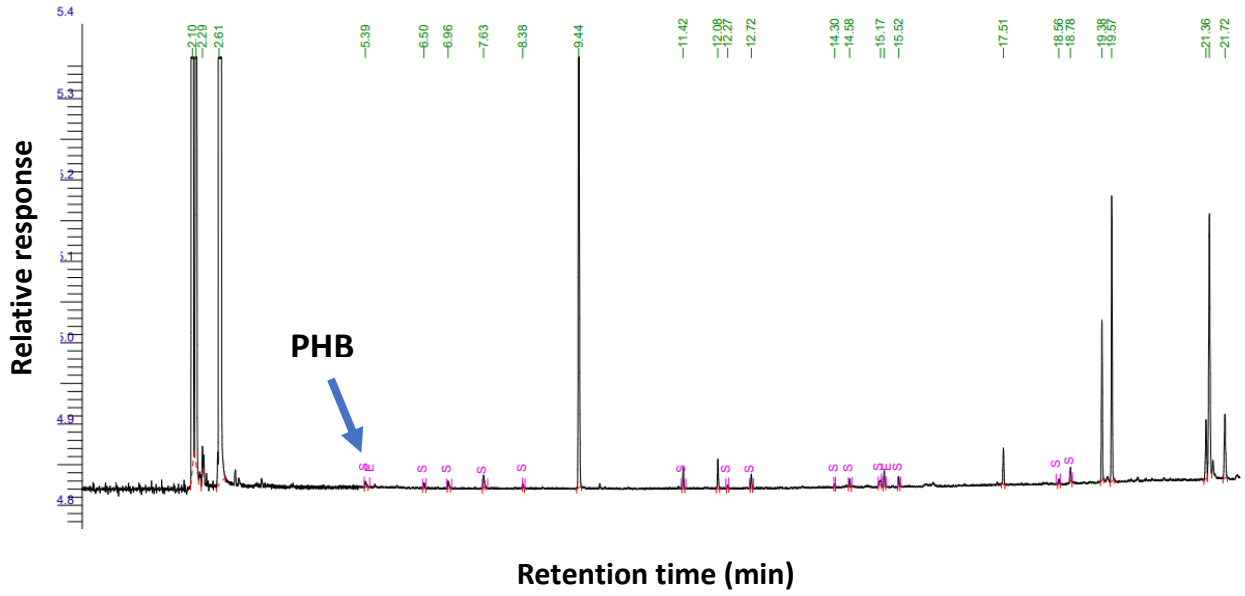

Figure 5.7: Gas Chromatography (GC) analysis of 3-hydroxybutyric acid produced in engineered yeast (retention time for PHB 5.39 mins) transformed with a plasmid containing PHA synthase gene, PhaC2 with PTS1 and without GFP (pAB7), cultured in rice wastewater media supplemented with glucose. In the chromatogram, the retention time for PHB is marked with an arrow. The retention time of the target PHB is 5.39 minutes.

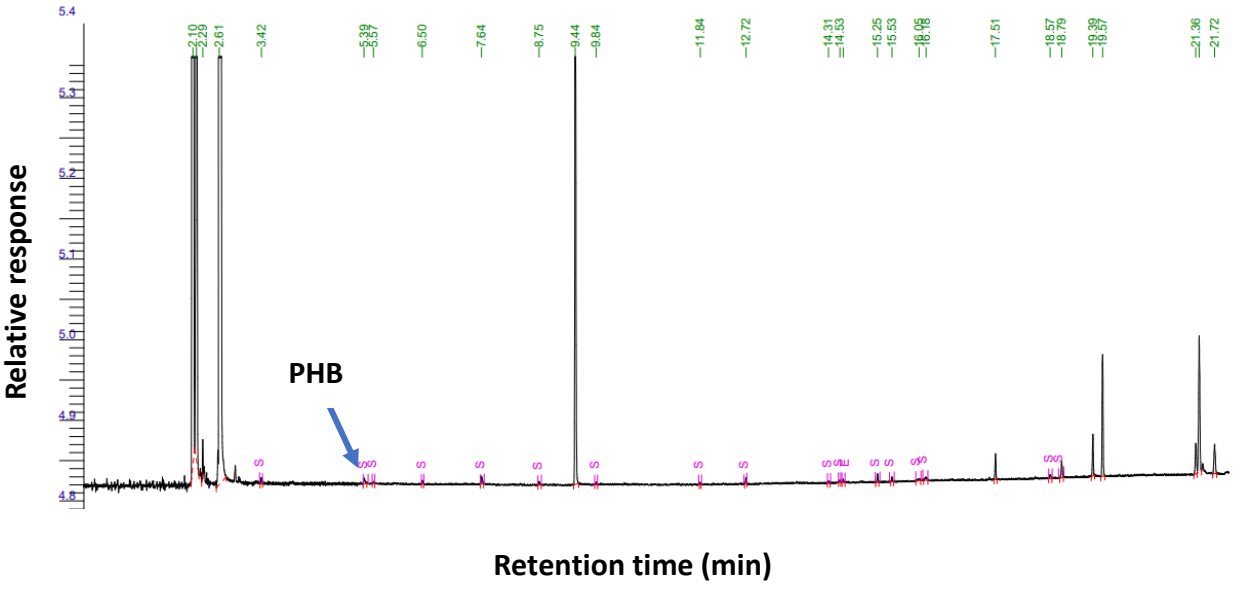

Figure 5.8: Gas Chromatography (GC) analysis of 3-hydroxybutyric acid produced in engineered yeast (retention time 5.39 mins, marked with arrow) transformed with a plasmid containing PHA synthase gene, PhaC2 with PTS1, without GFP (pAB7), cultured in

rice wastewater media only without any supplementation. In the chromatogram, the retention time for PHB is marked with an arrow. The retention time of the target PHB is 5.39 minutes.

Table 5.3: This table represents the quantification of polymer synthesised by recombinant *S. cerevisiae* **(***mdh3/gpd1Δ* with pAB7) grown in rice wastewater with supplements and without supplements utilising Gas Chromatography (GC). This analysis was performed with methanolysis derivatives, and the results are expressed as weight percent.

Samples	Dry Cell Weight (DCW) in $CHCl_3$			HB					[PHA]	
	DCW (g)	$CHCl_3$ (g/mL)	$CHCl_3$ (g/L)	Peak Area	$CHCl_3$ (mg/L)	Real (mg/L)	$CHCl_3$ (g/L)	M	%	g/L
Rice wastewater with glucose + *mdh3/gpd1Δ* with pAB7	0.0297	0.00743	7.425	12.10	4.26	8.52	0.01	0.0020	0.1%	0.009
Rice wastewater only + *mdh3/gpd1Δ* with pAB7	0.0163	0.00408	4.075	12.56	4.42	8.85	0.01	0.0021	0.2%	0.009
Rice wastewater with Yeast extract + *mdh3/gpd1Δ* with pAB7	0.0272	0.00680	6.800	11.32	3.99	7.97	0.01	0.0019	0.1%	0.008

The study revealed that cultures supplemented with yeast extract and glucose (Figures 5.6 and 5.7; Table 5.3) exhibited 0.1% PHA content. In contrast, rice wastewater only (Figure 5.8; Table 5.3) displayed a higher PHA level of 0.2%. This suggests that even in the absence of any supplementation, the nutrient profile of parboiled rice effluent supplies enough substrates to drive PHA accumulation. This analysis also highlights the viability of parboiled rice effluent as a suitable substrate for recombinant yeast. The application of GC analysis stands out as an accurate quantification and compositional study to gain valuable insights into the production process. Further exploration of metabolic pathways, supplement optimisation, fermentation

parameters, and downstream processing methods might serve insights for accelerating PHA production utilising parboiled rice wastewater as a sustainable option.

The observed PHA generation in this study, prompts a critical evaluation in the context of published findings reported in the literature. To ascertain the significance of our results, a comparative analysis with established benchmarks is essential. Upon reviewing published studies on PHA production in yeast strains, it becomes apparent that PHA accumulation can vary widely. Different yeast strains may have different capabilities and efficiencies for PHA production. In the broader landscape of PHA production, reported levels can vary significantly based on microbial strains, growth conditions, and the specific pathways engineered for PHA synthesis. A recent study has shown that PHB can be produced in yeast *Saccharomyces cerevisiae* using cellobiose as the only source of carbon. The yeast strains were modified to express PHB pathway genes from *Cupriavidus necator* and a cellodextrin transporter gene CDT-1 from *Neurospora crassa.* They were also complemented either with β-glucosidase gene GH1-1 from *N. crassa* or with cellobiose phosphorylase gene cbp from *Ruminococcus flavefaciens*. The study found that the production of PHB was much higher in better aerated and pH-controlled bioreactors than in shake flasks and the performance of the strains changed when they were grown in bioreactors. Notably, PHB accumulation levels per CDW of 13.4 ±0.9% and 18.5 ±3.9% were achieved with Cbp and Gh1-1 routes, respectively (Ylinen *et al.,* 2022). This observation highlights the significant impact of bioreactor conditions, with the genetic modifications of specific pathways exhibiting enhanced performance under controlled and well-aerated environments. Considering our measured production rate of 0.1%-0.2%, it falls within the lower range of reported values in the literature. While seemingly modest, the observed PHA yield reflects the success of our engineered yeast strain under the specific conditions outlined in our study, including growth in rice wastewater. It is important to note that the choice of growth medium, genetic modifications, and cultivation conditions can profoundly influence PHA synthesis.

5.6 Discussion

The outcome of this study offers a comprehensive understanding of the effect of numerous supplements on the growth of yeast, biomass production, and PHA accumulation in parboiled rice effluent. The findings shed light on the complex interrelationships among the metabolism of yeast, nutrient availability, synthesis of biomass, and biopolymer in the context of waste management and sustainable production.

When investigating the development of *S. cerevisiae* in parboiled rice effluent for the production of biomass and potential PHAs, it is pivotal to take into consideration the constituents of waste samples. The inherent organic contents, inorganic elements, and trace

minerals present in wastewater can all contribute to yeast cell vitality. Nonetheless, it is worth pointing out that the diversity of composition in wastewater emerging from distinct varieties of rice and different processing techniques might contribute to inconsistent outcomes. Thus, parboiled rice wastewater that contains a higher amount of nutrients, sugars, amino acids, and minerals, can stimulate cell growth to accelerate biomass production.

The successful *S. cerevisiae* cultivation in wastewater has been exhibited in this study. The observed acceleration in the growth of a double mutant strain of *S. cerevisiae, mdh3/gpd1Δ* highlighted that rice waste media supported the metabolic demands of cells. Optical density displayed acceleration over the period of cultivation (up to 48 hours) suggesting that constituents of parboiled wastewater were capable of cellular growth and underscoring the efficacy of utilisation of parboiled effluent as yeast growth media. The considerable production of biomass in parboiled wastewater conditions compared to standard culture media spotlights the advantage of agricultural byproducts for yeast cultures. This aligned with the previous studies that presented the various wastewaters as potential growth media for the culture of micro-organisms (Schneid *et al*., 2004; Gaboardi *et al.,* 2018; Santos *et al.,* 2018).

The miscellaneous supplements applied to parboiled rice waste effluent scenarios ultimately underscore the dynamic interactions between yeast metabolism and nutrient availability. The obtained results demonstrate that adding external supplements to rice wastewater can notably influence the growth of *S. cerevisiae* and simultaneously the production of biomass and potentially PHAs. Substrate utilisation by a double mutant strain of *S. cerevisiae, mdh3/gpd1Δ* emphasizes the suitability of the media and opens avenues for more research and development. While this investigation recommends worthwhile insights, future research is mandated to delve into the optimisation of the composition of wastewater for maximum microbial growth.

Incorporating fluorescence microscopic image analysis in this study has enriched the comprehensiveness and depth of research findings. Visual insights have made our understanding deeper regarding the effects of various supplements on the growth of *S. cerevisiae*. In the case of yeast extract supplementation, image analysis revealed vibrant and densely populated cells, aligning with the increased growth rate shown in Figure 5.5. This concurrence established the role of yeast extract in allocating essential nutrients to support cellular growth. Similarly, densely populated cells were observed with glucose-supplemented waste media suggesting an accelerated growth rate. Image analysis showed the visual evidence of enhanced cell numbers (Figure 5.5) underscoring that glucose is a robust carbon source for the proliferation of *S. cerevisiae*. The observed growth enhancement pointed toward the potential of the mentioned additives to optimise the waste used for sustainable byproducts.

The study underscores the potential of parboiled waste effluent as a growth media for recombinant *S. cerevisiae* and accumulation of PHA. The diverse supplement conditions for using rice waste effluent, reflect different scenarios extending from additive-free to nutrient-accelerated approaches. The elevated PHA content in recombinant yeast grown in rice parboiled water without additives (Figure 5.8, Table 5.3) compared to those with additives (Figures 5.6 and 5.7; Table 5.3) is remarkable and suggests that rice waste effluent carries intrinsic nutrients that support yeast growth and PHA synthesis. The existence of complex compounds in parboiled samples could act as precursors to produce PHA, emphasizing the potential of rice waste streams as a versatile candidate for sustainable PHA production. By harnessing the present inherent nutrients in agricultural waste and supplementing with specified nutrients, this study illustrated a path toward eco-friendly and cost-effective PHA synthesis.

While our study manifests the potential of the rice waste stream for polymer production in recombinant *S. cerevisiae*, future directions along with several challenges need to be considered. Future research could focus on achieving higher PHA yield by optimising the content and composition of additives, as well as the fermentation process. Alternatively, it would be advantageous to engineer the amylase gene into *S. cerevisiae* to hydrolyse the starch to use the waste stream as a suitable substrate while considering both the yield of the biopolymer and the economic feasibility of the process. We believe this to be the first attempt at the application of *S. cerevisiae* to the bioprocessing of parboiled rice wastewater. To fully harness the advantage of this novel approach, ongoing and deeper explorations are required for sustainable waste management and synthesis of cellular biomass and biopolymer.

Chapter 6: General Discussion

6.1 Introduction

Rice cultivation is a crucial element of agriculture in Southeast Asia including Bangladesh (Muthayya *et al*., 2014), which is supplying provisions for millions and contributing notably to the economy of Bangladesh. The rice parboiling process generates a substantial amount of wastewater (Islam *et al*., 2020), posing environmental challenges and presenting potential resources to be applied for biotechnology. This Chapter delves into the findings of the research conducted in this project, focusing on the innovative use of rice wastewater as a substrate for conventional yeast, *S. cerevisiae* expressing PHA synthase engineered from *P.mendocina*, with an emphasis on the composition of rice wastewater and as a sustainable source for biomass and biopolymer. This study aimed to establish the constituents of rice wastewater, assess the suitability of cultivating *S. cerevisiae*, and shed light on the waste stream as a potential resource in biotechnology.

This study focused on two critical aspects of biotechnology, firstly, the expression of PHA synthase from *P. mendocina*, a promising source of PHA synthase (Mozejko-Ciesielska *et al.,* 2019) into various cellular locations of *S. cerevisiae* to produce PHA. Secondly, the untapped potential of parboiled rice wastewater as a useful resource for biotechnology. We successfully demonstrated the heterologous expression of PHA synthase genes, *phaC1* and *phaC2* in peroxisomes and cytosols of *S. cerevisiae* cells. The synthesis of polymer in recombinant yeast was marked through powerful techniques namely NMR and GC. Our discussion manifests the significance, future perspectives, and potential limitations of this study.

6.2 Polymer synthesis in recombinant *S. cerevisiae*

In this study, we focused on a series of plasmids, some of which contained the PHA synthase gene, GFP, and with or without PTS1 to assess biopolymer production in engineered yeast carrying the corresponding plasmid. Despite the presence of the PHA synthase gene, recombinant *S. cerevisiae* did not produce PHA surprisingly. This was evident from multiple NMR analyses. This phenomenon raised questions regarding the role of GFP in the constructs. A few factors might contribute to this phenomenon such as the expression of GFP may consume the resources for metabolism that are essential for PHA synthesis (Deng *et al*., 2021). Foreign proteins like GFP expression could place a burden on the metabolism of host

cells and may trigger stress responses to divert resources away from the synthesis of PHA in the host organism (Scandella *et al.,* 2020). This finding highlights the interaction between engineered heterologous genes with native metabolic pathways. Consequently, the expression of a foreign gene could divert metabolic intermediates away from essential pathways, leading to unexpected outcomes (Scandella *et al.,* 2020). Or else it may be that the GFP domain binds to the PHA synthase domain and thus inhibits its activity directly. Further research is required to optimise the plasmid construct to achieve a balance between the expression of GFP and PHA synthase. This balance can be potentially achieved through the selection of inducible promoters or alternative fusion tags to promote visualisation as well as polymer production.

This study successfully expressed the PHA synthase from *P. mendocina* in peroxisomes and cytosols. We detected the presence of polyhydroxybutyrate in recombinant *S. cerevisiae* strains containing plasmid targeting peroxisomes (PHA synthase *phaC1*/*phaC2* with PTS1 and without GFP). However, the quantified level of PHB was low, and optimising the production has remained a challenge. This approach contributes to our understanding regarding the biosynthesis of polymer in eukaryotic hosts and delivers opportunities for further development, for example, the identification of additional genetic targets or optimisation of fermentation strategy. The potential of engineering yeast as a biopolymer producer is worthwhile and warrants further exploration.

6.3 Rice parboiled wastewater as a biotechnological resource

Parboiled wastewater from rice is a byproduct of rice processing mills and drew limited attention as an asset for biotechnological applications. We analysed the compositions of rice wastewater from Bangladesh and that highlights the potential of using this resourceful, abundant, and underused byproduct for numerous biotechnological purposes.

6.3.1 Constituents of rice wastewater from Bangladesh

We thoroughly analysed the physicochemical characteristics of rice-parboiled wastewater and revealed a complex mixture of organic components, inorganic, and trace elements present in the waste stream. These components create opportunities and can serve as a rich carbon source along with the nutrient source for yeast growth. Using waste streams not only serves as a solution for its disposal but also facilitates the sustainable production of biomass

and bioplastics. In Bangladesh, the cultivation of rice is a ruling industry, therefore the availability of rice-parboiled water is a locally accessible resource for biotechnological applications. The establishment of optimal rice waste stream constituents opens avenues for the cultivation of yeast leading to decentralised and localised bioproduction.

6.3.2 Utilisation of rice wastewater for yeast cultivation and production of biomass and biopolymer

The successful cultivation of recombinant yeast in rice-parboiled water in this study spotlights its potential as a nutrient-enriched growth media. Utilisation of rice waste stream for the cultivation of yeast offers an eco-friendly alternative to conventional media and aligns with the principles of making productive use of waste material. The study focused on adding various supplements to the waste stream, allowing the optimisation of the media to enhance the expected outcomes.

6.4 Challenges and future perspective

There are some challenges to be addressed, despite the potential of using rice-parboiled water for the cultivation of *S. cerevisiae* to produce biomass and biopolymer. These include PHA yield enhancement, fermentation condition optimisation, and potential contaminant mitigation, for instance, heavy metals in waste effluent. In addition, the requirement of pre-processing and conditioning of wastewater with additives to acquire optimal growth conditions for eukaryotes might introduce additional complexities regarding scalability and economic viability. The culmination of this study sets the stage for numerous future directions for further investigations. Future research should focus on:

6.4.1 Genetic engineering

Further optimisation of the expression of PHA synthase genes along with the metabolic pathways in *S. cerevisiae* to optimise PHA production. To achieve a higher PHA yield, PHA synthase genes from different microorganisms such as *Pseudomonas putida* (Muneer *et al*., 2020) or *Bacillus subtilis* (Wang *et al*., 2006) could be explored for expression in *S. cerevisiae*. Promoters play a key role in regulating the PHA synthase gene expression (Khadanga *et al.,* 2022). The choice of promoters with different strengths can be tested to gain a higher level

of gene expression. Synthetic promoters customised to yeast physiology might also be considered.

Beta-oxidation is a series of enzymatic reactions that degrades long-chain fatty acids to small two-carbon units known as acetyl-CoA which can be further metabolised or used as the precursor for the synthesis of PHA ((Anjum *et al*., 2016; Usman *et al*., 2022). PhaJ (Figure 1.12) plays a key role in one of the steps in this cycle. In the context of PHA synthesis, PhaJ enables the efficient use of fatty acids and the synthesis of PHA monomers such as 3-hydroxyacyl-CoA, which is essential for the polymerisation process (Liu *et al*., 2023). When fatty acids are used as a substrate, PhaJ converts the beta-oxidation intermediate, trans-2-enoyl-CoA to R-3-hydroxyacyl-CoA. The *R* isomer of 3-hydroxyacyl-CoA is expected to be a better substrate for the polymerase enzyme and so could significantly enhance the yield of polymer. By regulating the carbon flux between PHA biosynthesis and beta-oxidation, PhaJ turned out to be an important enzyme for the microbial synthesis of PHA. Engineering *phaJ* along with the PHA synthase gene, *phaC1* or *phaC2* could be a viable strategy for exploration of boosting PHA synthesis in conventional yeast, particularly when the primary carbon source is fatty acids or related precursors. This could allow the optimisation of both the supply of precursors and the polymerisation of PHA, ultimately would lead to the overall efficiency of the biosynthesis of PHA.

PHA production heavily depends on the availability of some precursors, primarily acetyl-CoA and NADPH (Amache *et al.,* 2013). Increasing the supply of precursors by regulating central carbon metabolism, for instance, the pentose phosphate pathway (Masi *et al.,* 2021) and glycolytic pathway (Wu *et al*., 2023) may improve PHA production.

A delicate balance between carbon and redox flux is essential (Vargas *et al*., 2011) for PHA biosynthesis. Few strategies for dynamic control of metabolic pathways can assist in achieving this balance for example overexpression of key enzymes, and cofactor engineering. Metabolic engineering could be employed to redirect carbon flux away from the competing pathways. This includes deleting or downregulating genes associated with carbon consumption or byproduct formation.

The introduction of the amylase gene in *S. cerevisiae* may serve as an intriguing opportunity for starch hydrolysis (Sakwa *et al*., 2018) to promote growth in the rice waste stream while concurrently facilitating the production of biomass and biopolymer. Amylase is an enzyme, that plays a critical role in breaking down starch molecules into simple sugars such as glucose and maltose (Gupta *et al*., 2003). By engineering the amylase gene into *S. cerevisiae* can acquire the ability to hydrolyse starch, a key component of rice waste effluent to fermentable sugars. This genetic engineering may facilitate the conventional yeast with a metabolic advantage to thrive in the complex growth media. Starch conversion to simple sugars in rice

waste stream would not support only yeast growth but also manifest a way of recycling nutrients.

6.4.2 Wastewater management

Development of efficient and cost-effective methods to remove contaminants (heavy metals) from rice waste stream to retain its suitability for conventional yeast as a growth media. Additionally, wastewater could be concentrated by heating to boost the starch content. Although this approach is energy-intensive but could be effective in concentrating the organic content, mainly starch to be used as a feedstock for the cultivation of yeast. It is possible that the heat energy could come from burning rice husks, which would make good use of all the waste from the milling process.

6.4.3 Assessment of environmental impact

The assessment of the environmental impact associated with utilising rice wastewater for yeast growth and the subsequent production of value-added products represents a critical facet of sustainable biotechnological processes. Our results revealed several noteworthy findings regarding the environmental impact of employing rice wastewater as a growth medium for yeast. Firstly, the wastewater quality was assessed in accordance with WHO and USEPA standards and guidelines. The analysis indicated that various key parameters, including physical characteristics, nutrient content, and heavy metal concentrations although all were well below the acceptable levels outlined by the WHO. This suggests that the utilization of rice wastewater as a growth medium for yeast does not introduce contaminants or pollutants beyond permissible limits, thereby minimizing the environmental burden associated with wastewater disposal.

Moreover, the efficient assimilation of nutrients by yeast during growth in rice wastewater was indicative of a sustainable and resource-effective process. The utilization of a waste stream for microbial cultivation not only repurposes a potential environmental pollutant but also reduces the reliance on conventional nutrient sources, contributing to resource conservation.

6.4.4 Scale-up

To evaluate its feasibility and economic viability, the process needs to be scaled up to the industrial level. The process of transitioning from laboratory-scale operations to industrial-scale production requires careful consideration of various factors to ensure feasibility and economic viability. When it comes to using rice wastewater for yeast growth and value-added polymer production, several strategies and considerations must be taken into account to guide the scale-up process. Scaling up requires a systematic approach to replicate and optimize the process on a larger scale. The choice of yeast strains for industrial-scale production is crucial, with strains such as atg36Δ and mdh3/gpd1Δ transformed with plasmid containing PhaC1+PTS1 without GFP being potential options. Strains with robust growth characteristics, high product yields, and tolerance to variations in environmental conditions are preferred.

Scaling up the process of utilizing rice wastewater for yeast growth requires a multidimensional approach including strain selection, nutrient management, downstream processing, economic viability, and environmental impact assessment. Successfully navigating these challenges can lead to the establishment of a sustainable and economically viable industrial bioprocess, demonstrating the potential for converting a waste stream into valuable products on a large scale.

6.5 Conclusion

In conclusion, this study explored the dual facets of producing PHA in *S. cerevisiae* through genetic engineering and the potential of rice-parboiled wastewater as a resourceful material for biotechnology. This research presents exciting opportunities for the development of green technologies that align with global sustainability goals. We have made notable strides in establishing the constituents of rice waste effluent for the cultivation of conventional yeast. Our research manifests valuable insights into the complex interconnection between microbial engineering and sustainable resource employment, offering a blueprint for the advancement of the future to produce biodegradable polymers and the management of waste streams. Addressing challenges, for instance, optimisation of the media, a cost-effective pathway for production will be vital in achieving the full potential of this technology. The combination of genetic engineering, innovative growth media, and metabolic optimisation offers a promising roadmap to make an advancement in the bio-based polymer field.

References

Adams, G. (2007). The principles of freeze-drying. *Cryopreservation and freeze-drying protocols*, pp.15-38.

Afrad, M.S.I., Monir, M.B., Haque, M.E., Barau, A.A. and Haque, M.M. (2020). Impact of industrial effluent on water, soil and Rice production in Bangladesh: a case of Turag Riverbank. *Journal of Environmental Health Science and Engineering*, *18*, pp.825-834.

Akaraonye, E., Keshavarz, T. and Roy, I. (2010). Production of polyhydroxyalkanoates: the future green materials of choice. *Journal of Chemical Technology & Biotechnology*, *85*(6), pp.732-743.

Al-Saryi, N.A., Al-Hejjaj, M.Y., van Roermund, C.W., Hulmes, G.E., Ekal, L., Payton, C., Wanders, R.J. and Hettema, E.H. (2017). Two NAD-linked redox shuttles maintain the peroxisomal redox balance in *Saccharomyces cerevisiae*. *Scientific reports*, *7*(1), pp. 1-9.

Amache, R., Sukan, A., Safari, M., Roy, I. and Keshavarz, T. (2013). Advances in PHAs production. *Chemical engineering transactions*, *32*, pp.931-936.

Anjum, A., Zuber, M., Zia, K.M., Noreen, A., Anjum, M.N. and Tabasum, S. (2016). Microbial production of polyhydroxyalkanoates (PHAs) and its copolymers: a review of recent advancements. *International journal of biological macromolecules*, *89*, pp.161-174.

Ansari, S. and Fatma, T. (2016). Cyanobacterial polyhydroxybutyrate (PHB): screening, optimization and characterization. *PLoS One*, *11*(6), p.e0158168.

Arefin, M.A. and Mallik, A. (2018). Sources and causes of water pollution in Bangladesh: A technical overview. *Bibechana*, *15*, pp. 97-112.

Awual, M.R., Ismael, M., Khaleque, M.A. and Yaita, T. (2014). Ultra-trace copper (II) detection and removal from wastewater using novel meso-adsorbent. *Journal of Industrial and Engineering Chemistry*, *20*(4), pp.2332-2340.

Azizullah, A., Khattak, M.N.K., Richter, P. and Häder, D.P. (2011). Water pollution in Pakistan and its impact on public health—a review. *Environment international*, *37*(2), pp.479-497.

Badotti, F., Dário, M.G., Alves, S.L., Cordioli, M.L.A., Miletti, L.C., de Araujo, P.S. and Stambuk, B.U. (2008). Switching the mode of sucrose utilization by *Saccharomyces cerevisiae*. *Microbial Cell Factories*, *7*(1), pp.1-11.

Braunegg, G., Sonnleitner, B. Y., & Lafferty, R. M. (1978). A rapid gas chromatographic method for the determination of poly-β-hydroxybutyric acid in microbial biomass. *European journal of applied microbiology and biotechnology*, *6*, pp. 29-37.

Breuer, U., Terentiev, Y., Kunze, G. and Babel, W. (2002). Yeasts as producers of polyhydroxyalkanoates: genetic engineering of *Saccharomyces cerevisiae*. *Macromolecular bioscience*, *2*(8), pp.380-386.

Brown, L.A. and Baker, A. (2003). Peroxisome biogenesis and the role of protein import. *Journal of cellular and molecular medicine*, *7*(4), pp.388-400.

Chen, D. C., Yang, B. C., and Kuo, T. T. (1992). One-step transformation of yeast in stationary phase. *Current Genetics*, 21(1), pp. 83–84.

Chen, J.Y., Liu, T., Zheng, Z., Chen, J.C. and Chen, G.Q. (2006). Polyhydroxyalkanoate synthases PhaC1 and PhaC2 from Pseudomonas stutzeri 1317 had different substrate specificities. *FEMS microbiology letters*, *234*(2), pp.231-237.

Chiha, M., Samar, M.H. and Hamdaoui, O. (2006). Extraction of chromium (VI) from sulphuric acid aqueous solutions by a liquid surfactant membrane (LSM). *Desalination*, *194*(1-3), pp.69-80.

Chopra, A.K. and Pathak, C. (2015). Accumulation of heavy metals in the vegetables grown in wastewater irrigated areas of Dehradun, India with reference to human health risk. *Environmental monitoring and assessment*, *187*, pp.1-8.

Chopra, S.L. and Kanwar, J.S. (1982). Analytical agricultural chemistry Kalyani Publishers. *Ludhiana, India*.

Cripwell, R.A., Rose, S.H., Favaro, L. and Van Zyl, W.H. (2019). Construction of industrial *Saccharomyces cerevisiae* strains for the efficient consolidated bioprocessing of raw starch. *Biotechnology for biofuels*, *12*, pp.1-16.

Deng, Y., Beahm, D.R., Ionov, S. and Sarpeshkar, R. (2021). Measuring and modeling energy and power consumption in living microbial cells with a synthetic ATP reporter. *BMC biology*, *19*(1), p.101.

Dixit, S., Yadav, A., Dwivedi, P.D. and Das, M. (2015). Toxic hazards of leather industry and technologies to combat threat: a review. *Journal of Cleaner Production*, *87*, pp.39-49.

Fang, Y., Morrell, J.C., Jones, J.M. and Gould, S.J. (2004). PEX3 functions as a PEX19 docking factor in the import of class I peroxisomal membrane proteins. *The Journal of cell biology*, *164*(6), pp.863-875.

Fehrenbach, G.W., Sitowski, A., Novo, D.L.R., Mesko, M.F., Gil de los Santos, D. and Leite, F.P.L. (2022). Nutrient Removal and Biomass Production by Culturing *Saccharomyces Cerevisiae* in Parboiled Rice Effluent. *Ecological Engineering & Environmental Technology*, *23*.

Fidaleo, M. (2010). Peroxisomes and peroxisomal disorders: the main facts. *Experimental and Toxicologic Pathology*, *62*(6), pp.615-625.

Gaboardi, G., de Los Santos, D.G., Mendes, L., Centeno, L., Meireles, T., Vargas, S., Griep, E., Silva, A.D.C.J., Moreira, Â.N. and Conceição, F.R. (2018). Bioremediation and biomass production from the cultivation of probiotic *Saccharomyces boulardii* in parboiled rice effluent. *Journal of environmental management*, *226*, pp.180-186.

Gao, C., Qi, Q., Madzak, C. and Lin, C.S.K. (2015). Exploring medium-chain-length polyhydroxyalkanoates production in the engineered yeast Yarrowia lipolytica. *Journal of Industrial Microbiology and Biotechnology*, *42*(9), pp.1255-1262.

Gautam, P.K., Gautam, R.K., Banerjee, S., Chattopadhyaya, M.C. and Pandey, J.D. (2016). Heavy metals in the environment: fate, transport, toxicity and remediation technologies. *Nova Sci Publishers*, *60*, pp.101-130.

Gietz, R. D., and Woods, R. A. (2002). Transformation of yeast by lithium acetate/single-stranded carrier DNA/polyethylene glycol method. *Methods in Enzymology*, 350, pp. 87– 96.

Gil de los Santos, D., Gil de los Santos, J.R., Gil-Turnes, C., Gaboardi, G., Fernandes Silva, L., Franca, R., Gevehr Fernandes, C. and Rochedo Conceição, F. (2018). Probiotic effect of *Pichia pastoris* X-33 produced in parboiled rice effluent and YPD medium on broiler chickens. *Plos one*, *13*(2), p.e0192904.

Goffeau, A., Barrell, B.G., Bussey, H., Davis, R.W., Dujon, B., Feldmann, H., Galibert, F., Hoheisel, J.D., Jacq, C., Johnston, M. and Louis, E.J. (1996). Life with 6000 genes. *Science*, *274*(5287), pp.546-567.

Gopinath, S.C., Anbu, P., Arshad, M.M., Lakshmipriya, T., Voon, C.H., Hashim, U. and Chinni, S.V. (2017). Biotechnological processes in microbial amylase production. *BioMed research international*, *2017*.

Gould, S.J., Keller, G.A., Hosken, N., Wilkinson, J. and Subramani, S. (1989). A conserved tripeptide sorts of proteins to peroxisomes. *The Journal of cell biology*, *108*(5), pp.1657-1664.

Green, M.R. and Sambrook, J. (2017). Isolation of high-molecular-weight DNA using organic solvents. *Cold Spring Harbor Protocols*, *2017*(4), pp.pdb-prot093450.

Griffiths, C., Klemick, H., Massey, M., Moore, C., Newbold, S., Simpson, D., Walsh, P. and Wheeler, W. (2012). US Environmental Protection Agency valuation of surface water quality improvements. *Review of Environmental Economics and Policy*.

Gupta, R., Gigras, P., Mohapatra, H., Goswami, V.K. and Chauhan, B. (2003). Microbial α-amylases: a biotechnological perspective. *Process biochemistry*, *38*(11), pp.1599-1616.

Haddouche, R., Poirier, Y., Delessert, S., Sabirova, J., Pagot, Y., Neuvéglise, C. and Nicaud, J.M., (2011). Engineering polyhydroxyalkanoate content and monomer composition in the oleaginous yeast *Yarrowia lipolytica* by modifying the *ß*-oxidation multifunctional protein. *Applied microbiology and biotechnology*, *91*, pp.1327-1340.

Hahn, S. K., Chang, Y. K., Kim, B. S., Lee, K. M., & Chang, H. N. (1993). The recovery of poly (3-hydroxybutyrate) by using dispersions of sodium hypochlorite solution and chloroform. *Biotechnology techniques*, *7*, pp. 209-212.

Hakobyan, L., Gabrielyan, L. and Trchounian, A. (2012). Yeast extract as an effective nitrogen source stimulating cell growth and enhancing hydrogen photoproduction *by Rhodobacter sphaeroides* strains from mineral springs. *international journal of hydrogen energy*, *37*(8), pp.6519-6526.

Hammer Sr, M.J. and Hammer Jr, M.J. (2013). *Water and Wastewater Technology: Pearson New International Edition*. Pearson Higher Ed.

Hanahan, D. (1983). Studies on transformation of *Escherichia coli* with plasmids. *Journal of Molecular Biology,* 166(4), pp. 557–580.

Heinemann, R.J.B., Fagundes, P.D.L., Pinto, E.A., Penteado, M.D.V.C. and Lanfer-Marquez, U.M. (2005). Comparative study of nutrient composition of commercial brown, parboiled and milled rice from Brazil. *Journal of Food Composition and Analysis*, *18*(4), pp.287-296.

Helen (2021) *What food has the most starch*. Available at: What food has the most starch? | - From Hunger To Hope (Accessed: 25 June 2023).

Hettema, E.H., Erdmann, R., van der Klei, I. and Veenhuis, M. (2014). Evolving models for peroxisome biogenesis. *Current opinion in cell biology*, *29*, pp.25-30.

Higuchi-Takeuchi, M., Morisaki, K., Toyooka, K. and Numata, K. (2016). Synthesis of high-molecular-weight polyhydroxyalkanoates by marine photosynthetic purple bacteria. *Plos one*, *11*(8), p.e0160981.

Holesh, J. E., Aslam, S., & Martin, A. (2022). Physiology, Carbohydrates. In *StatPearls [Internet]*. StatPearls Publishing.

Hossain MA. (2014). Chemical constituents and suitability studies of ground water for irrigation uses in Dinajpur. M.S. Thesis, Department of Agricultural Chemistry, Hajee Mohammad Danesh Science and Technology University, Dinajpur.

Huppelschoten, Y., Elhebieshy, A.F., Hameed, D.S., Sapmaz, A., Buchardt, J., Nielsen, T.E., Ovaa, H. and van der Heden van Noort, G.J. (2022). Total chemical synthesis of a functionalized GFP nanobody. *ChemBioChem*, *23*(19), p.e202200304.

Hutch, F. (2012) *OD660 vs number of cells*. Available at: Untitled (fredhutch.org) (Accessed: 21 August, 2023).

Islam, M., Nasrin, T., Rahman, M., Islam, M. and Ray, T.K. (2020). Quantitative Constituents Analysis of Rice Mill Wastewater. *Turkish Journal of Agriculture-Food Science and Technology*, *8*(10), pp.2034-2039.

Järup, L., Hellström, L., Alfvén, T., Carlsson, M.D., Grubb, A., Persson, B., Pettersson, C., Spång, G., Schütz, A. and Elinder, C.G. (2000). Low level exposure to cadmium and early kidney damage: the OSCAR study. *Occupational and environmental medicine*, *57*(10), pp.668-672.

Khadanga, B., Sherpa, T., Chanwala, J. and Dey, N. (2022). Synthetic Promoters in Regulating Disease Gene Expression. In *Transcription Factors for Biotic Stress Tolerance in Plants* (pp. 33-50). Cham: Springer International Publishing.

Kouras, A., Katsoyiannis, I. and Voutsa, D., (2007). Distribution of arsenic in groundwater in the area of Chalkidiki, Northern Greece. *Journal of Hazardous materials*, *147*(3), pp.890-899.

Kovalcik, A., Obruca, S., Fritz, I. and Marova, I. (2019). Polyhydroxyalkanoates: their importance and future. *BioResources*, *14*(2), pp.2468-2471.

Kozlowski, H., Janicka-Klos, A., Brasun, J., Gaggelli, E., Valensin, D. and Valensin, G. (2009). Copper, iron, and zinc ions homeostasis and their role in neurodegenerative disorders (metal uptake, transport, distribution and regulation). *Coordination Chemistry Reviews*, *253*(21-22), pp.2665-2685.

Kumar, A., Lal, M.K., Nayak, S., Sahoo, U., Behera, A., Bagchi, T.B., Parameswaran, C., Swain, P. and Sharma, S. (2022). Effect of parboiling on starch digestibility and mineral bioavailability in rice (Oryza sativa L.). *Lwt*, *156*, p.113026.

Kumar, S. and Deswal, S. (2021). A review on current techniques used in India for rice mill wastewater treatment and emerging techniques with valuable by-products. *Environmental Science and Pollution Research*, *28*, pp.7652-7668.

Lamberts, L., Gomand, S.V., Derycke, V. and Delcour, J.A. (2009). Presence of amylose crystallites in parboiled rice. *Journal of Agricultural and Food Chemistry*, *57*(8), pp.3210-3216.

Lazarow, P.B. and Fujiki, Y. (1985). Biogenesis of peroxisomes. *Annual review of cell biology*, *1*(1), pp.489-530.

Lemoigne, M. (1926). Products of dehydration and of polymerization of β-hydroxybutyric acid. *Bull Soc Chem Biol*, *8*, pp.770-782.

Liu, S., Narancic, T., Tham, J.L. and O'Connor, K.E. (2023). β-oxidation–polyhydroxyalkanoates synthesis relationship in *Pseudomonas putida* KT2440 revisited. *Applied Microbiology and Biotechnology*, *107*(5-6), pp.1863-1874.

Mannan, M.A., Nuruzzaman, M., Bari, M.S. and Rahman, M.S. (2022). Impact of Rice Mill Pollution on Surrounding Environment: A Case Study in Sadar Upazila, Dinajpur, Bangladesh. *Asian Journal of Research in Agriculture and Forestry*, *8*(4), pp. 88-96.

Martin, C. and Smith, A.M. (1995). Starch biosynthesis. *The plant cell*, *7*(7), p.971.

Masih, D., Seida, Y. and Izumi, Y. (2009). Arsenic removal from dilute solutions by high surface area mesoporous iron oxyhydroxide. *Water, Air, & Soil Pollution: Focus*, *9*, pp.203-211.

Masi, A., Mach, R.L. and Mach-Aigner, A.R. (2021). The pentose phosphate pathway in industrially relevant fungi: Crucial insights for bioprocessing. *Applied Microbiology and Biotechnology*, *105*(10), pp.4017-4031.

Mattanovich, D., Sauer, M. and Gasser, B. (2014). Yeast biotechnology: teaching the old dog new tricks. *Microbial cell factories*, *13*(1), pp.1-5.

Meinecke, M., Bartsch, P. and Wagner, R. (2016). Peroxisomal protein import pores. *Biochimica Et Biophysica Acta (BBA)-Molecular Cell Research*, *1863*(5), pp.821-827.

Mezzolla, V., D'Urso, O.F. and Poltronieri, P. (2018). Role of PhaC type I and type II enzymes during PHA biosynthesis. *Polymers*, *10*(8), p.910.

Miah, M.K., Haque, A., Douglass, M.P. and Clarke, B. (2002). Parboiling of rice. Part II: Effect of hot soaking time on the degree of starch gelatinization. *International journal of food science & technology*, *37*(5), pp.539-545.

Miyata, N. and Fujiki, Y. (2005). Shuttling mechanism of peroxisome targeting signal type 1 receptor Pex5: ATP-independent import and ATP-dependent export. *Molecular and cellular biology*, *25*(24), pp.10822-10832.

Muneer, F., Rasul, I., Azeem, F., Siddique, M.H., Zubair, M. and Nadeem, H. (2020). Microbial polyhydroxyalkanoates (PHAs): efficient replacement of synthetic polymers. *Journal of Polymers and the Environment*, *28*, pp.2301-2323.

Muthuraj, R., Valerio, O. and Mekonnen, T.H., (2021). Recent developments in short-and medium-chain-length Polyhydroxyalkanoates: Production, properties, and applications. *International Journal of Biological Macromolecules*, *187*, pp.422-440.

Muthayya, S., Sugimoto, J.D., Montgomery, S. and Maberly, G.F. (2014). An overview of global rice production, supply, trade, and consumption. *Annals of the new york Academy of Sciences*, *1324*(1), pp.7-14.

Myers, J. (2017) *Where is the Yeast cell located or found?* Available at: Where is the Yeast Cell located or found? by Jack Myers (prezi.com) (Accessed: 4 July, 2023).

Nickens, K.P., Patierno, S.R. and Ceryak, S. (2010). Chromium genotoxicity: A double-edged sword. *Chemico-biological interactions*, *188*(2), pp.276-288.

Nocon, J., Steiger, M.G., Pfeffer, M., Sohn, S.B., Kim, T.Y., Maurer, M., Rußmayer, H., Pflügl, S., Ask, M., Haberhauer-Troyer, C. and Ortmayr, K., (2014). Model based engineering of *Pichia*

pastoris central metabolism enhances recombinant protein production. *Metabolic Engineering*, *24*, pp.129-138.

Okoroafor, R. (2023) *13 Biggest rice producing countries in the world*. Available at: 13 Biggest rice producing countries in the world (2023) - MakeMoney.ng (Accessed: 22 June 2023).

Okumoto, K., Tamura, S., Honsho, M. and Fujiki, Y. (2020). Peroxisome: metabolic functions and biogenesis. *Peroxisome Biology: Experimental Models, Peroxisomal Disorders and Neurological Diseases*, pp.3-17.

Paiva, F.F., Vanier, N.L., Berrios, J.D.J., Pinto, V.Z., Wood, D., Williams, T., Pan, J. and Elias, M.C. (2016). Polishing and parboiling effect on the nutritional and technological properties of pigmented rice. *Food chemistry*, *191*, pp.105-112.

Payen, A. and Persoz, J.F. (1833). Mémoire sur la diastase, les principaux produits de ses réactions, et leurs applications aux arts industriels. *Ann. chim. phys*, *53*(2), pp.73-92.

Poirier, Y., Erard, N. and Petétot, J.M.C. (2001). Synthesis of polyhydroxyalkanoate in the peroxisome of *Saccharomyces cerevisiae* by using intermediates of fatty acid β-oxidation. *Applied and environmental microbiology*, *67*(11), pp.5254-5260.

Pulingam, T., Appaturi, J.N., Parumasivam, T., Ahmad, A. and Sudesh, K. (2022). Biomedical applications of polyhydroxyalkanoate in tissue engineering. *Polymers*, *14*(11), p.2141.

Rajaram, T. and Das, A. (2008). Water pollution by industrial effluents in India: Discharge scenarios and case for participatory ecosystem specific local regulation. *Futures*, *40*(1), pp.56-69.

Ralser, M., Heeren, G., Breitenbach, M., Lehrach, H. and Krobitsch, S. (2006). Triose phosphate isomerase deficiency is caused by altered dimerization–not catalytic inactivity–of the mutant enzymes. *PLoS One*, *1*(1), p.e30.

Raza, Z.A., Abid, S. and Banat, I.M. (2018). Polyhydroxyalkanoates: Characteristics, production, recent developments and applications. *International Biodeterioration & Biodegradation*, *126*, pp.45-56.

Rehm, B.H.A. (2021) Polyhydroxyalkanoates. Available at: https://lipidlibrary.aocs.org/chemistry/physics/microbial-lipid/polyhydroxyalkanoates (Accessed: 26 June 2023).

Rios, D.A.D.S., Borba, T.D.M.D., Kalil, S.J. and Burkert, J.F.D.M. (2015). Rice parboiling wastewater in the maximization of carotenoids bioproduction by *Phaffia rhodozyma*. *Ciência e Agrotecnologia*, *39*, pp.401-410.

Robyt, J.F. (2008). Starch: structure, properties, chemistry, and enzymology. *Glycoscience*, p.1437.

Rozpędowska, E., Hellborg, L., Ishchuk, O.P., Orhan, F., Galafassi, S., Merico, A., Woolfit, M., Compagno, C. and Piškur, J. (2011). Parallel evolution of the make–accumulate–consume strategy in *Saccharomyces* and *Dekkera* yeasts. *Nature communications*, *2*(1), p.302.

Sakwa, L., Cripwell, R.A., Rose, S.H. and Viljoen-Bloom, M. (2018). Consolidated bioprocessing of raw starch with *Saccharomyces cerevisiae* strains expressing fungal alpha-amylase and glucoamylase combinations. *FEMS yeast research*, *18*(7), p. foy085.

Sambrook, J., & Russell, D. W. (2006). Purification of nucleic acids by extraction with phenol: chloroform. *Cold Spring Harbor Protocols*, *2006*(1), pdb-prot4455.

Sanitation and Water for All (2020) *People's Republic of Bangladesh Country Overview*. Available at: Microsoft Word - 2020 Country-Overview Bangladesh.docx (sanitationandwaterforall.org) (Accessed: 24 July 2023).

Sasidharan, K., Soga, T., Tomita, M. and Murray, D.B. (2012). A yeast metabolite extraction protocol optimised for time-series analyses.

Sayanthan, S. and Thusyanthy, Y. (2018). Rice parboiling and effluent treatment models; a review. *International Journal of Research Studies in Agricultural Sciences (IJRSAS)*, *4*(5), pp.17-23.

Scandella, V., Paolicelli, R.C. and Knobloch, M. (2020). A novel protocol to detect green fluorescent protein in unfixed, snap-frozen tissue. *Scientific reports*, *10*(1), p.14642.

Schneid, A.S., de los Santos, J.G., Elıas Jr, M. and Gil-Turnes, C. (2004). Wastewater of rice parboiling process as substrate for probiotics. In *Proceedings of the 2nd International Probiotic Conference* (p. 66).

Seitz, A. (2023) *MCT Oil 101*: *A Review of Medium Chain Triglycerides*. Available at: MCT Oil 101: A Review of Medium-Chain Triglycerides (healthline.com) (Accessed: 26 September 2023).

SGDWiki (2019) *What are yeast*. Available at: What are yeast? - SGD-Wiki (yeastgenome.org) (Accessed: 25 June 2023).

Shafique, S., Bajwa, R. and Shafique, S. (2010). Mutagenesis and genetic characterisation of amylolytic *Aspergillus niger*. *Natural Product Research*, *24*(12), pp.1104-1114.

Shahbandeh, M. (2023) *Statista: Rice statistics and facts*. Available at: https://www.statista.com/topics/1443/rice/#topicOverview (Accessed: 10 June 2023).

Shallcross, L. (2022) *Aluminum in Water: What You Need to Know in 2023*. Available at: Aluminum in Water: What You Need to Know in 2023 (waterfilterguru.com) (Accessed: 10 August 2023).

Sharma, V.K. and Sohn, M. (2009). Aquatic arsenic: toxicity, speciation, transformations, and remediation. *Environment international*, *35*(4), pp.743-759.

Sherri. (2023) *How yeast feeds on starch: A look at fermentation*. Available at: How Yeast Feeds On Starch: A Look At Fermentation – The Well-Floured Kitchen (Accessed: 25 June 2023).

Singh, R., Singh, S., Parihar, P., Singh, V.P. and Prasad, S.M. (2015). Arsenic contamination, consequences and remediation techniques: a review. *Ecotoxicology and environmental safety*, *112*, pp.247-270.

Singh, A.K., Singh, D.P., Panday, K.K. and Singh, V.N., (1988). Wollastonite as adsorbent for removal of Fe (II) from water. *Journal of Chemical Technology & Biotechnology*, *42*(1), pp.39-49.

Swinkels, B.W., Gould, S.J. and Subramani, S. (1992). Targeting efficiencies of various permutations of the consensus C-terminal tripeptide peroxisomal targeting signal. *FEBS letters*, *305*(2), pp.133-136.

Svihus, B., Uhlen, A.K. and Harstad, O.M. (2005). Effect of starch granule structure, associated components and processing on nutritive value of cereal starch: A review. *Animal Feed Science and Technology*, *122*(3-4), pp.303-320.

The University of Sheffield (2023) '*Inductively Coupled Plasma spectroscopy'. Faculty of Science Mass Spectrometry Centre.*

Available at: https://www.sheffield.ac.uk/mass-spectrometry/chemms/inductively-coupled-plasma-spectroscopy (Accessed: 2nd May 2023).

Uddin, M.G. (2004). *Comparative studies of ground water quality at different aquifers of Dinajpur district* (Doctoral dissertation, MS Thesis, Department of Agricultural Chemistry, Bangladesh Agricultural University, Mymensingh).

Usman, M., Zhao, S., Jeon, B.H., Salama, E.S. and Li, X. (2022). Microbial β-oxidation of synthetic long-chain fatty acids to improve lipid biomethanation. *Water Research*, *213*, p.118164.

Vadahanambi, S., Lee, S.H., Kim, W.J. and Oh, I.K. (2013). Arsenic removal from contaminated water using three-dimensional graphene-carbon nanotube-iron oxide nanostructures. *Environmental science & technology*, *47*(18), pp.10510-10517.

Van den Bosch, H., Schutgens, R.B.H., Wanders, R.J.A. and Tager, J. (1992). Biochemistry of peroxisomes. *Annual review of biochemistry*, *61*(1), pp.157-197.

Vargas, F.A., Pizarro, F., Pérez-Correa, J.R. and Agosin, E. (2011). Expanding a dynamic flux balance model of yeast fermentation to genome-scale. *BMC systems biology*, *5*(1), pp.1-12.

Vasu, A.E. (2008). Adsorption of Ni (II), Cu (II) and Fe (III) from aqueous solutions using activated carbon. *Journal of Chemistry*, *5*, pp.1-9.

Verlinden, R.A., Hill, D.J., Kenward, M.A., Williams, C.D. and Radecka, I. (2007). Bacterial synthesis of biodegradable polyhydroxyalkanoates. *Journal of applied microbiology*, *102*(6), pp.1437-1449.

Vieira Gomes, A.M., Souza Carmo, T., Silva Carvalho, L., Mendonça Bahia, F. and Parachin, N.S., 2018. Comparison of yeasts as hosts for recombinant protein production. *Microorganisms*, *6*(2), p.38.

Walter, T. and Erdmann, R. (2019). Current advances in protein import into peroxisomes. *The Protein Journal*, *38*(3), pp.351-362.

Wang, Y., Ruan, L., Chua, H. and Yu, P.H. (2006). Cloning and expression of the PHA synthase genes phaC1 and phaC1AB into *Bacillus subtilis*. *World Journal of Microbiology and Biotechnology*, *22*, pp.559-563.

Ward, P.G., de Roo, G. and O'Connor, K.E. (2005). Accumulation of polyhydroxyalkanoate from styrene and phenylacetic acid by Pseudomonas putida CA-3. *Applied and environmental microbiology*, *71*(4), pp.2046-2052.

WaterAid (2020*) Bangladesh- Facts and Statistics*. Available at: Bangladesh - Facts and Statistics | WaterAid Bangladesh (Accessed: 25 May 2023).

Water Quality Association (2023*) Manganese fact sheet*. Available at: Manganese Fact Sheet - Water Quality Association (wqa.org) (Accessed: 9 August 2023).

Wood, V., Gwilliam, R., Rajandream, M.A., Lyne, M., Lyne, R., Stewart, A., Sgouros, J., Peat, N., Hayles, J., Baker, S. and Basham, D. (2002). The genome sequence of *Schizosaccharomyces pombe*. *Nature*, *415*(6874), pp.871-880.

World Health Organization. (2004). *Guidelines for drinking-water quality* (Vol. 1). World Health Organization.

Worldometer (2023) *Bangladesh Population*. Available at: Bangladesh Population (2023) - Worldometer (worldometers.info) (Accessed: 24 July 2023).

Wu, Z., Liang, X., Li, M., Ma, M., Zheng, Q., Li, D., An, T. and Wang, G. (2023). Advances in the optimization of central carbon metabolism in metabolic engineering. *Microbial Cell Factories*, *22*(1), pp.1-11.

Yang, S. T., Liu, X. and Zhang, Y. (2007). Metabolic engineering–applications, methods, and challenges. In *Bioprocessing for value-added products from renewable resources* (pp. 73-118). Elsevier.

Yang, Y. T., Bennett, G.N. and San, K.Y. (1998). Genetic and metabolic engineering. *Electronic Journal of Biotechnology*, *1*(3), pp.20-21.

Yiu, A. (2021*) Rice, types of rice and alternative grains.* Available at: Rice, Types of Rice and Alternative Grains - Health Stand Nutrition (Accessed: 3 July, 2023).

Ylinen, A., De Ruijter, J.C., Jouhten, P. and Penttilä, M. (2022). PHB production from cellobiose with Saccharomyces cerevisiae. *Microbial Cell Factories*, *21*(1), p.124.

Zhang, B., Carlson, R. and Srienc, F. (2006). Engineering the monomer composition of polyhydroxyalkanoates synthesized in *Saccharomyces cerevisiae*. *Applied and environmental microbiology*, *72*(1), pp.536-543.

Zhang, X., Liu, X.Y., Yang, H., Chen, J.N., Lin, Y., Han, S.Y., Cao, Q., Zeng, H.S. and Ye, J.W. (2022). A Polyhydroxyalkanoates-Based Carrier Platform of Bioactive Substances for Therapeutic Applications. *Frontiers in Bioengineering and Biotechnology*, *9*, p.798724.

Zhang, Y., Chi, H., Zhang, W., Sun, Y., Liang, Q., Gu, Y. and Jing, R. (2014). Highly efficient adsorption of copper ions by a PVP-reduced graphene oxide based on a new adsorption's mechanism. *Nano-Micro Letters*, *6*, pp.80-87.

Zuriani, R., Vigneswari, S., Azizan, M. N. M., Majid, M. I. A., & Amirul, A. A. (2013). A high throughput Nile red fluorescence method for rapid quantification of intracellular bacterial polyhydroxyalkanoates. *Biotechnology and bioprocess engineering*, *18*, pp. 472-478.